Identification of
DNA damage-induced autophagic cargo
by mass-spectrometry based proteomics

Dissertation

zur Erlangung des Grades

Doktor der Naturwissenschaften

am Fachbereich Biologie

der Johannes Gutenberg-Universität Mainz

vorgelegt von

Thomas Johannes Juretschke

geboren am 11.05.1990

in Frankfurt am Main, Deutschland

Mainz, Oktober 2021

Dekan:

1. Gutachterin:

2. Gutachter:

Tag der mündlichen Prüfung: 03.12.21

Preface

1 TABLE OF CONTENT

Table of content

2 LIST OF PUBLICATIONS

3 SUMMARY

Autophagy is a catabolic recycling pathway initiated under periods of starvation with energy-saving and cytoprotective effects. Previously considered a non-targeted process that degrades bulk cytoplasmic material, the discovery of autophagy receptors revealed that autophagy also leads to the targeted turnover of different cargo.

Upon its perception, DNA damage triggers tailor-made signaling and repair pathways, collectively designated as the DNA damage response (DDR) that can also result in apoptosis or cellular senescence. Kinases that orchestrate the DDR are ATM, ATR and DNA-PKcs. Autophagy succeeds DNA damage, but the signaling pathways required to transmit the information for autophagy activation from the nucleus to the cytoplasm as well as its purpose remain poorly understood.

This study focused on two aspects of DNA damage-induced autophagy. First, I investigated whether the DDR kinases play a role in the activation of autophagy after DNA double strand breaks. Second, I employed mass spectrometry (MS)-based proteomics to probe the cargo of DNA damage-induced autophagy to investigate its relevance in the DDR.

To assess the role of the DDR kinases in DNA damage-induced autophagy, the conversion of the autophagy marker protein LC3B into its lipidated form and the degradation of the receptor p62 were monitored in DDR kinase knockdown cells. As a complementary approach, the tandem-LC3B assay was engaged to measure DNA damage-induced autophagy in the presence of DDR kinase inhibitors. Using different read-out systems, we came to indecisive results indicating no, mild or strong involvement of the DDR kinases in DNA damage-induced autophagy. The off-target effects of commonly used DDR kinase inhibitors that might also cause the inhibition of the phosphatidylinositol-3-kinase VPS34 could explain observed inconsistency between the results obtained in knockdown and chemical inhibitor-treated cells.

I established a MS-based proximity proteomics approach to identify systematically DNA damage-induced autophagic cargo. Applying this technique, many known and previously undescribed putative cargo proteins were identified. Computational analyses permitted to associate the identified cargo with focal adhesions proteins, ribosomal proteins, the subunits of the TRiQ/CCT chaperonin complex as well as with nuclear-localized proteins. The proteinase K protection assay enabled to validate most of the selected proteins as autophagic cargo. Ultimately, the cargo that was identified indicates that micronuclei might be degraded by autophagy after genotoxic stress. Further, identification of focal adhesions proteins and validation of the metastasis suppressor NME1 could indicate for a metastasis-promoting role of autophagy after treatment with chemotherapeutic agents. This study presents the first approach to investigate DNA damage-induced autophagic cargo using proximity proteomics and reveals a role for autophagy in the degradation of nuclear proteins in human cells.

4 ZUSAMMENFASSUNG

Autophagie ist ein katabolischer Wiederverwertungsmechanismus der durch Mangel an Nahrungsmitteln ausgelöst wird und der energiesparende und zellschützende Auswirkungen hat. Ursprünglich als nicht zielgerichteter Prozess betrachtet, der lose und große Mengen cytoplasmatischen Materials abbaut, hat sich mit der Entdeckung selektiver Autophagierezeptoren gezeigt, dass Autophagie auch zum zielgerichteten Abbau unterschiedlicher Fracht führen kann.

Schäden in der DNS können, sobald sie wahrgenommen wurden, maßgeschneiderte Signal- und Reparatur-Wege auslösen, die zusammengenommen als die DNS-Schadensreaktion (engl. DDR) bezeichnet werden und auch zur Apoptose oder der zellulären Seneszenz führen können. ATM, ATR und DNA-PKcs sind die Kinasen, welche die DDR orchestrieren. Auf Schäden in der DNS folgt die Autophagie, aber die Signalwege, welche erforderlich sind, um die Information zur Autophagieaktivierung vom Nukleus in das Cytoplasma zu übertragen sowie ihr Zweck, sind wenig verstanden.

Diese Studie hat sich auf zwei Aspekte der durch DNS-Schäden induzierten Autophagie fokussiert. Erstens habe ich untersucht, ob die DDR-Kinasen eine Rolle in der Autophagieaktivierung nach DNS-Doppelstrangbrüchen spielen. Zweitens habe ich Massenspektrometrie (engl. MS)-basierte Proteomik verwendet, um die Fracht der durch DNS-Schäden induzierten Autophagie und ihre Relevanz in der DDR zu untersuchen.

Um die Rolle der DDR Kinasen in der durch DNS-Schäden induzierten Autophagie festzustellen, wurde die Konvertierung des Autophagiemarkerproteins LC3B in seine lipidierte Form und der Abbau des Rezeptors p62 in Knockdownzellen der DDR-Kinasen untersucht. In einem komplementären Ansatz wurde der Tandem-LC3B Assay in Anspruch genommen, um die durch DNS-Schäden induzierten Autophagie in Anwesenheit von Inhibitoren der DDR-Kinasen zu messen. Mittels verschiedener Auslesesysteme sind wir zu nicht eindeutigen Ergebnissen gekommen, welche auf keine, eine milde oder eine starke Beteiligung der DDR-Kinasen in der durch DNS-Schäden induzierten Autophagie hinweist. Die Fehlschusseffekte allgemein üblicher Inhibitoren der DDR-Kinasen, die auch die Hemmung der Phosphaditylinositol-3-Kinase VPS34 verursachen könnten, könnte die beobachteten Widersprüchlichkeiten zwischen den Ergebnissen aus Knockdownzellen und mittels chemischer Inhibitoren behandelter Zellen erklären.

Ich habe einen MS-basierten Annäherungs-Proteomik Versuch etabliert, um systematisch die durch DNS-Schäden induzierte Autophagiefracht zu identifizieren. Diese Technik verwendend, konnten viele bekannte und vorher nicht beschriebene potentielle Frachtproteine identifiziert werden. Eine bioinformatische Analyse stellte die identifizierte Fracht mit fokalen Adhäsionsproteinen, ribosomalen Proteinen und Untereinheiten des TRiQ/CCT-Chaperonin Komplexes, aber auch mit Proteinen nuklearer Lokalisation in Verbindung. Der Proteinase K Schutz-Assay ermöglichte es die meisten der ausgewählten Proteine als autophagische Fracht

zu validieren. Schlussendlich weist die identifizierte Fracht darauf hin, dass Mikronuklei durch DNS-Schäden induzierten Autophagie abgebaut werden. Des Weiteren könnte die Identifizierung von fokalen Adhäsionsproteinen und die Validierung der Metastase unterdrückenden Proteins NME1 auf eine Metastase fördernde Rolle der Autophagie nach Behandlung mit chemotherapeutischen Mitteln hindeuten. Diese Studie präsentiert den ersten Versuch die durch DNS-Schäden induzierten Autophagiefracht mittels Annäherungs-Proteomik zu untersuchen und konnte eine potentielle Rolle der Autophagie im Abbau nuklearer Proteine in Humanzellen aufzeigen.

5 INTRODUCTION

5.1 PROTEOSTASIS

The proteome of a cell is defined as the sum of all proteins. It is under constant change as proteins can fold wrong or encounter damage, which requires their control and regulation. Keeping the proteome in balance ensures correct development, response to environmental stresses and healthy aging [1]. Two major protein quality control mechanisms have evolved that regulate the proteome: the autophagy-lysosome pathway and the ubiquitin-proteasome system (UPS) [2,3]. Autophagy is a recycling system that collects cellular entities such as proteins or cell organelles in specific vesicles, autophagosomes, that eventually fuse with lysosomes and direct the cargo for proteolytic degradation [4]. The UPS is based on a posttranslational modification (PTM), ubiquitylation, which targets a protein for degradation via the proteasome (Figure 1). Ubiquitin (Ub), a protein of 76 amino acids is attached to an internal lysine of another protein in a mechanism that requires three steps: the activation, conjugation and ligation of Ub conducted by the interplay of an E1-activating, E2-conjugating and E3-ligating enzyme [5]. Ub itself can be ubiquitylated on seven internal lysines (K6, K11, K27, K29, K33, K48 and K63) and the amino-terminal methionine (M1), which enables to build up poly-ubiquitin chains that can be of homotypic nature or branch into heterotypic Ub chains of different linkage types. Proteins that have been modified with Ub chains of the K48 type are most often directed for proteasomal degradation. K63 linkages are associated with other mechanisms such as DNA repair or protein sorting [6–8]. Different Ub linkage types have also been associated with autophagy. In contrast to the UPS, there is no particular Ub linkage type known that directs proteins or cell organelles for autophagosomal removal [9]. Different linkage types on M1, K6, K11, K33, K48 and K63 have been associated with different aspects of autophagy [10–12]. Recent studies estimate that the UPS is capable to degrade about 90% of the cellular proteome, whereas autophagy is responsible for the turnover of long-lived proteins such as nuclear lamins and proteins that assemble either into large complexes or protein aggregates [13]. Autophagy has been linked to many pathologies such as neurodegenerative, immunological and infectious diseases, aging and cancer [14,15].

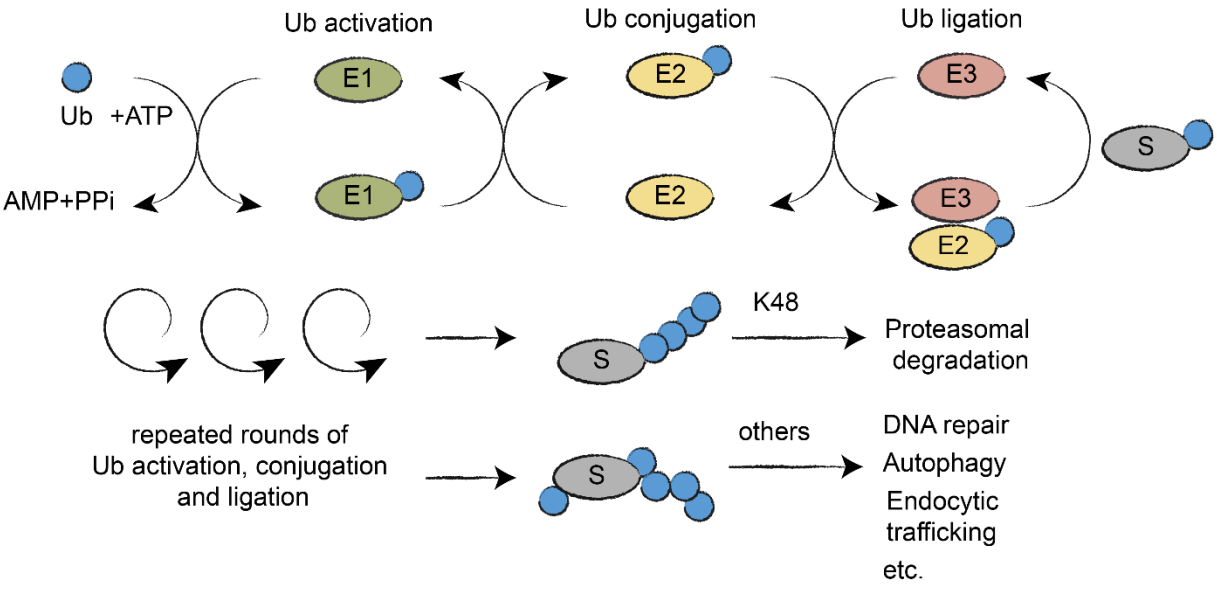

Figure 1: Ubiquitylation and its role as a PTM. Activation of Ub requires the hydrolysis of ATP by an Ub-activating enzyme (E1), which is followed by the covalent conjugation to an Ub-conjugating enzyme (E2) and the ligation by an Ub-ligase (E3) to the substrate. The process can be repeated, which results in the formation of different homotypic or heterotypic Ub chains. Chains of the K48 linkage-type are associated with proteasomal degradation of the substrate protein. Other chain types have been reported to be involved in other biological processes such as autophagy, DNA repair or endocytic trafficking. S: Substrate.

5.2 AUTOPHAGY

Autophagy, (name derives from the Greek words auto = oneself and phagei = eating), is a ubiquitous cellular degradation process conserved from lower to higher eukaryotes. It involves the transport of macromolecules, organelles or pathogens into the lysosome, where they are catabolized into their biochemical constituents [16]. Autophagy is triggered by physiological perturbations and has mostly been studied under starvation conditions. It is believed to be a cytoprotective pro-survival mechanism. However, excessive activation of autophagy can lead to autophagic cell death (ACD, a type II programmed cell death) [17,18]. Moreover, autophagy-related (ATG) proteins interact with proteins from apoptosis pathways indicating an intricate interplay between the two processes [19–21]. Generally, there are three main autophagy types in higher eukaryotic cells: macroautophagy, microautophagy and chaperone-mediated autophagy (CMA) (Figure 2).

In macroautophagy a cup-shaped membrane structure, the phagophore, is formed at the endoplasmic reticulum (ER). It grows around cytoplasmic material and matures to an autophagosome, a vesicle with two lipid bilayers. Eventually, the autophagosome will fuse with a lysosome and form the autolysosome. Thereby, the inner lipid bilayer of the autophagosome and the captured cargo is degraded by lysosomal hydrolases. The catabolites, free fatty acids, amino acids and monosaccharides are finally exported by permeases into the cytoplasm, where they can serve for anabolic purposes [2,16].

An important marker for autophagosomal vesicles is the ubiquitin-like (UBL) protein Microtubule-associated proteins 1A/1B light chain 3 (MAP1LC3, also known as LC3) [22]. It resides as a soluble protein (referred to as LC3-I) in the nucleus and is exported into the

cytoplasm upon autophagy activation [23]. Here, it is lipidated with phosphatidylethanolamine (PE) in an UBL conjugation system that depends on ATG proteins [24–26]. The lipidated version of LC3 (known as LC3-II) resides in the autophagosomal bilayers. Yeast have only one orthologue of LC3, which is ATG8. Humans however, have in total six homologues: the LC3 family consisting of LC3A, LC3B and LC3C and the γ-aminobutyric acid receptor-associated protein (GABARAP) family consisting of GABARAP, GABARAPL1 and GABARAPL2 (hereafter referred to as human ATG8 proteins). Interestingly, two different genes MAP1LC3B and MAP1LC3B2 encode LC3B [27]. Due to their high sequence similarity, it is difficult to define specific and redundant functions of the human ATG8 proteins (hATG8s). However, it is believed that the LC3 family proteins function in early steps of autophagosome formation such as phagophore elongation, whereas the proteins of the GABARAP family are considered to act later, when sealing the autophagosome [28].

Macroautophagy can lead to the targeted degradation of macromolecules, organelles and intracellular pathogens. These selective autophagy pathways are named after the respective cargo that is destined for elimination. Over 14 types of selective autophagy have been reported, e.g. mitophagy, reticulophagy, nucleophagy, xenophagy and aggrephagy that describe the targeted capture and degradation of mitochondria, parts of the ER, nuclei, intracellular bacteria and protein aggregates, respectively [29–35]. During selective autophagy the lipidated versions of hATG8s interact with selective autophagy receptors (SARs), e.g. Sequestosome-1 (SQSTM1, also known as p62) via their ATG8-family interacting motifs/LC3 interacting regions (AIMs/LIRs). The affinity between SARs and hATG8s is generally relatively low (dissociation constant in µM range) so that receptor di-, multi- or oligomerization is required to increase the avidity and to target the cargo efficiently for autophagy [36]. More than 20 SARs have been identified, which can be divided into soluble and membrane-associated SARs that either freely diffuse within the cytoplasm or are attached to the membrane of a particular cell organelle [37]. Among the soluble SARs, SQSTM1-like receptors contain an Ub-binding domain that enables them to interact with ubiquitylated target proteins. Hence, SARs provide specificity to the autophagic process in Ub-dependent or –independent ways [38]. Due to the nature of the proteolytic pathway, SARs are constantly degraded upon autophagy activation [37,39]. Autophagy can be seen as a stress response towards a plethora of stress stimuli although the connection between autophagy trigger and autophagy target often remains elusive [40,41]. Hence, it is largely unknown how or when a selective autophagy pathway is triggered and whether the SARs fulfill redundant or exclusive functions during the process.

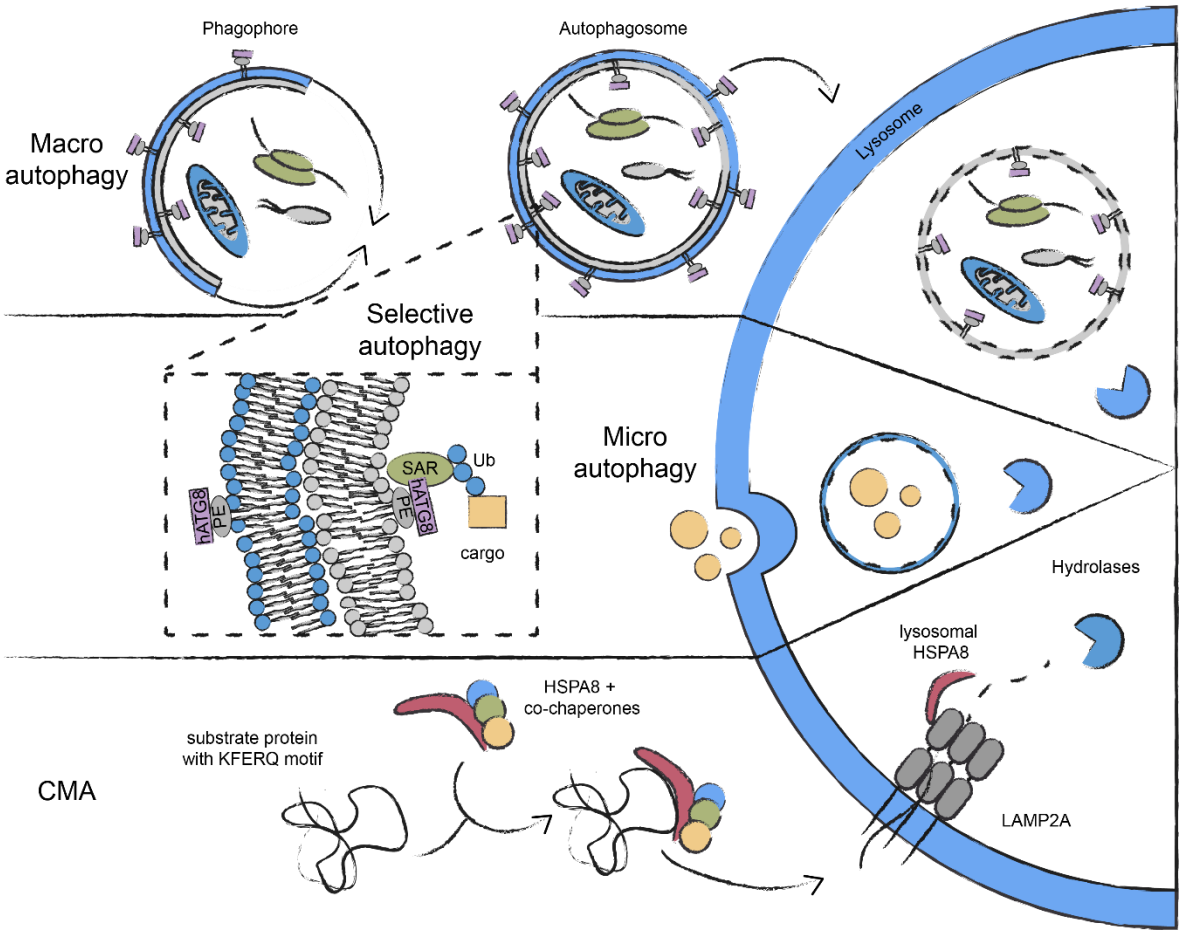

Figure 2: The three main autophagy pathways in mammals. Autophagosomes engulf cellular material and deliver it to the lysosome in macroautophagy. SARs mediate selective forms of macroautophagy where they interact with the (ubiquitylated) cargo and the hATG8s that are attached to the autophagosomal membrane by PE. In microautophagy, local invaginations of the lysosomal membrane lead to the engulfment of cellular material. In CMA target proteins with a KFERQ-like motif are recognized by the chaperone HSPA8. The target protein is transported across the lysosomal membrane with the help of LAMP2A and lysosomal HSPA8. The cargo is degraded in the lysosome by hydrolases. Adapted from Juretschke et al. [42].

Microautophagy describes a local invagination of the lysosomal membrane that leads to the direct uptake of cellular material [16]. It is capable of degrading large cellular structures, including mitochondria, peroxisomes and parts of the nucleus [43–45]. Hence, microautophagy can also be selective. The molecular determinants of microautophagy remain largely unknown, but might involve ATG proteins, the endosomal sorting complexes required for transport machinery and soluble N-ethylmaleimide-sensitive-factor attachment receptor proteins [46].

CMA relies on a chaperone complex formed around Heat shock cognate 71 kDa protein (HSPA8) that binds proteins and transports them across the lysosomal membrane into the lumen [16]. The translocation of the proteins through the lysosomal membrane is dependent on Lysosome-associated membrane glycoprotein 2A (LAMP2A) and the lysosomal fraction of HSPA8 . Proteins that are degraded via CMA possess a KFERQ-like pentapeptide motif, which allows HSPA8 to bind them. According to sequence analysis, KFERQ-like motifs are present in about 30-40% of the human proteome [47,48]. The identification of *bona fide* CMA target

proteins remains challenging as the KFERQ-like motif can be hidden or become active by different PTMs. CMA is independent of ATG proteins [48].

5.2.1 AUTOPHAGY INITIATION SIGNALING

Macroautophagy (hereafter referred to as autophagy) is under the control of the cell proliferation regulator mechanistic Target Of Rapamycin (mTOR) Complex 1 (mTORC1). It is composed of mTOR, Regulatory-associated protein of mTOR (RPTOR), DEP domain-containing mTOR-interacting protein (DEPTOR), Target of rapamycin complex subunit LST8 (MLST8) and Proline-rich AKT1 substrate 1 (AKT1S1) [49–52]. mTORC1 is localized in its active state at the lysosome where it regulates the metabolic state of the cell [53]. Information about amino acid availability, growth factor supply, energy status and oxygen level converge at mTORC1, which is why it is considered a cellular signaling hub [54]. When active, mTORC1 promotes the biosynthesis of lipids, nucleotides and proteins by phosphorylation of several downstream effectors such as p70S6 kinase 1 and members of the eIF4E binding protein family [55–58]. Inactivation of mTORC1 leads to its detachment from the lysosome and results in a cellular switch from anabolic to catabolic metabolism including the initiation of autophagy (Figure 3).

The major counter player of mTORC1 is AMP-activated protein kinase (AMPK), which promotes autophagy under hypoxic conditions and low energy levels [59,60]. It is a heterotrimeric protein complex composed of a catalytically active α-subunit and two regulatory subunits, β and γ. The γ-subunit can bind different adenine nucleotides and therefore measure cellular levels of ATP [61]. A high cellular ratio of AMP or ADP to ATP leads to AMPK activation resulting in the phosphorylation of the mTORC1 subunit RPTOR and members of the Uncoordinated-51-like kinase 1 (ULK1) complex, the apical kinase in autophagy signaling [62]. Phosphorylation of RPTOR via AMPK has an inactivating effect on the mTORC1 complex. Another signaling pathway via AMPK to inactivate mTORC1 is the activation of the heterotrimeric GTPase-activating protein tuberous sclerosis complex (TSC) consisting of TSC1, TSC2 and TBC1 domain family member 7 [63]. Activation of the TSC leads to its localization to the lysosome where it converts GTP-binding protein Rheb (RHEB) to the GDP-bound form. RHEB is an interactor of the mTORC1 complex at the lysosome and is required in the GTP-bound form to keep mTORC1 active. Inactivation of RHEB causes the re-localization of mTORC1 from the lysosome, which results in its inactivation [55,60]. AMPK can also be activated by upstream kinases liver kinase B1 (LKB1), Calcium/calmodulin-dependent protein kinase kinase 2 or Nuclear receptor subfamily 2 group C member 2 that phosphorylate the α-subunit on T172 [64–68]. Each AMPK subunit is encoded by multiple genes, which makes 12 distinct AMPK complexes possible suggesting tissue- and cell-specific functions [69].

The common downstream target of mTORC1 and AMPK is the protein complex ULK1 [70]. Particular phosphorylation sites on the subunits of the complex are regulated by mTORC1 and AMPK and can be used as a read-out for the cellular activity of autophagy. The ULK1 protein complex is composed of the serine/threonine kinase ULK1 or ULK2, ATG13, RB1-inducible coiled-coil protein 1 (RB1CC1, also known as FIP200) and ATG101 [70–73]. ULK1 has five

homologues of which ULK1 and ULK2 are considered to be involved in autophagy [74]. The loss of ATG genes such as ATG5 and ATG7 has been associated with neonatal lethality in mice [75]. This phenotype is only resembled when both kinases ULK1 and ULK2 are knocked-out, indicating partial redundancy of the kinases in mice [74]. In most cell lines, loss of ULK1 leads to a complete abrogation of autophagy highlighting its importance for the pathway. In the early steps of autophagy activation, the ULK1 complex forms punctate structures in close proximity to the ER, where it co-localizes with different autophagy-associated proteins, such as Vacuole membrane protein 1. Here, it phosphorylates downstream ATG proteins to start autophagosome biogenesis [76–78].

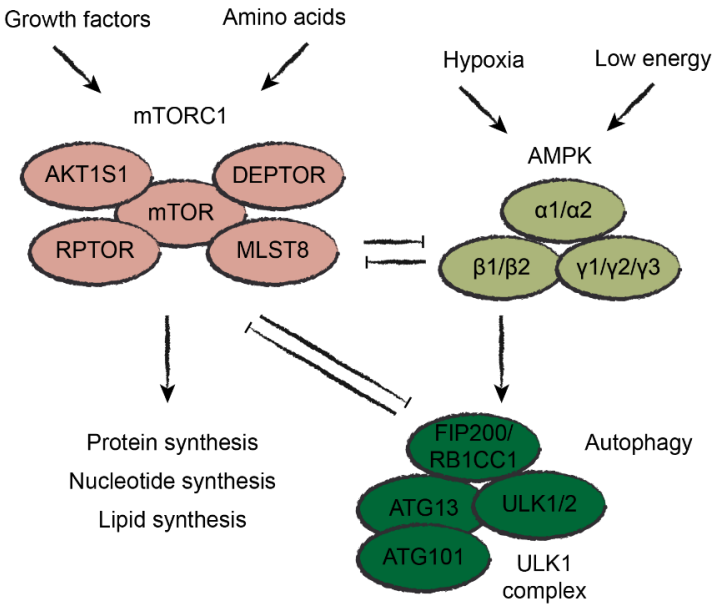

Figure 3: Regulation of the apical autophagy kinases. mTORC1 regulates anabolic and catabolic processes such as autophagy in response to nutrient availability. AMPK can inactivate mTORC1 via different pathways under hypoxic conditions or low cellular levels of ATP. The ULK1 complex is kept in active or inactive states by different phosphorylation events. Activation of the ULK1 complex promotes autophagy.

5.2.2 AUTOPHAGOSOME FORMATION AND THE AUTOPHAGIC MACHINERY

Groundbreaking work led to the identification of many ATG genes in yeast, which was awarded with the Nobel prize in 2016 [79–82]. Today, about 40 core ATG genes and proteins have been characterized in yeast and mammalian systems. The function of yeast and mammalian ATG proteins is relatively well conserved and the processes are very alike [16,83]. However, differences between yeast and human autophagy exist. First, the mammalian ATG protein family is expanded by several homologues, which indicates for a higher level of complexity in mammals [29]. Second, the mammalian omegasome, a cup-shaped ER-associated structure that gives rise to the phagophore, can form simultaneously at multiple sites at the ER, whereas yeast cells possess only one phagophore assembly site [84–86]. Third, instead of lysosomes, yeast have one large vacuole with which the autophagosomes fuse.

The core ATG proteins can be categorized into five different groups that fulfill specific functions during autophagosome biogenesis [83]. These are in mammals: the ULK1 complex, the class III phosphatidylinositol (PtdIns) 3-kinase (PtdIns3K) complex I, the UBL conjugation

machineries around the UBL hATG8s and ATG12, the phosphatidylinositol-3-phosphate (PtdIns3P) binding proteins of the WD repeat domain phosphoinositide-interacting protein (WIPI) family, ATG2A and ATG2B and the transmembrane proteins ATG9A and ATG9B. This machinery is triggered upon mTORC1 inactivation e.g. due to nutrient deprivation and starts with the formation of an autophagosome at the omegasome (Figure 4). The biogenesis of an autophagosome can be divided into initiation, nucleation, elongation and maturation. Its life cycle ends when it fuses with a lysosome [87].

The initiation requires the activated ULK1 complex (described above) that localizes to the ER, where it phosphorylates subunits of the second large autophagy protein complex, the PtdIns3K complex I (also known as VPS34/Beclin-1 complex). The latter consists of the lipid kinase Phosphatidylinositol 3-kinase catalytic subunit 3 (PIK3C3, also known as VPS34), its regulatory subunit Phosphoinositide 3-kinase regulatory subunit 4 (PIK3R4, also known as VPS15), Beclin-1 and ATG14L [88]. When active, the VPS34 complex phosphorylates PtdIns to PtdIns3P in the omegasome that starts the nucleation of a growing phagophore. PtdIns3P recruits many ATG factors that can bind phospholipids such as Zinc finger FYVE domain-containing protein 1 (ZFYVE1), ATG2A, ATG2B and the WIPI family proteins [85,89,90]. Recent studies suggest that ATG2A tethers the phagophore to the ER membrane where it transfers lipids with the help of WIPI family proteins into the nascent autophagic structure [91–93]. A consecutively supply of lipids is secured by the ATG9 system. ATG9A and ATG9B are the only transmembrane proteins of the core autophagy machinery. They are inserted in the membranes of vesicles that shuttle from the Golgi and the plasma membrane to the omegasome, where they eventually fuse with the phagophore to deliver membrane material [94,95].

PtdIns3P has been shown to promote the lipidation process of hATG8s via an UBL conjugation system [96]. Analogous to ubiquitylation of proteins, the UBL hATG8s are covalently attached to PE, which anchors them into the membranes of the phagophore and promotes its elongation to finally mature to a closed autophagosome [97]. The UBL conjugation system in autophagy is composed of ATG7, the E1 activating-like protein, ATG3, an E2 conjugating-like protein, and a protein complex formed by ATG5, ATG12 and ATG16L1, which functions as an E3 ligase-like protein. The latter complex is assembled itself via a second UBL conjugation system where the UBL protein ATG12 is covalently attached to ATG5 in a process involving ATG7 and the E2 conjugating-like protein ATG10 [25,98,99]. Prior to the lipidation via the UBL conjugation machinery, hATG8s undergo proteolytic cleavage at the C-terminus. This is conducted by the cysteine proteases ATG4A, ATG4B, ATG4C and ATG4D [100,101]. The lipidation is reversible and is also conducted by the ATG4 homologues. Here, ATG4D seems to be the main player to recover hATG8s from endolysosomal vesicles, which are then re-used for a newly forming phagophore [102,103].

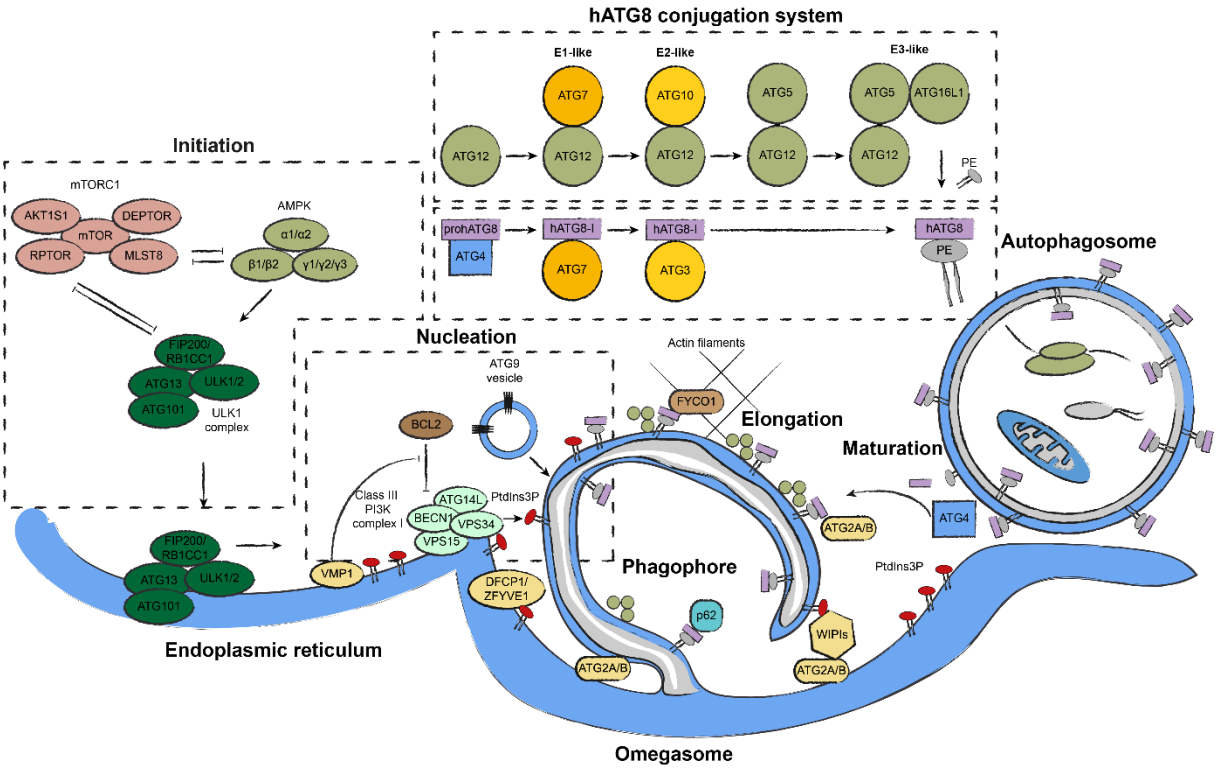

Figure 4: Autophagosome biogenesis. Initiation, nucleation, elongation and maturation are depicted along with the two UBL conjugation machineries for hATG8 lipidation. The role of important core autophagy proteins and complexes in autophagosome biogenesis and regulation is shown. The omegasome is indicated by accumulated PtdIns3P. Adapted from Mizushima et al. [2].

5.3 GENOME STABILITY AND THE DNA DAMAGE RESPONSE

The genome of a cell encodes the cellular proteome. It is duplicated in S-phase and equally distributed as chromosomes towards the cell poles in mitosis. Two genetically identical cells result from a completed round of cell division. Endogenous or exogenous threats, such as naturally occurring replication errors or chemotherapeutic treatment, can interfere with faithful cell division and cause mutations, intra-chromosomal breaks and aneuploidy with severe effects on genome stability [104,105]. To minimize serious aberrations in the DNA, dedicated DNA surveillance and maintenance mechanism have evolved, collectively designated as the DNA damage response (Figure 5) [104]. The DDR comprises a tailored set of DNA repair and signaling pathways that are initiated upon DNA damage detection to prevent further harm on the genome. Particular proteins detect DNA lesions in the nucleus, such as single- or double-stranded DNA breaks and trigger the DDR. PTMs of proteins including phosphorylation, ubiquitylation and poly-ADP-ribosylation (parylation) play a central role in driving and fine-tuning the DDR [106]. The apical protein kinases of the DDR Ataxia telangiectasia mutated (ATM) and DNA-dependent protein kinase (DNA-PK) are activated after DNA double strand breaks (DSBs) and Ataxia telangiectasia and Rad3-related protein (ATR) is activated after replication stress and DNA single strand breaks (SSBs). These serine/threonine kinases phosphorylate a plethora of proteins involved in DNA repair, chromatin remodeling and RNA metabolism as well as the checkpoint kinases

Serine/threonine-protein kinase Chk1 (CHK1) and Chk2 (CHK2) [107]. The integrated response of these phosphorylations is required for coordination of DNA repair with gene expression and proliferation to maintain genome stability in the nucleus. A signaling hub in the DDR is the tumor suppressor Cellular tumor antigen p53 (TP53, also known as p53), a transcription factor, that regulates cell proliferation, DNA repair, senescence, apoptosis and autophagy [108]. DNA damage-induced activation of p53 leads to the transcriptional upregulation of DNA repair factors and Cyclin-dependent kinase inhibitor 1 (CDKN1A, also known as p21), which promotes cell cycle arrest and senescence. Further, pro-apoptotic and ATG proteins are under the control of p53 [109,110]. Taken together, characteristic cellular consequences of the DDR is checkpoint activation to facilitate DNA repair, entrance into a senescent state or the induction of cell death- or cell survival-promoting programs such as apoptosis or autophagy.

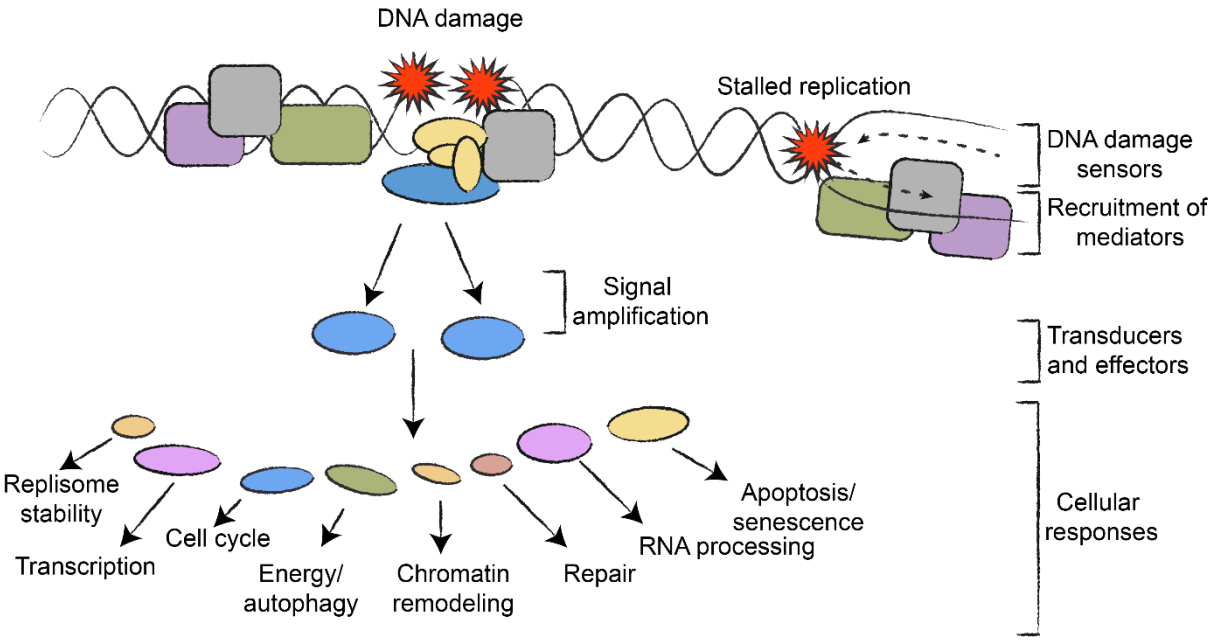

Figure 5: Model of the DDR. Genotoxic stress in form of DNA lesions or stalled replication forks are recognized by different sensor proteins. Recognition of the DNA damage activates a signaling cascade with impact on a multitude of cellular processes. Adapted from Jackson et al. [104].

5.3.1 DNA REPAIR MECHANISMS

Every cell of the human body encounters thousands of DNA lesions per day [111]. As the perturbations can have different causes, the types of lesions vary. These include base modifications, mismatches between bases, bulky adducts, inter-and intra-strand crosslinks, protein-DNA crosslinks and DNA single and double strand breaks (Figure 6). These lesions cannot be repaired by a single overarching repair machinery, but require specific mechanisms or the orchestrated interplay of several repair pathways to reinstall genomic stability. For example, oxidized, alkylated or deamidated DNA bases are corrected by base excision repair (BER), faulty inserted bases are exchanged by DNA mismatch-repair (MMR), ultra violet (UV) light-induced pyrimidine dimers (bulky adducts) are removed by nucleotide excision repair (NER) and inter-strand crosslinks are dealt by inter-strand crosslink repair (ICLR) [112–116]. DSBs are repaired by two major repair mechanisms, NHEJ and HR [117,118]. Genomic

perturbations, particularly in the DDR, are a major source for the development of human disorders such as premature aging and cancer [119]. Cells that are perturbed in HR, e.g. by the loss or downregulation of the Breast cancer type 1/2 susceptibility protein (BRCA1/BRCA2) genes, are highly dependent on NHEJ to remove DSBs. These cells are characterized by an increased mutation rate and genomic instability [120]. Cancer therapies try to exploit this instability and recent strategies focus on synthetic lethality [121]. One example is the targeted inhibition of Poly (ADP-ribose) polymerase 1 (PARP1), a nuclear protein that attaches poly (ADP-ribose) to many chromatin-associated proteins and which is involved in a variety of DNA repair mechanisms [122]. Hence, inhibition of PARP1 leads to an increased cell death in cells with dysregulated DNA repair pathways [123,124].

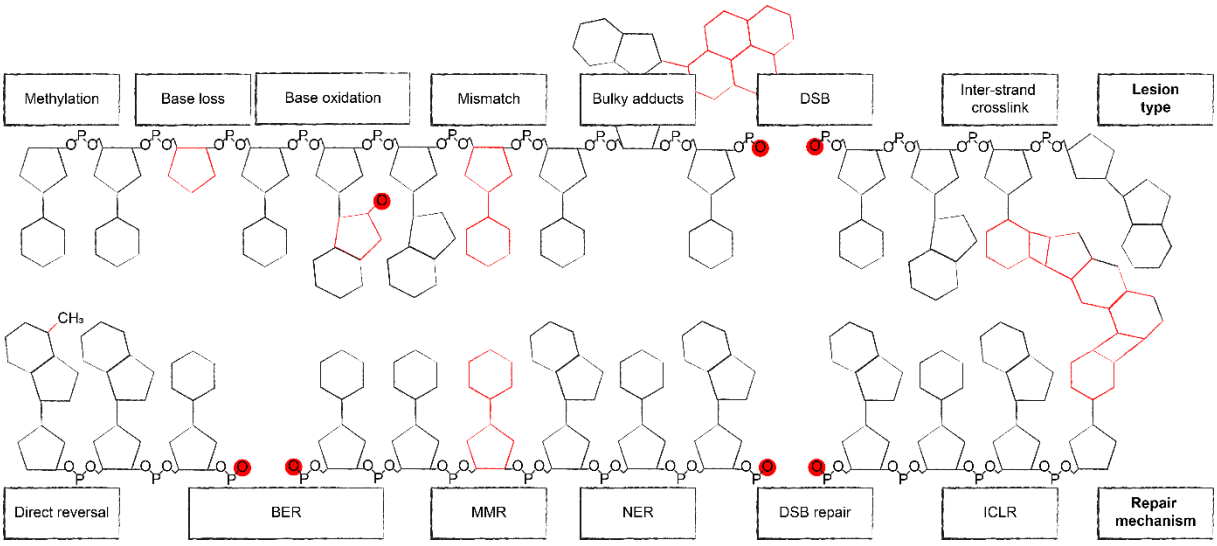

Figure 6: DNA lesions and repair mechanisms. The lesion type is indicated at the upper DNA strand. The adequate repair mechanism is named below. For example, methylation can be removed by direct reversal, whereas base loss or oxidation is repaired by BER. Adapted from Fang et al. [125].

5.3.2 DNA DOUBLE STRAND BREAK REPAIR

DNA double strand breaks are among the most severe DNA lesions as they have a high risk to cause loss of genetic information. They can result from unrepaired single strand breaks or from exposure to ionizing radiation (IR) or chemotherapeutic treatment, e.g. with topoisomerase poisons [105]. They also occur under physiological conditions, e.g. during meiotic recombination or in maturating lymphocytes during class-switch recombination [126]. DSBs are recognized by PARP1, which is one of the earliest events in DSB repair [127]. Its activation leads to the parylation of itself, histones and other chromatin associated proteins and causes the recruitment of other DNA repair proteins [128,129]. DSBs are repaired by NHEJ and HR (Figure 7). In NHEJ broken DNA ends are rapidly detected by the X-ray repair cross-complementing protein 6 (XRCC6, also known as Ku70)/XRCC5 (also known as Ku80) heterodimer, which forms the heterotrimeric kinase DNA-PK with the catalytic subunit of DNA-dependent protein kinase (DNA-PKcs) [130]. PARP1 might parylate DNA-PKcs to increase its activity, which increments the phosphorylation of DNA repair proteins such as the nuclease Protein artemis (DCLRE1C) that removes single nucleotides from DNA ends [131,132]. End

resection enables the ligation of the broken DNA ends, which is conducted by a ligase complex including DNA ligase 4 (LIG4) [133]. Due to the removal of nucleotides and the subsequent end joining of the DNA ends, NHEJ can be error-prone. NHEJ is not restricted to any of the cell cycle phases, but is primarily engaged in G1-phase.

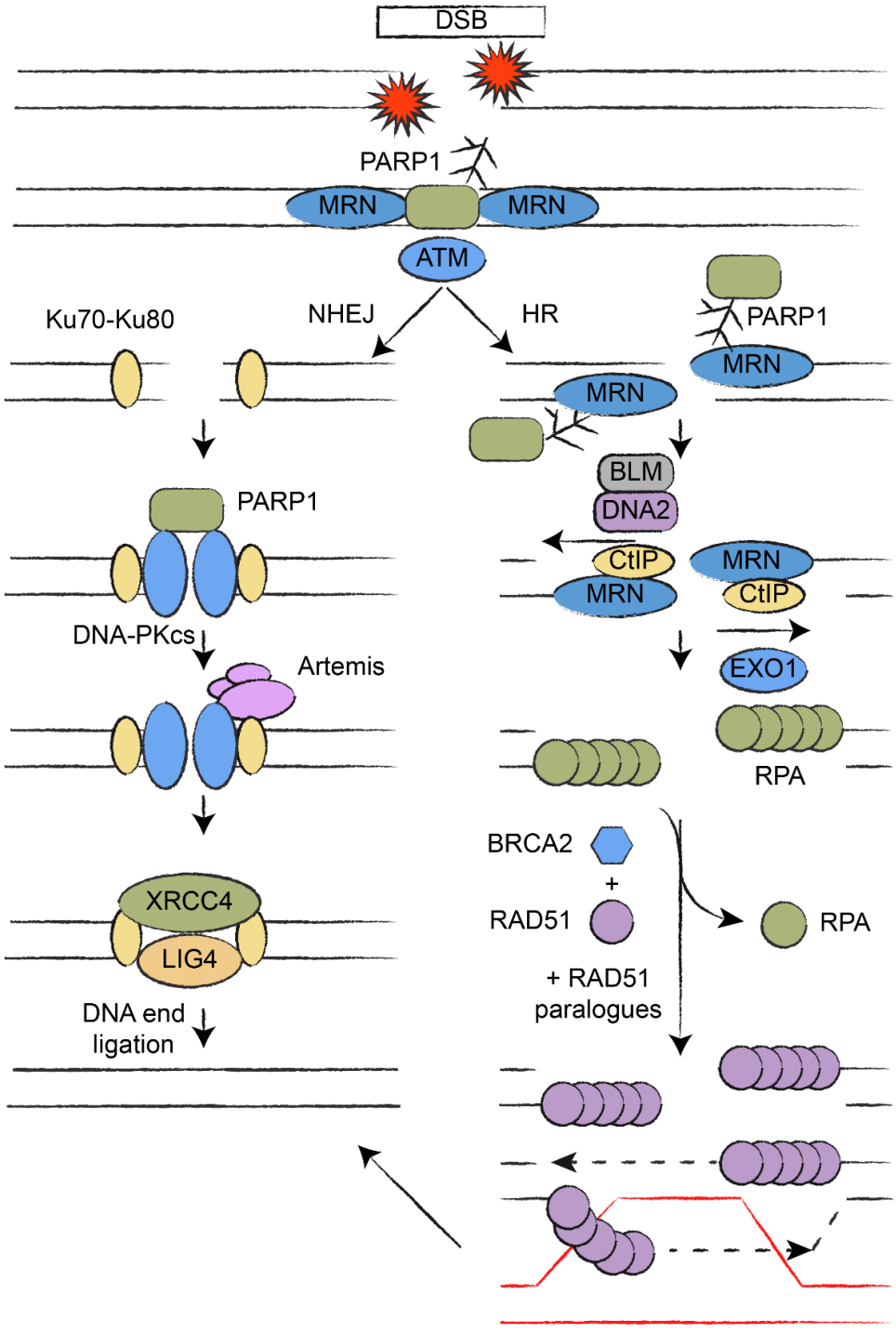

Figure 7: DSB repair by NHEJ and HR. A DSB is recognized by PARP1, which recruits the MRN complex and ATM. The latter phosphorylates a multitude of downstream proteins to initiate DSB repair. In NHEJ the Ku70-Ku80 heterodimer recruits DNA-PKcs to the lesion. PARP1 might increase the activity of the latter. The nuclease Artemis removes nucleotides from the DNA ends, which are finally ligated by LIG4. In HR, PARP1-recruited MRN complex promotes DNA end resection by a number of exonucleases such as BLM, DNA2, CtIP and EXO1. Single stranded DNA stretches are stabilized by RPA, which is later exchanged with RAD51 by the interplay of BRCA2 and RAD51 paralogues. Strand invasion into an unperturbed sister chromatid (red) occurs, which forms a D-loop that is finally resolved to form two unperturbed sister chromatids. Adapted from Schwertman et al. and Chaudhuri et al. [134,135].

As HR requires a template strand to repair faithfully DSBs, it is restricted to late S- and G2-phase of the cell cycle, where DNA replication has already been completed. In HR extended regions of single-stranded DNA (ssDNA) are generated by several nucleases that catalyze DNA end resection [136]. First, the MRE11-RAD50-NBS1 (MRN) complex is recruited to DSBs by PARP1, where it promotes resections on the DNA strands together with CtBP-interacting protein (CtIP) [137,138]. Resection of the DNA ends by CtIP engages the HR pathway. The MRN complex recruits ATM to the DSBs, which phosphorylates many proteins needed for their removal by HR. The resections are extended by Exonucleases 1 (EXO1) and Bloom syndrome protein (BLM)-DNA replication ATP-dependent helicase DNA2 (DNA2) and covered with Replication protein A (RPA), which stabilizes the ssDNA stretches [139]. BRCA2 and DNA repair protein RAD51 (RAD51) paralogues exchange RPA for RAD51 [140,141]. The RAD51-ssDNA recombinase filament executes homology search and strand invasion of the homologous template strand, which results in the formation of a displacement loop (D-loop). Resolvases finish the repair process by separating the D-loop and restoring unperturbed DNA strands. The third DDR kinase, ATR, is recruited to single stranded DNA via ATR-interacting protein ATRIP that binds to the RPA complex [142]. ssDNA is generated in response to replication stress as well as in intermediate steps during different DNA repair pathways. The DDR kinases DNA-PK, ATM and ATR function in similar ways and overlap in their substrates [107]. The nature of the DNA lesion determines their degree of activation [143].

5.3.3 DNA TOPI AND TOPII POISONS

Topoisomerases remove torsional stress originating from DNA helix supercoiling during biological processes such as DNA replication or transcription. They bind DNA and cleave the DNA phosphate backbone to untangle or unwound it and to re-seal the DNA backbone again. DNA topoisomerase I (TOP1) induces an intermediate nick into one strand of the DNA, which allows passing the other strand through the break. DNA topoisomerase II (TOP2) catalyzes a similar reaction, but cleaves both DNA strands, which results in an intermediate double strand break [144]. Chemical inhibitors of TOP1 and TOP2 are camptothecin (CPT) and etoposide (ETO), respectively. ETO and derivatives of CPT are frequently used in cancer therapy as they cause DNA damage. CPT binds TOP1 and DNA, which stabilizes the complex and traps TOP1 on the DNA without re-ligating it [145,146]. The DNA-protein crosslink that is covalently connected by a phosphodiester bond is designated as TOP1 cleavage complex (TOP1cc) [144]. When unresolved, TOP1ccs lead to conflicts with the replication and transcription machinery and result in DNA replication fork collapse and DSBs [147]. The cellular mechanisms that allow the removal of TOP1ccs are not entirely understood. The phosphodiester bond between TOP1 and DNA is known to be hydrolyzed by tyrosyl-DNA phosphodiesterase 1 (TDP1) [148,149]. However, TDP1 is hindered in assessing its substrate due to the TOP1cc structure, leaving the open question of how TOP1ccs are removed from chromatin. A recent study could show that the reticulophagy SAR Testis-expressed protein 264 (TEX264) can bind CPT-induced TOP1ccs and recruit the ATPase Valosin-containing protein (VCP, also known as p97) and the DNA-dependent metalloprotease SPRTN (SPRTN) [150]. The interaction of TEX264 with TOP1 was

partially dependent on small ubiquitin-related modifier 1 (SUMO1), an UBL modification. The authors propose a model, in which VCP re-arranges the TOP1cc, so that SPRTN can cleave it (Figure 8). This enables TDP1 to access the phosphodiester bond and remove TOP1 from DNA. TOP2 cleavage complexes induced by ETO treatment are believed to be resolved in a similar manner. Here, TDP1 is replaced by tyrosyl-DNA phosphodiesterase 2 [151,152].

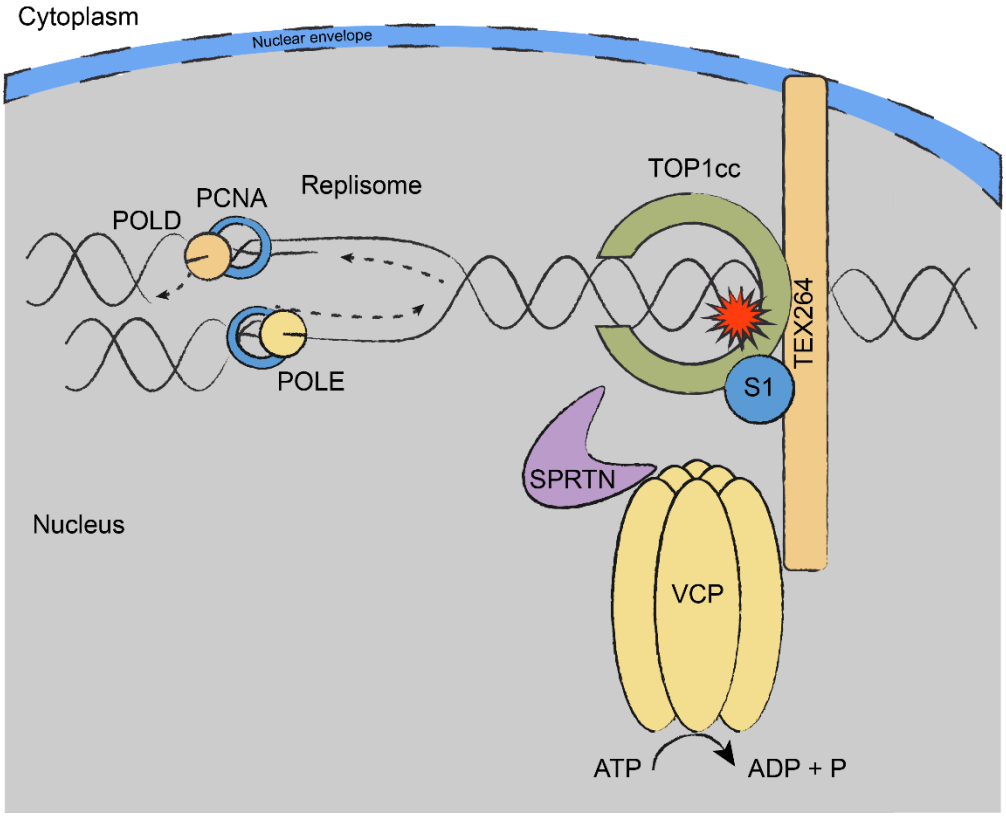

Figure 8: The role of TEX264 in TOP1cc removal. TEX264 is attached to the inner nuclear membrane. Upon formation of TOP1ccs, TEX264 can interact with TOP1 in a partially SUMO1-dependent manner. TEX264 recruits VCP and SPRTN that rearrange the TOP1cc allowing TDP1 (not shown) to cleave the phosphodiester bond between TOP1 and DNA. Unresolved TOP1ccs interfere with faithful DNA replication. Adapted from Fielden et al. [150]. S1: SUMO1.

5.4 DNA DAMAGE-INDUCED AUTOPHAGY

Autophagy can be stimulated by multiple perturbations such as starvation, hypoxia, increased concentrations of reactive oxygen species (ROS), bacterial invasion, viral infection and DNA damage [153–159]. Whereas starvation-induced autophagy promotes cell survival as an energy-saving mechanism, the physiological role of autophagy activation after genotoxic stress remains largely enigmatic. Moderate DNA damage is believed to induce pro-survival autophagy, whereas critical amounts of DNA damage are supposed to cause excessive autophagy resulting in ACD. The former is based on the idea that DNA repair might deplete cellular ATP and nucleotide pools that need to be replenished by the autophagy pathway [125,160]. The latter follows the hypothesis that autophagy can be an alternative cell death pathway, particularly in cancer cells with perturbed apoptosis mechanisms [17,161–163]. As autophagy is known to be a consequence of the DDR, the question arises which signaling events lead to its activation after genotoxic stress [104]. Although the DDR kinases and p53

have been associated with autophagy activation after DNA damage, the exact signaling events remain unresolved [153–155,164–166]. Another open question is whether DNA damage-induced autophagy compels the selective degradation of cell organelles or particular proteins, which would influence the cell's fate towards survival or cell death.

5.4.1 DNA DAMAGE TO AUTOPHAGY SIGNALING

Studies in budding yeast and higher eukaryotes have shown that DNA damage induces autophagy [167–170]. A first systematic study to identify proteins important for DNA damage-induced autophagy was performed in budding yeast [167]. The alkylating agent methyl methanesulfonate (MMS) that induces DNA replication stress was used to trigger autophagy [171]. As ATG11, an ATG protein required for selective autophagy in yeast, was needed for the MMS-induced pathway, the mechanism was termed Genotoxin-induced Targeted Autophagy (GTA). Other proteins that were identified as important signaling factors for GTA were Mec1 and Tel1 (yeast orthologues of ATR and ATM, respectively) and their downstream target Rad53 (yeast orthologue of CHK2). Interestingly, CHK1 was dispensable for GTA. Activation of autophagy was explained by the induction of the histone demethylase Rph1 (homologue of KDM4) by CHK2, which under non-perturbed conditions keeps ATG genes repressed. A genome-wide screen identified further, positive and negative regulators of GTA. One of the negative regulators, *PPH3* encodes the catalytic subunit of the PP4 phosphatase. The latter inhibits Rad53, which tempted the authors to reason that the hits of the screen affect DDR signaling.

FOXK proteins, transcription factors that repress ATG genes, are phosphorylated in response to cisplatin (CIS) and etoposide (ETO) treatment in human cells [172]. The signaling pathway is exclusively ATM-CHK2-dependent and results in the interaction of FOXK with 14-3-3-γ and subsequent nuclear exclusion. Consequently, ATG genes are no longer repressed and autophagosome biogenesis can start. The same study could show that KDM4A, the mammalian homologue of yeast Rph1, which had been associated previously with GTA, was dispensable for DNA damage-induced autophagy in human cells. Another study showed that DNA damaging agents such as CPT, doxorubicin (DOX), UV light and MMS also activate autophagy [166]. Interestingly, only UV light and MMS were able to trigger an ATR-CHK1-dependent interaction between TSC2 and Rho-related GTP-binding protein RhoB (RHOB), which caused their relocalization to the lysosome, where RHEB was inactivated and in turn, mTORC1 inhibited (Figure 9).

DNA-PKcs has been identified as a kinase that alters basal and ETO-induced autophagy in an siRNA-based screen performed in Michigan Cancer Foundation - 7 (MCF-7) cells [164]. Mechanistically, DNA-PKcs shall facilitate the activation of AMPK via its phosphorylation on the γ-subunit by LKB1. Although prior studies had reported a role for LKB1 in DNA damage-induced autophagy after IR and ETO, LKB1 itself was not among the top hits of the screen [173,174]. The role of DNA-PKcs in affecting autophagy was independent of XRCC5 suggesting that the association of DNA-PKcs with lysosomes (co-localization with about 20% LAMP2-

positive puncta) represented a DNA repair-independent function. The mechanisms underlying the relocalization of DNA-PKcs to the lysosome remained unresolved. Interestingly, several studies have also suggested functions for ATM outside DNA repair: ATM can trigger autophagy in response to glucose deprivation or ROS by activating LKB1-AMPK-TSC2 or via CHK2-Beclin 1 pathway [153,175,176].

PARP1 knockout (KO) or PARP1-inhibited mouse embryonic fibroblasts (MEFs) show impaired starvation- and DNA damage-induced autophagy suggesting a role of PARP1 in autophagy activation [177,178]. It was proposed that autophagy promotes cell survival after DNA damage as PARP1- and autophagy-deficient cells show an increased sensitivity to DNA damage [177]. Starvation can lead to increased cellular concentrations of ROS due to dysfunctional mitochondria. These elevated ROS levels might damage DNA and result in PARP1 activation. It has been shown that PARP1 can parylate the α-subunit of AMPK under starvation conditions, which leads to its nuclear export and autophagy activation. In line, parylation of the catalytic subunit of AMPK was prevented by chemical inhibition of PARP1 [179]. Poly-ADP-ribosylation polymerase (PARP) family proteins conduct parylation. They require nicotinamide adenine dinucleotide (NAD^+) for their catalytic activity. The activity of Sirtuin-1 deacetlyase (SIRT1) is also dependent on NAD^+. Accordingly, PARPs and SIRT1 compete for NAD^+ and regulate each other [125]. SIRT1-mediated deacetylation of autophagy-associated proteins can promote autophagy and is required for the nuclear export of hATG8s [180–182]. As PARP1 is considered to have a higher affinity towards NAD^+ compared to SIRT1, DNA damage-induced parylation might prevent SIRT1 activity, hence autophagy [183]. Given that PARP1 activity reduces cellular ATP (probably due to energy-consuming chromatin remodeling) and NAD^+ levels in response to DNA damage, autophagy might be a consequence of this depletion and be engaged to later time points, when SIRT1 has access to NAD^+ [184].

Alternative autophagy (also known as Golgi-membrane-associated degradation pathway) is a pathway that was discovered in yeast and mammalian cells by the Shimizu lab [185,186]. The autophagic vesicles in alternative autophagy derive from Golgi membranes. Different stimuli such as DNA damage lead to a reduction of Golgi associated phosphatidylinositol 4-phosphate, which causes structural rearrangements of the Golgi apparatus and initiates alternative autophagy. Substrates of alternative autophagy are accumulated and undelivered proteins such as insulin granules and ceruloplasmin or entire cell organelles such as mitochondria during erythrocyte differentiation [187–189]. Alternative autophagy is independent of those ATG proteins involved in the Ub-like conjugation system of the hATG8 and the ATG9 system, but depends on ULK1 and VPS34 complexes that mediate autophagosome initiation and nucleation [186]. The Shimizu lab reports ULK1-S746 phosphorylation by RIPK3 as an important marker for alternative autophagy, which also requires ULK1 dephosphorylation by PPM1D at S637 [190,191]. However, they could show that PPM1D-mediated dephosphorylation of ULK1 is needed for both (regular and alternative) DNA damage-induced autophagy pathways. Other proteins involved in alternative autophagy are p53, DRAM1, RAB9

and WIPI3 [186,189,192]. Whether the DDR kinases are involved in upstream signaling of this alternative autophagy is unknown.

The signaling pathways leading to DNA damage-induced autophagy described so far include either mTORC1 inhibition or direct phosphorylation of transcription factors that activate autophagy by different kinases including ATM, ATR, DNA-PKcs, CHK1 and CHK2.

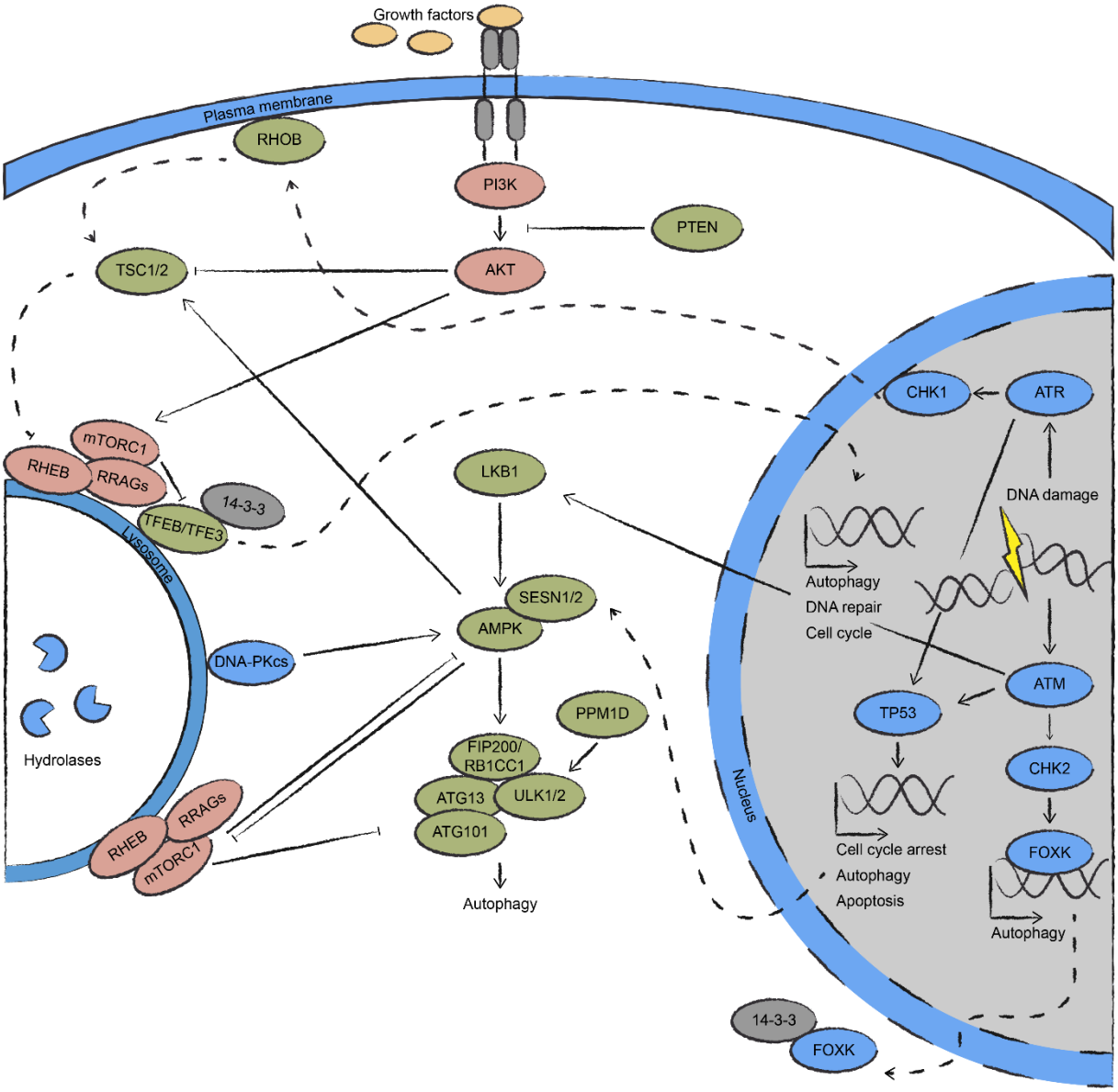

Figure 9: Signaling pathways for DNA damage-induced autophagy. Genotoxic stress induces p53-mediated gene expression of ATG genes and the ATM-CHK2 and ATR-CHK1 signaling axis. The former leads to nuclear exclusion of FOXK by 14-3-3, which results in ATG gene expression. The latter axis leads to relocalization of RHOB-TSC2 to the lysosome, which inactivate RHEB and mTORC1. Inactivation of mTORC1 results in translocation of TFEB/TFE3 into the nucleus to promote p53-dependent expression of ATG genes. DNA-PKcs and LKB1 phosphorylate AMPK and promote autophagy. The ULK1 complex is activated by AMPK, which initiates autophagosome biogenesis. PTEN counteracts PI3K-AKT signaling and relocalizes to the nucleus in an ATM-dependent manner to induce ATG gene expression. PPM1D dephosphorylates ULK1 prior to DNA damage-induced autophagy. Proteins in green/red are autophagy-promoting/suppressing factors, respectively. 14-3-3 has ambivalent effects and is grey. Proteins in blue are considered to fulfill nuclear functions. Adapted from Juretschke et al. [42].

5.4.2 TRANSCRIPTIONAL REGULATION OF DNA DAMAGE-INDUCED AUTOPHAGY

The list of transcription factors regulating ATG gene expression is constantly growing. However, the transcriptional regulation of ATG genes after genotoxic stress is under the control of p53 (Figure 9). First, it was shown that ETO and IR initiated autophagy in a p53- and TSC1/2-dependent way [193,194]. Following studies revealed that p53 activation led to the systematic transcriptional upregulation of ATG genes [155]. These are involved in different stages of catabolic process, including apical kinases, members of the Ub-like conjugation system and lysosomal proteins. Interestingly, there have been contradicting studies on the role of p53 on autophagy. However, today, it is clear that p53's impact on autophagy is context- and largely localization-dependent. Whereas transcriptionally active nuclear p53 promotes autophagy in response to stress, cytoplasmic p53 can inhibit autophagy by binding RB1CC1, which probably interferes with ULK1 complex-dependent autophagosome biogenesis [195–197]. Interestingly, cancer cells that are devoid of p53 or express a mutated version of p53 can activate autophagy after DNA damage by ATM-dependent phosphorylation of PTEN [198]. Phosphorylation leads to the nuclear translocation of PTEN, where it might activate JUN, a known regulator of ATG genes. Other members of the p53 family, p63 and p73, have also been connected to ATG gene upregulation in response to DNA damage [155].

TFEB, TFE3, TFEC and MITF are the members of the microphthalmia family of transcription factors. They were recently identified as regulators of lysosomal and ATG gene expression. Although they share many common target genes, KO mouse models show different phenotypes, which suggests that they cover different purposes [199]. Under nutrient-rich conditions, TFEB and TFE3 are localized at the lysosome, where they interact with Ras-related GTP binding proteins (RRAGs). They are phosphorylated by mTORC1, which enables 14-3-3 proteins to bind them and to prevent their translocation into the nucleus [200,201]. Inactivation of mTORC1 causes their release from 14-3-3 binding and enables TFEB and TFE3 to initiate the expression of lysosome and ATG genes [202].

DNA damage activates TFEB and TFE3 in a p53- and mTORC1-dependent way [203]. RNA-sequencing data from TFEB/TFE3 double knockout (DKO) cells that were treated with ETO revealed that p53-regulated transcripts were significantly downregulated compared to wild type cells. The E3 ubiquitin-protein ligase Mdm2 is the major regulator of p53. Its protein levels were increased in TFEB/TFE3 DKO cells after ETO treatment, which led to reduced levels of p53. Hence, the authors concluded that TFEB and TFE3 amplify and sustain the expression of p53-dependent genes after DNA damage [203].

As mentioned above, FOXK proteins are inactivated in response to DNA damage, which enables the expression of ATG genes [172]. Other transcription factors are also known to be involved in autophagy regulation [204]. Whether some of these factors can also be activated by DNA damage is currently unknown, as they have mostly been studied in the background of nutrient deprivation or chemical inhibition of mTORC1.

5.4.3 DNA DAMAGE-INDUCED AUTOPHAGIC CARGO

One hypothesis in the field is that DNA damage-induced autophagy is required to refuel deoxynucleotide triphosphate (dNTP) pools that were emptied for DNA repair [160]. RNA- or DNA-containing cell organelles, such as ribosomes, mitochondria or factors that negatively regulate dNTP biosynthesis could therefore represent potential targets of autophagy (Figure 10). The cell cycle regulates the biosynthesis of dNTPs, which peaks during S-phase, when enzymes such as ribonucleotide reductase (RNR) that form deoxyribonucleotides from ribonucleotides are upregulated [205]. In line with this, a study in budding yeast could show that autophagy regulates the levels of Ribonucleoside-diphosphate reductase large chain 1 (RNR1, orthologue of human RRM1) after genotoxic stress [206]. The large subunit of the RNR complex is composed of different homo- or heterodimers that have different catalytic activities. The authors reasoned that degradation of RNR1 would favor the assembly of the large subunit based on Ribonucleoside-diphosphate reductase large chain 2 (RNR3) and RNR1 heterodimers that show synergistic increase of activity compared to RNR3 homodimers [207]. Hence, dNTP biosynthesis would be balanced by autophagy-mediated RNR1 degradation after DNA damage. As mentioned above, MMS-treatment was shown to induce GTA in yeast, an ATG11-dependent, hence selective type of autophagy [167]. Although experiments with GFP-tagged proteins from different subcellular compartments (reporters for mitophagy, pexophagy, reticulophagy, nucleophagy, ribophagy and aggrephagy) were performed, no specific cargo was detected for GTA. Whether RNR1 is degraded in an ATG11-dependent fashion was not assessed.

Recent publications attributed a more direct role to autophagy in DNA repair. Loss of autophagy, led to the nuclear accumulation of p62, which caused the proteasomal breakdown of nuclear FLNA and RAD51, proteins that are involved in the repair of DSBs by HR [208,209]. Similarly, it was shown that loss of autophagy caused perturbed activity of the Ub E3 ligase RNF168 due to elevated levels of p62. Under physiological conditions RNF168 ubiquitylates histones for the recruitment of DNA repair proteins to their place of action [210]. In contrast, another study suggested that the effect on RNF168 was a consequence of decreased autophagic clearance of USP14, which is a regulator of RNF168, rather than an inhibitory effect due to the accumulation of nuclear p62 [211].

It has been reported that mouse embryonic fibroblasts (MEFs) devoid of autophagy show increased proteasomal degradation of CHK1 [212]. Downregulation of CHK1 in these cells led to perturbed ATR-CHK1 signaling that would be required for repair of DSBs by HR. Hence, autophagy-deficient MEFs were highly dependent on NHEJ to remove DSBs [212]. A study with a similar experimental design in MEFs came to different results. Here, DNA damage-induced CMA was reported that caused the selective degradation of (p)CHK1 [168]. MEFs devoid of CMA showed decreased survival rates after genotoxic stress due to the dysregulated phosphorylation and hence perturbed complex formation of the CHK1 target MRN.

Another target of autophagy has been suggested in mammalian cells. Genotoxic stress induced by UV light, MMS or ETO has been associated with mitophagy [166,193]. Interestingly, changes in the mitochondrial network have been reported in response to CPT, which has also been shown to inhibit mitochondrial TOP1 *in vitro* [213–215]. However, mitochondrial DNA damage and hence mitophagy induced by agents such as CPT is only likely with prolonged treatment duration due to limited mitochondrial permeability [216]. Whether DNA damage-induced mitophagy promotes cell death or cell survival depends probably on the severity and the duration of the genotoxic stress. UV light and MMS treatment have been reported to activate a signaling pathway that engages ATR-CHK1-mediated and RHOB-dependent mitophagy to promote cell death [166]. The same study demonstrated CPT- and DOX-induced autophagy, which was independent of RHOB. The equitoxicity of the treatments was not compared, but it remains plausible that RHOB-dependent autophagic cell death was triggered by strong DNA damage, whereas moderate DNA damage resulted in RHOB-independent pro-survival autophagy. A different study showed that about 50% of p53-positive ETO-treated cells initiated mitophagy [193]. Interestingly, p53-negative cells that were treated with ETO triggered mitophagy in only below 10% of the cells, which corroborates that p53 is crucial for DNA damage-induced autophagy, but which is also indicative for p53-independent pathways. Of note, ATM has been associated with mitochondria and has been shown to orchestrate mitophagy induced by spermidine, which could indicate that the DDR kinase is engaged for mitophagy in response to DNA damage as well [217,218]. Another study showed that PEX5 can recruit ATM to peroxisomes through a PEX5-binding sequence to induce pexophagy [154]. This could suggest that similar mechanism might exist for the recruitment of ATM to other cell organelles. DNA damage-induced cytoprotective autophagy has been reported in thymocytes. Here, ETO and IR treatment led to PPM1D-dependent autophagic degradation of the pro-apoptotic protein Phorbol-12-myristate-13-acetate-induced protein 1 (NOXA), probably by the interaction of its LIR domain with LC3 [191].

Several forms of nucleophagy and nucleoporinophagy have been reported in budding yeast [43,219–223]. Physiologically, nucleophagy is known to occur in humans during epidermal differentiation [34]. Further, a perturbed cell cycle, due to exogenous DNA damage or oncogene activation, can promote mis-segregation of DNA during cell division. This can cause the formation of micronuclei (MN) that consist of chromatin surrounded by its own nuclear envelope. MN have recently been associated with selective autophagy [224]. Thereby, the nuclear lamina protein Lamin-B1 (LMNB1) can directly be bound by LC3 to direct the MN into the autophagic vesicle [225,226]. ATG proteins were associated already earlier with MN [227]. However, only few MN (about 2-5%) showed co-localization with the marker protein LC3.

Damaged nuclear DNA accumulated as buds or small speckles in the cytoplasm of cells devoid of autophagy or the lysosomal nuclease Deoxyribonuclease-2-alpha, which indicates a role for autophagy in the removal of extranuclear DNA [228,229]. In line with this, it has been shown that the DNA-sensing Cyclic GMP-AMP synthase (CGAS)-Stimulator of interferon genes protein (STING) pathway promotes the removal of DNA damage-induced cytoplasmic DNA in an

autophagy-dependent fashion [230]. Mechanistically, LC3 lipidation is promoted by STING that relocalized to the endoplasmic reticulum-Golgi intermediate compartment upon activation. The surveillance of MN has also been associated with the CGAS-STING pathway, suggesting that CGAS-STING-mediated autophagy is crucial to preserve genomic stability by the removal of extranuclear chromatin fragments or micronucleated DNA [224,228,230–232]. This was recently confirmed by a study that identified CGAS as a SAR for the LC3-mediated degradation of MN via selective autophagy [233].

Moreover, it has been shown that DNA and RNA molecules can be taken up and be degraded by lysosomes [234–236]. The mechanism requires ATP and is dependent on the lysosomal transmembrane proteins LAMP2C and SID1 transmembrane family member 2 (SIDT2) [237,238]. Further, LAMP2C and SIDT2 show specificity towards guanosine-containing polymers of deoxy-/ribonucleotide triphosphates, which they bind by arginine-rich motifs in the cytoplasm [239,240]. The authors pointed out that repeated guanosine-rich DNA stretches can form G-quadruplexes and that such secondary structures in DNA or RNA could mediate the lysosomal uptake by binding of LAMP2C or SIDT2 [236].

Recently, it was reported that cells undergoing oncogenic transformation due to disabled Retinoblastoma-associated protein and p53 pathways induced a strong autophagic response towards damage in telomeric DNA [163]. Telomeric DNA damage in cells with functional autophagy led to elevated levels of cytoplasmic DNA species in the form of nucleoplasmic bridges, MN and cytoplasmic chromatin fragments (in about 50% of the cell population), which were observed to much lower levels in IR-treated cells (in about 5-10% of the cell population) with intrachromosomal DNA damage. Whereas autophagy-proficient cells activated autophagy based on the CGAS-STING pathway, which was followed by mitotic catastrophe and cell death, autophagy- or CGAS-STING-deficient cells continued to proliferate and bypassed replicative crisis. Of note, ATG proteins have been associated with mitotic catastrophe before: it has been reported that ETO and CIS treatments can lead to Focal adhesion kinase 1-dependent proteasomal degradation of ATG3. However, when ATG3 degradation was inhibited, BAG family molecular chaperon regulator 3 interacted with ATG3 and promoted mitotic catastrophe[241]. Further, it was demonstrated that sub-lethal doses of ETO and CIS led to the upregulation and translocation of ATG5 into the nucleus, where it interacted with Baculoviral IAP repeat-containing protein 5 (BIRC5), a member of the chromosomal passenger complex (CPC). Consequently, Aurora kinase B, another member of the CPC and binding partner of BIRC5, mis-localized, resulting in increased cell death [242].

In summary, CGAS-STING activation promotes autophagy to remove MN and cytopolasmic DNA species derived from genotoxic stress. However, telomeric DNA damage triggers a CGAS-STING-dependent autophagy-pathway that leads to mitotic catastrophe in cells undergoing oncogenic transformation. Further, DNA damage-induced autophagy can lead to the selective degradation of distinct proteins such as RNR1, USP14, (p)CHK1 and NOXA, which influences

directly or indirectly DNA repair and cell survival. The genotoxic induction of mitophagy has mostly been associated with cell death.

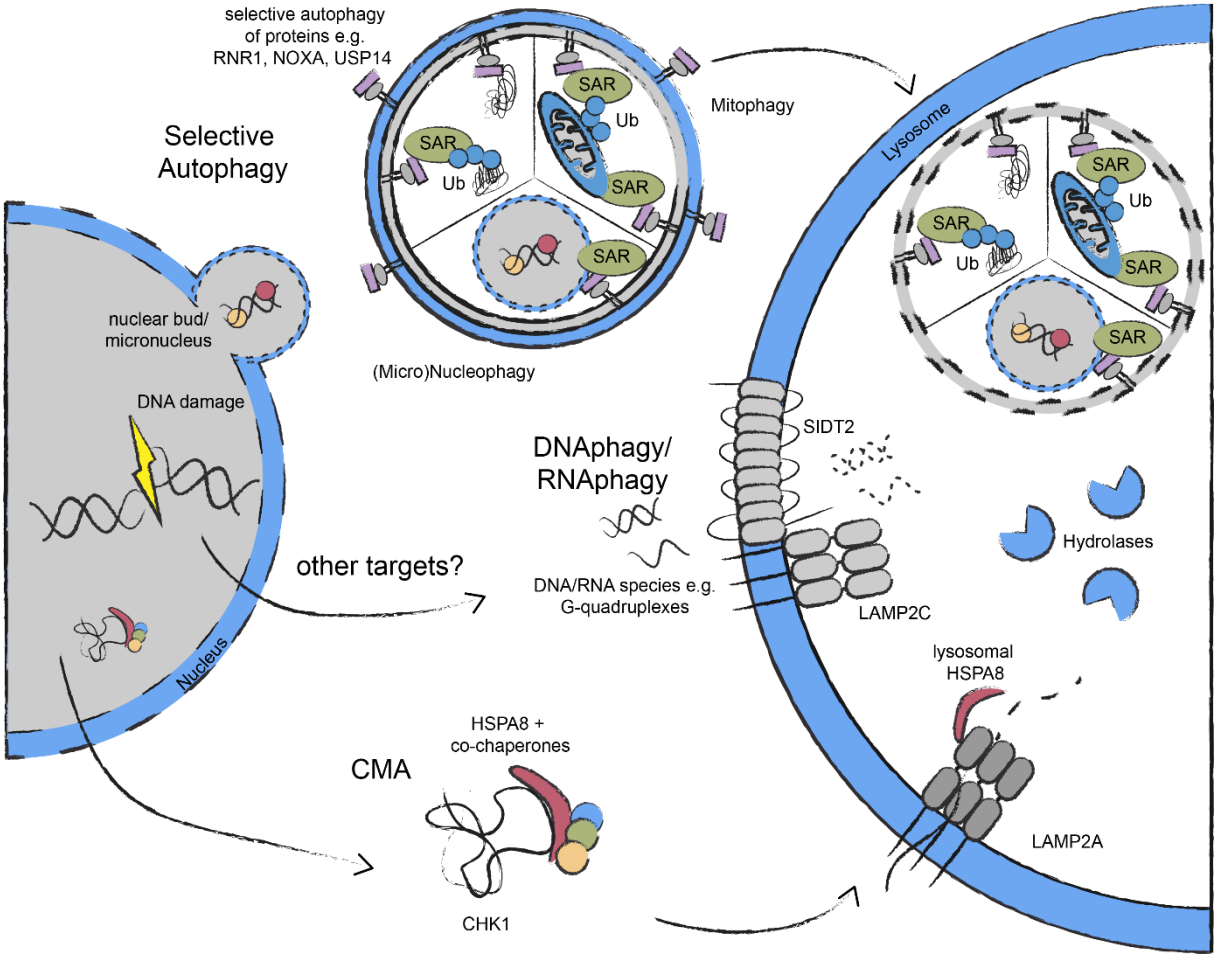

Figure 10: The potential targets of the autophagy response towards DNA damage. Genotoxic stress can active selective forms of autophagy leading to the targeted sequestration of specific proteins (e.g. NOXA and USP14 in mammals and RNR1 in yeast), of mitochondria and of micronuclei (including LMNB1 and CGAS). CHK1 is regulated by CMA. Extranuclear DNA/RNA might be degraded in a LAMP2C/SIDT2-dependent manner by the lysosome. Adapted from Juretschke et al. [42].

5.4.4 METHODS TO VALIDATE AUTOPHAGIC CARGO

Classical approaches to validate autophagosomal cargo involve the use of autophagy inhibitors, which enable to block autophagic flux. Their use allows recording the time-dependent increase of the signal of the cargo of interest, detectable e.g. via Western blotting or confocal microscopy [243]. Widely used chemical inhibitors are bafilomycin A_1 (BafA) and chloroquine. These chemicals target the lysosomal Vacuolar H^+-translocating ATPase (V-ATPase), which prevents the acidification of the lysosome. Consequently, lysosomal hydrolases become less efficient. Further, BafA and chloroquine inhibit the fusion capability of the lysosome with other vesicles preventing maturation of autophagosomes to autolysosomes [244–246]. Inhibitors of phosphoinositide 3-kinases (PI3Ks, also known as PtdIns3Ks), such as wortmannin (targets all classes of PtdIns3Ks) and 3-Methyladenine

(targets class I and III PtdIns3Ks) result in nonspecific autophagy inhibition due to suppression of the VPS34 complex [247–249]. Since these inhibitors can also target other kinases e.g. members of the PI3K-related kinases (PIKKs) such as ATM and mTOR, caution is needed when interpreting results [249–251]. Alternatively, combinations of protease inhibitors are used such as the aspartyl protease inhibitor Pepstatin A with the membrane-permeable cysteine protease inhibitor trans-epoxysuccinyl-L-leucylamido-(4-guanidino)butane (E-64) D that block the activity of subsets of lysosomal hydrolases [252,253]. To confirm the results obtained from inhibitor studies ATG KO cell lines can be used to shut down autophagy. Here, KOs in ATG7 or ATG5 are widely used as they are part of the UBL conjugation machinery and do not possess redundant isoforms [210,212,253,254]. SiRNA-mediated knockdown of ATG proteins has been reported to insufficiently block the autophagic flux and might therefore turn out inefficient at least in some cell lines [22,254]. Cycloheximide (CHX) chase experiments are also an option to validate autophagosomal cargo in combination with aforementioned inhibitors or cell lines. CHX inhibits protein synthesis, so that autophagy-regulated proteins would accumulate compared to UPS-regulated proteins in the background of autophagy inhibition. A potential caveat is here that autophagy is considered to regulate rather long-lived proteins, which might exclude CHX chase experiments for their validation due to cytotoxic long-term effects. Here, radioactive pulse-chase experiments might be an alternative [255,256]. Historically, transmission electron microscopy (TEM) is a powerful method to identify characteristic cell organelles such as autophagosomes with their two lipid bilayers [257]. Non-selective and selective sequestration of cytoplasmic material or cell organelles such as mitochondria or the ER can be detected. However, morphological changes during autophagy are quite dynamic, which complicates classification of discrete vesicles along the process [258]. Immuno-electron microscopy combines TEM with antibodies that are labeled with gold particles. Hence, the localization of proteins can be visualized at the ultrastructural level by generating an electron-dense label at their position [259,260]. To systematically analyze autophagic cargo mass spectrometry (MS)-based proteomics can be engaged. A number of studies employed mass (MS)-based proteomics to mammalian cells under basal, starvation- or rapamycin-induced conditions [261–263]. Most of these approaches relied on the enrichment of autophagosomes by gradient ultracentrifugation prior to their analysis by quantitative MS. A different strategy was developed by the Behrends lab that took advantage of a fusion protein of ascorbate peroxidase 2 (APEX2)-LC3 allowing *in vitro* biotinylation of autophagosomal cargo [45,264]. A systematic study profiling the autophagic cargo after genotoxic stress is still missing. Taken together, a set of methods exist to validate *bona fide* autophagic cargo. Due to the individual caveats of the methods, but also of the protein of interest, it is recommended to acquire solid data by a combined use of them [243].

5.5 QUANTIFICATION METHODS IN MS-BASED PROTEOMICS

MS-based proteomics allows systematically identifying and quantifying proteins from biological specimen such as cell culture or tissues [265]. In ‘bottom-up’ proteomics proteins are usually extracted from their specimen and digested by proteases such as trypsin [266,267].

To decrease the complexity of the sample, the generated peptides are often separated by reversed-phase liquid chromatography (LC) before they are directed via different methods, such as electrospray ionization or matrix-assisted laser desorption ionization, in form of peptide ions into a mass spectrometer [268–270]. Inside the device, ionized peptides are measured as a ratio of mass over charge (*m/z*) [271]. State of the art mass spectrometer pick automatically among the most intense ionized peptides from the top N parent ions (MS1 level) and subject them for fragmentation into a high collision induced fragmentation cell, which allows determining their primary amino acid structure (MS2 level) [271,272]. Tailored software enables identification of the protein(s) that were the origin of the measured parent and fragment ions, which is represented as a protein group [273–275].

Depending on the experimental design and workflow, different quantification techniques have its advantages. In general, label-free quantification (LFQ) is discriminated from quantification methods that are based on chemical labeling or metabolic labeling of amino acids [276]. As LFQ is independent of expensive chemicals or isotope-labeled amino acids it is the most cost efficient method. However, it is sensitive towards batch effects and requires therefore high consistency in sample preparation and stable performance of the LC-MS [277]. A common chemical label are tandem mass tags (TMT), which are added to the samples on the peptide level [278]. Chemical labeling has the advantage that it allows reliably to quantify samples from specimen that require complicated sample preparation, which would exclude LFQ. Further, it can be applied, where metabolic labeling methods are not suitable, such as in samples derived from tissues or complete organisms. Another advantage of recent chemical labeling methods is that it allows for multiplexing of many conditions, so that different treatments can directly be compared in replicates [279]. A major drawback of chemical labeling by TMT is its cost, which exceed the costs of LFQ and metabolic quantification methods [280]. Using TMT, obstacles in quantification may appear when more than one peptide was subjected for fragmentation causing co-isolation interference. This issue can be solved by MS3, but requires expensive tribrid instruments [281].

The quantification approach that I have relied on for my work is stable isotope labeling by amino acids in cell culture (SILAC) [282]. The method is based on naturally occurring isotopes of carbon, nitrogen and hydrogen that when enriched can be incorporated into amino acids such as arginine (R) and lysine (K). These amino acids complete the cultivation medium of the cells that lack the natural amino acids without enriched isotopes [283]. Hence, the cellular metabolism will slowly lead to the almost entire labeling of the proteome with isotopically labeled amino acids. One advantage of SILAC is that the labeling process takes place on the cellular level, which results in the lowest variation between samples compared to LFQ or labeling by chemicals [266]. Disadvantages are that only few conditions can be tested in parallel, meaning that there are combinations of isotopically labeled amino acids that result in SILAC media with virtually no isotopes (designated as ‘light’ condition) and SILAC media with heavy isotopes (designated as ‘heavy’ condition). A third SILAC medium contains isotopically labeled amino acids that are less heavy compared to the ones used in ‘heavy’ SILAC medium

(designated as 'medium' condition). Finally, the same peptide that was labelled in the three different SILAC media will cause peaks with different *m/z* as the mass of the peptide is shifted according to the respective isotopically labeled amino acids [266]. This allows quantifying SILAC ratios between the peptides from the different SILAC conditions. These ratios are relative to each other and do not allow for absolute quantification of protein numbers. An obstacle is here that quantification is only successful, when for each SILAC condition a signal was detected. Otherwise, no ratio can be built and a protein group might be identified, but not quantified.

A major advantage of SILAC is that the different conditions can be mixed in equal shares on the cell or protein level, which reduces the sample number to one (Figure 11). The earlier the mixing, the lower will be the risk of unwanted effects on the individual SILAC condition that could compromise quantification [276]. This makes SILAC the method of choice when workflows require a high demand of hands-on time.

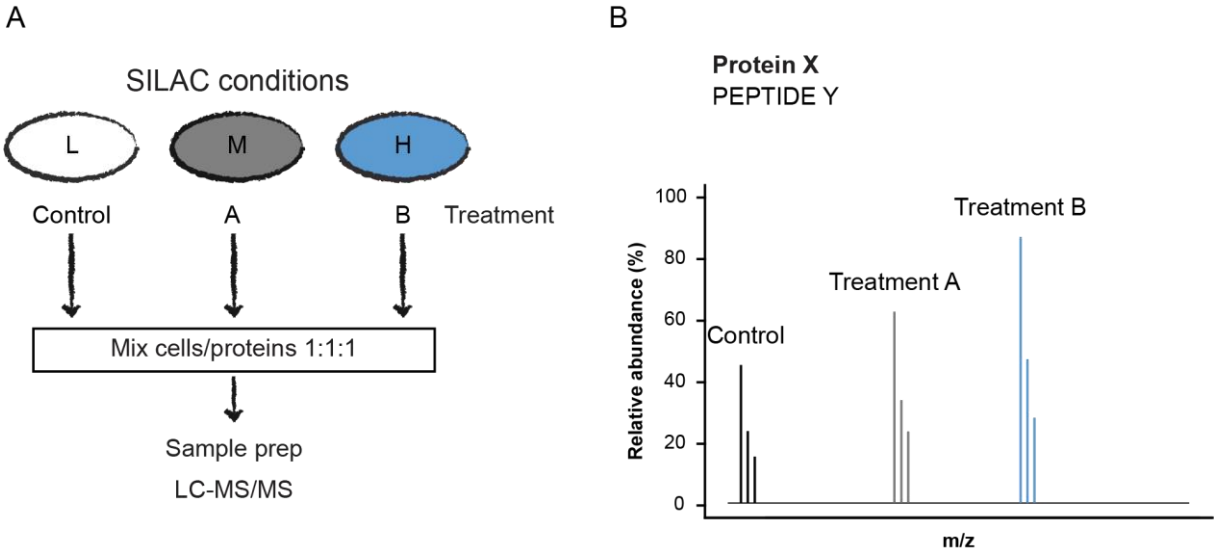

Figure 11: SILAC workflow and quantification principles. (A) A general workflow in SILAC approaches contains labeling of cells with different SILAC media allowing the quantitative comparison of peptides from 'light', 'medium' and 'heavy' conditions. SILAC allows reducing the samples size on the cell or protein level. Afterwards, samples are prepared for MS-based analysis. **(B)** Parent ion scan indicating the relative abundance of a given peptide Y derived from a given protein X from the experiment conducted in (A). According to the mass shift based on the differently labeled amino acids in the different SILAC conditions, peptide Y is measured at different *m/z*. The triplets indicate naturally occurring isotopes of elements within the peptide and is referred to as isotopic envelope. Treatment B and treatment A show a higher abundance of the measured peptide Y compared to the control.

5.6 AIM OF THIS STUDY

Autophagy is a degradative recycling pathway that takes place in the cytoplasm and is initiated in response to many stresses. It can degrade entire protein aggregates, dysfunctional cell organelles or invading bacteria contributing to cellular homeostasis. Its activation after genotoxic stress is believed to play an important role in cell fate determination. To show that DNA damage can induce autophagy, different types of DNA damage will be applied and their impact on autophagy will be assessed. As autophagy is initiated within the DDR, the question arises how the signal is transmitted from the nucleus to the cytoplasm. The DDR kinases ATM, DNA-PKcs and ATR have been associated with autophagy before. However, in human cells, this has been reported when using chemical inhibitors of these kinases that might have off-target effects. We aim to dissect how the DDR kinases may be involved in DNA damage-induced autophagy activation using a variety of assays.

A second aspect that we want to address is the physiological role of autophagy after DNA damage. To tackle this issue, we will perform a systematic identification of DNA damage-induced autophagic cargo. This could unveil previously unknown connections between DDR and autophagy. To this end, we will establish autophagosome content profiling in our lab, which is a quantitative MS-based proteomics method. Human osteosarcoma (U2OS) cells that express LC3B with engineered ascorbate peroxidase APEX2 will be used to characterize autophagosomal cargo after inducing double strand DNA breaks using topoisomerase I or II inhibitors CPT and ETO. This endeavor could also address the question whether DNA damage-induced autophagy causes the selective or bulk turnover of proteins or cell organelles.

6 RESULTS

6.1 DNA DAMAGE INDUCES AUTOPHAGY

Conversion of hATG8s is considered a hallmark of autophagy induction and can be visualized via Western blotting [284]. Here, conversion of the hATG8 LC3B was monitored. A LC3B-specific antibody was used to detect lipidation of soluble LC3B-I to LC3B-II in wild-type (WT) U2OS cells that were treated with the topoisomerase inhibitors I or II, CPT and ETO, respectively, or starvation medium Earle's Balanced Salt Solution (EBSS) that lacks growth factors, amino acids and sugars (Figure 12). LC3B conversion was observed in all conditions, particularly when used in combination with BafA, which inhibits the turnover of lipidated LC3B. Under basal conditions, LC3B-II was only detected upon long exposure. The SAR p62 showed decreased signal under all stress conditions, but increased signal when autophagy was blocked simultaneously. mTORC1 activity was monitored by blotting for phospho (p)-p70S6K (T389). Whereas lack of nutrients caused reduced signal of the phosphorylation site, DNA damage showed no effect on the mTORC1-regulated site suggesting different modes of activation of autophagy. Although PPM1D-dependent de-phosphorylation of p-ULK1 (S638) has been reported to precede DNA damage-induced autophagy, no changes of p-ULK1 (S638) signal could be detected when U2OS cells were treated with CPT or ETO [191]. DNA damage detection and DDR activation was monitored by blotting for p-CHK2 (T68).

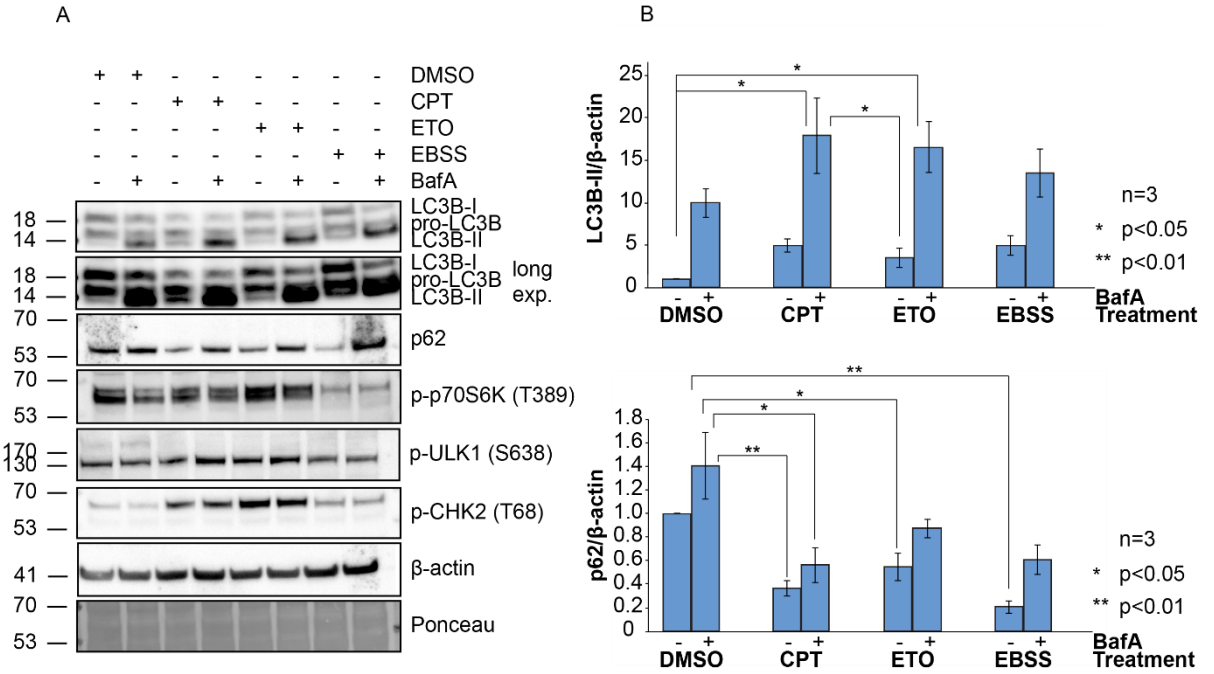

Figure 12: Semi-quantitative analysis of DNA damage-induced autophagy using LC3 conversion assay. (A) U2OS cells were treated for 16h with DMSO, CPT (10 µM), ETO (10 µM) or EBSS medium. BafA (200 nM) was added in the last 4 hours of the respective treatment. **(B)** Quantification of LC3B-II and p62 signal normalized to β-actin signal. Error bars represent standard deviation. *P<0.05, **P<0.01. Two-way ANOVA followed by Tukey`s *post hoc* test.

Recent studies showed that LC3B-II can have roles independent of autophagy that makes the interpretation of the LC3B conversion difficult. Novel methods such as the tandem-LC3B assay, which is a flow cytometry based assay involving a fluorescent fusion protein of LC3B with e.g.

enhanced GFP (eGFP) and mCherry, become the new gold standard in autophagy research [285–287]. Upon fusion of autophagosome and lysosome the eGFP signal is quenched fast whereas the mCherry signal remains more stable in the acidic environment of the autolysosome [22]. By calculating a ratio of eGFP to mCherry signal, one can measure autophagy initiation (Figure 13). U2OS cells stably expressing tandem-LC3B were treated with different types of DNA damage and autophagy induction was monitored. IR, CPT and ETO treatment generate DNA double strand breaks, whereas UV leads to the formation of bulky lesions within the DNA. CIS causes inter-strand crosslinks and HU leads to replication stress that can result in replication fork collapse. Among the different DNA damaging conditions, CPT and ETO showed strongest effects for autophagy induction and were picked to initiate genotoxic stress in following experiments (Figure 13C). Persistent treatment with CPT showed significant autophagy activation in U2OS cells from 6h on and was measured for up to 24h (Figure 13D). 16h CPT and 24h CPT induced autophagy to a similar extent as 4h treatment with starvation medium. To keep the genotoxic stress as short as possible, but to initiate autophagy potently, 16h CPT was chosen as a treatment for the investigation of DNA damage-induced autophagy in U2OS cells.

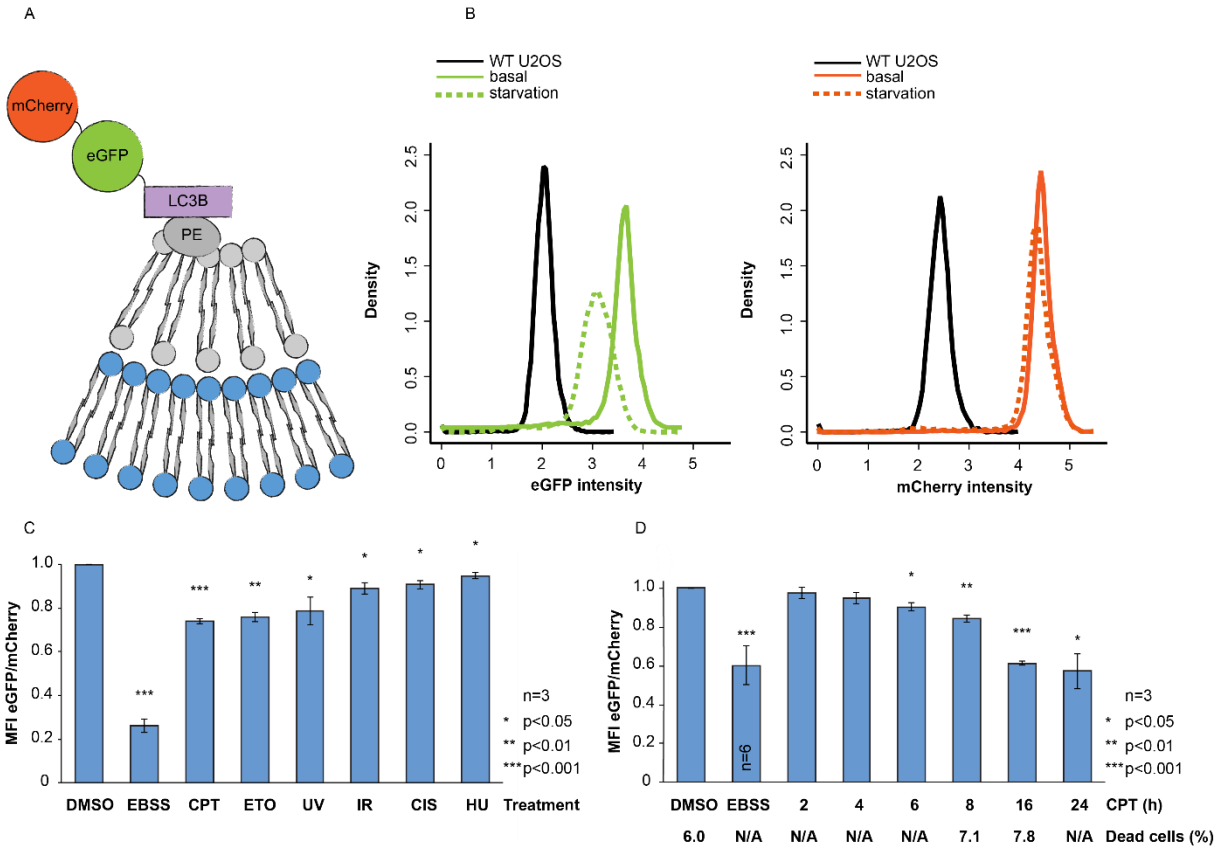

Figure 13: Quantitative analysis of DNA damage-induced autophagy by tandem-LC3B assay. (A) The assay is based on a fusion protein of LC3B-II with eGFP and mCherry. **(B)** eGFP and mCherry intensity as measured by tandem-LC3B assay during basal and starvation-induced autophagy. **(C)** Autophagy induction was measured in U2OS cells expressing tandem-LC3B after following treatments: DMSO (16h), EBSS (16h), CPT (16h, 10 µM), ETO (16h, 10 µM), UV (16h recovery after 40 J/m²), IR (16h recovery after 5 Gy), CIS (16h, 10 µM), hydroxyurea (16h, 2 mM). **(D)** Autophagy induction after different persistent treatments with 10 µM CPT or 4h EBSS. Dead cells were measured for indicated timepoints by Annexin V assay. Error bars represent standard deviation. P-values were calculated using Welch test. HU: hydroxyurea.

In order to assess the lethality of the respective treatments, the amount of cells with cell death-associated phenotypes was determined for indicated time points using Annexin V assay (Figure 13D and Figure 14A). Summing up dead, apoptotic and necroptotic U2OS cells after 16h of CPT treatment about 13% of the measured cells showed cell death-associated phenotypes. This was an increase of about 2-fold compared to control cells that showed cell death-associated phenotypes in about 7% over the whole cell population. To investigate whether CPT-treated cells would die at later stages Annexin V assay was performed 24h and 48h after recovery. Cells with cell death-associated phenotypes were in similar amounts as control cells or with a 16h insult of CPT, indicating that few cells died ultimately, whereas most cells managed to survive. The effect of 16h CPT and ETO treatment on apoptosis was investigated further in different concentrations, by monitoring the cleavage of CASP3 and PARP1, which is an indicator for cell death pathways (Figure 14B). Faint bands of cleaved CASP3 were detected in U2OS cells that were treated for 16h with 50 µM or 100 µM of CPT or ETO, whereas no cleavage was detected in cells that were treated with 10 µM of the respective compound. PARP1 cleavage was detected in cells treated with 100 µM CPT or ETO, but not in lower concentrations. Taken together, the low amount of cells with cell death-associated phenotypes as assessed by Annexin V assay and the absence of cleaved CASP3 and PARP1 in the 16h period with 10 µM CPT indicate that these treatments are in a sub-lethal range.

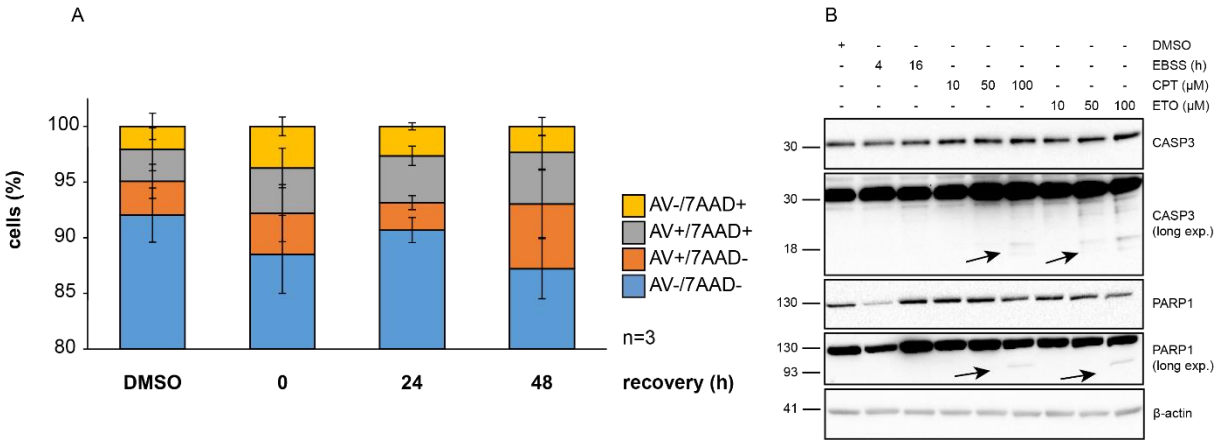

Figure 14: Quantification of the cytotoxicity of the treatment by Annexin V assay and CASP3 or PARP1 cleavage. **(A)** Annexin V assay was used to determine the amount of U2OS cells with cell death-associated phenotypes after treatment with 10 µM CPT for 16h and two recovery timepoints. AV-/7AAD- = alive, AV+/7AAD- = apoptotic, AV+/7AAD+ = dead, AV-/7AAD+ = necroptotic. **(B)** U2OS cells were treated for 16h with CPT or ETO with indicated concentrations or with EBSS for the indicated timepoints. Cleavage of CASP3 and PARP1 was assessed. CASP3 is cleaved to a ~17 kDa and ~12 kDa product upon activation. PARP1 is cleaved by CASP3 to a ~24 kDa and a ~89 kDa product.

Similar experiments were performed in human retinal pigment epithelial-1 (RPE-1) cells (Figure 15). RPE-1 cells that expressed the tandem-LC3B assay showed strong induction of autophagy after 18h treatment with 2 µM CPT, which was associated with low levels of cytotoxicity as assessed via Annexin V assay (Figure 15B, Figure 15D). Thus 2 µM CPT for 18h was chosen as a treatment in RPE-1 cells for further experiments. Interestingly, some of the treatments led to an increase of the eGFP to mCherry ratio, which would indicate more eGFP signal compared to mCherry. A possible explanation could be that maturation times for eGFP are shorter than for mCherry and that at the acquired time points tandem-LC3B expression is

increased leading to a short overrepresentation of the eGFP singal. Similar observations are known to collaborators and seem to be cell line-specific (personal communication with Alexandra Stolz and Paolo Grumati, Goethe University, Frankfurt). To confirm the specificity of the tandem-LC3B assay CPT- and starvation-induced autophagy was monitored in the presence of BafA treatment in the last two hours of the respective treatment (Figure 15C).

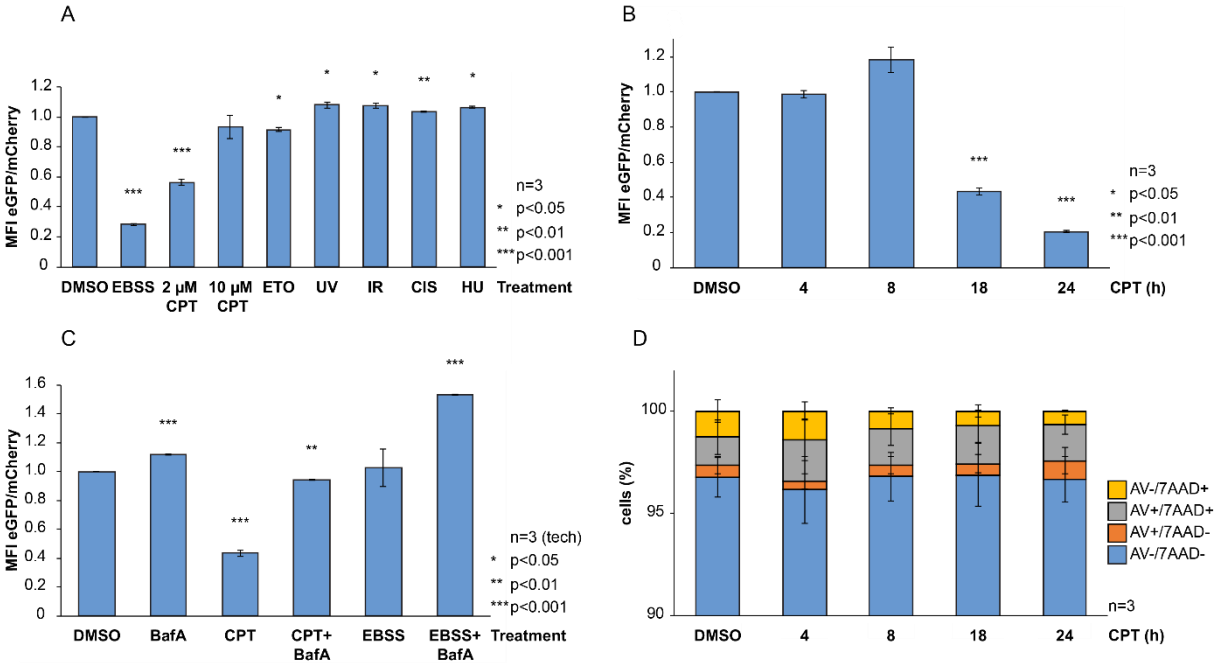

Figure 15: DNA damage-induced autophagy in RPE-1 cells. (A) RPE-1 cell that express the tandem-LC3B assay were treated with different types of DNA damage to monitor autophagy activation. CPT treatment was tested in two different concentrations. Treatments: DMSO (18h), EBSS (18h), CPT (18h, 2 µM and 10 µM), ETO (18h, 10 µM), UV (18h recovery after 40 J/m²), IR (18h recovery after 5 Gy), CIS (18h, 10 µM), hydroxyurea (18h, 2 mM). **(B)** RPE-1 cell that express the tandem-LC3B assay were treated with 2 µM CPT for the indicated time points. The 18 h time point was used for further experiments. **(C)** RPE-1 cell that express the tandem-LC3B assay were treated with 2 µM CPT for 18 h or EBSS for 4 h to monitor autophagy activation. BafA was added in the last 2 h of the treatment to show specificity of the assay. N= 3 technical replicates. **(D)** Annexin V assay was used to assess the lethality of 2 µM CPT treatment for the indicated time points on RPE-1 cells. AV-/7AAD- = alive, AV+/7AAD- = apoptotic, AV+/7AAD+ = dead, AV-/7AAD+ = necroptotic. P-values were calculated using Welch test.

6.2 THE DDR KINASES IN AUTOPHAGY

The DDR kinases have been reported to be involved in autophagy activation during conditions of starvation, elevated cellular concentrations of reactive nitrogen species, ROS and DNA damage [153,164,166,167,172,175,288–290]. Studies in yeast indicate a direct role for the DDR kinases Mec1, Tel1 and Rad53 (orthologues of ATR, ATM and CHK2, respectively) in DNA damage-induced autophagy [167]. Further, reports in yeast and mammals suggest a role for ATR and ATM in mitophagy and pexophagy, respectively [154,217,290]. In mammals, the role of the DDR kinases in DNA damage-induced autophagy is less clear although ROS production as a consequence of IR has been linked recently to ATM-mediated activation of autophagy via CHK2-Beclin1 or AMPK-TSC2 [153,175]. ATM-CHK2 activation has also been reported to mediate autophagy after DNA damage via FOXK2 inactivation, whereas ATR-CHK1 signaling was associated with RHOB-TSC2-mediated inactivation of mTORC1 in response to DNA damage [166,172]. In order to investigate the role of the DDR kinases in DNA damage-induced autophagy, U2OS cells that expressed tandem-LC3B were treated with respective kinase

inhibitors while inducing DNA damage with CPT. The kinases JNK1 and p38α have also been associated to the DDR and autophagy, previously and were therefore included into these experiments by respective inhibitors [291–294]. Inhibition of ATM, DNA-PKcs and ATR had significant effects on DNA damage-induced autophagy (Figure 16A). The inhibition of the checkpoint kinases CHK1 and CHK2 and the kinases JNK1 and p38α had no significant effects on autophagy induction by CPT. Similar results were obtained in RPE-1 cells expressing tandem-LC3B (Figure 16B).

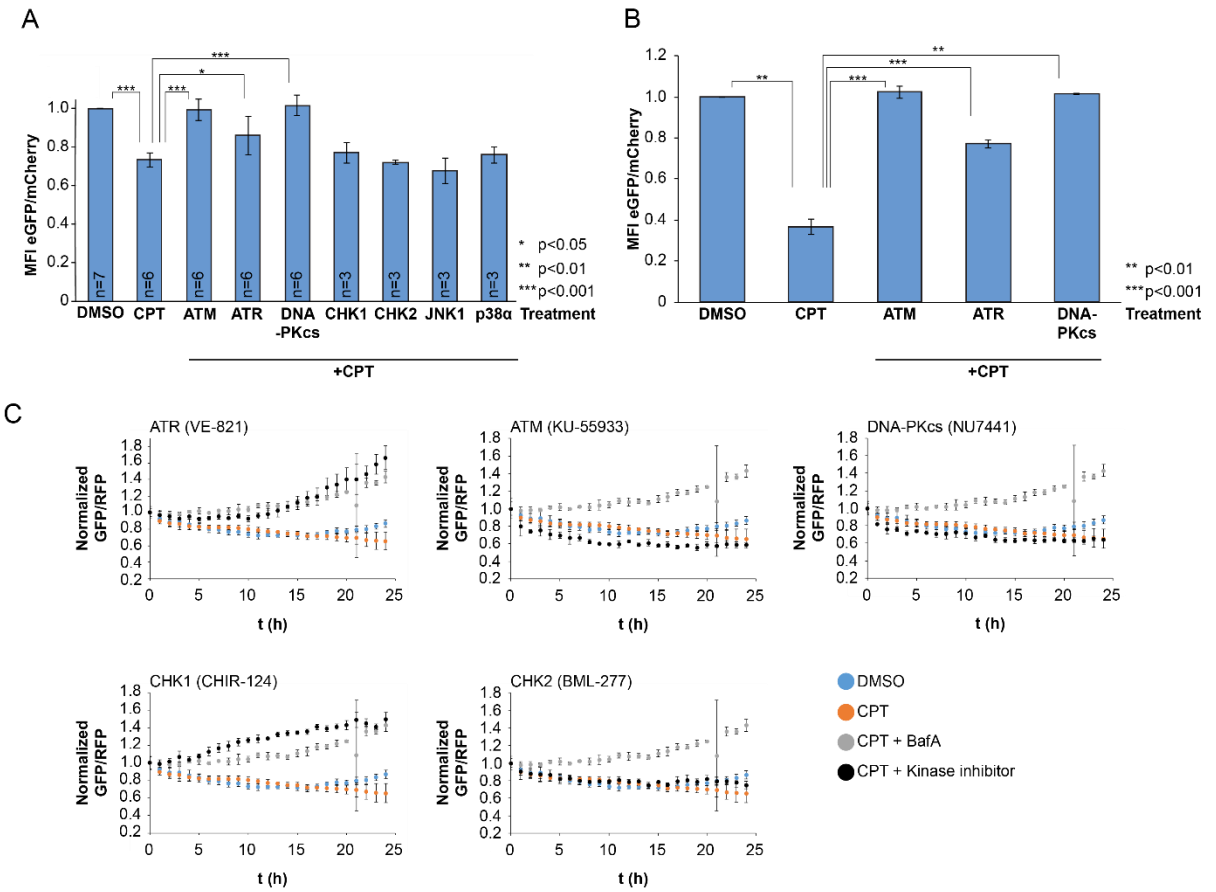

Figure 16: Analysis of DDR kinase inhibitors on DNA damage-induced autophagy. (A) U2OS cells expressing tandem-LC3B were pre-treated for 1 h with 5 µM JNK inhibitor, 10 µM p38 inhibitor, 2 µM ATR inhibitor, 10 µM ATM inhibitor, 2 µM DNA-PKcs inhibitor, 2 µM CHK1 inhibitor or 5 µM CHK2 inhibitor before application of 10 µM CPT for 16h. Statistically significant differences in CPT-induced autophagy are indicated. **(B)** RPE-1 cells expressing tandem-LC3B were pre-treated for 1 h with 2 µM ATR inhibitor, 10 µM ATM inhibitor, 2 µM DNA-PKcs inhibitor, 2 µM CHK1 inhibitor or 5 µM CHK2 inhibitor before application of 2 µM CPT for 18h. Statistically significant differences in CPT-induced autophagy are indicated. **(C)** Live cell imaging data from RPE-1 cells expressing tandem-LC3B. Cells were pre-treated with inhibitors as in (A), but DNA damage was induced with 2 µM CPT final concentration. Autophagy induction was monitored over a course of 24h. Data from basal autophagy (blue), CPT-induced autophagy (orange) and BafA-inhibited CPT-induced autophagy (grey) are shown in all plots. Data of CPT-induced autophagy with parallel inhibition of the respective kinase is shown individually according to the labeling (black). All data points are derived from at least three technical replicates that represent the mean of the ratio of GFP to RFP intensity. Error bars represent standard deviation. P-values were calculated using Welch test.

To validate the tandem-LC3B data obtained by flow cytometry, the experiments were repeated in a similar set-up using live cell imaging in collaboration with the Stolz lab (Goethe University Frankfurt). RPE-1 cells were used that expressed tandem-LC3B based on GFP-LC3B-RFP-LC3BΔG. The construct is cleaved by endogenous ATG4 proteases, which releases two reporters in equimolar amounts. As the RFP-LC3BΔG cannot be attached to autophagosomal

membranes, the RFP signal remains relatively stable compared to GFP-LC3B that is regulated by autophagy [295]. This tandem-LC3B assay should lead to similar results as the tandem-LC3B constructs used in U2OS and RPE-1 cells before (Figure 16A and Figure 16B). The cells were pre-treated for 1 h with the respective kinase inhibitor, before autophagy was induced by CPT over a time course of 24h. Each hour, the intensity of GFP and RFP was measured and the ratio of GFP to RFP signal was calculated. DMSO treated cells showed a gradual decrease in the ratio indicating a slight shift towards the RFP signal representing basal activity of autophagy that causes a constant degradation of GFP on a low level (Figure 16C). In CPT treated cells, the gradual shift in the ratio was more prominent indicative for a more persistent autophagy activation. Autophagy activation was blocked in cells that were treated simultaneously with BafA represented by a strong shift of the ratio towards GFP. Addition of the ATR and CHK1 inhibitors resembled the data obtained from BafA-mediated inhibition of autophagy, whereas inhibition of ATM, CHK2 or DNA-PKcs caused similar ratios obtained from CPT treatment alone. Hence, the data obtained from the live cell imaging approach indicates that CPT-induced autophagy is ATR-CHK1-mediated, whereas the kinases ATM, DNA-PKcs and CHK2 play no role in this signaling pathway. This is in contrast with the tandem-LC3B data obtained by flow cytometry where CPT-induced autophagy was blocked strongest by ATM and DNA-PKcs inhibition and where the inhibition of ATR had a mild effect (Figure 16A and Figure 16B).

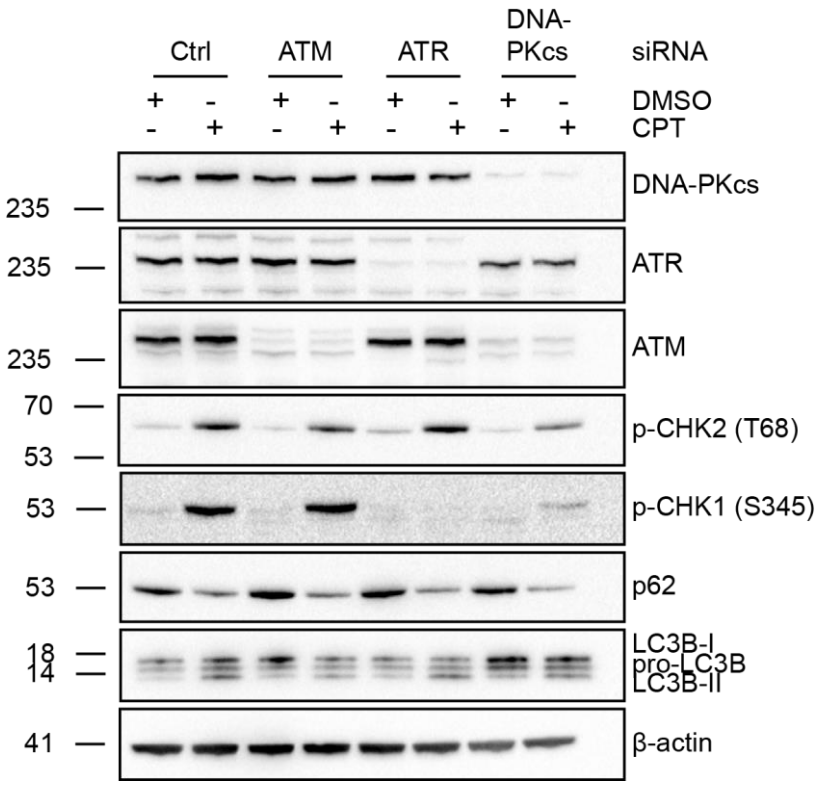

Figure 17: Analysis of DDR kinases in DNA damage-induced autophagy. The DDR kinases were knocked down in WT U2OS cells by siRNA pools containing four specific siRNAs towards their target mRNA. Subsequently, the cells were treated with 10 µM CPT for 16h, before the effect of the knockdown on DDR signaling and autophagy activation was assessed.

As the data obtained from flow cytometry- and live cell imaging-based tandem-LC3B did not resemble each other, LC3B conversion assay was used as an alternative approach to assess

the role of the DDR kinases on DNA damage-induced autophagy. WT U2OS cells were treated with CPT after the knockdown of the DDR kinases, which was confirmed by Western blotting (Figure 17). Knockdown of ATM caused simultaneous downregulation of DNA-PKcs, which had been reported conversely [296]. DDR activation was assessed by blotting for p-CHK1 (S345) and p-CHK2 (T68). The ATR-CHK1 signaling axis was perturbed in cells that had reduced levels of ATR and DNA-PKcs, whereas the ATM-CHK2 signaling was affected in cells with low levels of ATM and DNA-PKcs. Protein levels of LC3B-II and p62 were affected upon autophagy activation by DNA damage. Knockdown of the DDR kinases seemed to have no effect on the turnover of p62 by CPT-induced autophagy or the conversion of LC3B-I to LC3B-II. This describes for the first time in a direct comparison the effect of the DDR kinases on DNA damage-induced autophagy using a knockdown approach.

6.3 AUTOPHAGOSOMAL CONTENT PROFILING

The enzymatic protein tag APEX2 enables *in vitro* biotinylation of proteins in close proximity to a protein of interest. This facilitates the identification of direct and indirect interactors of the respective protein. Biotin-phenol (BP) is added to the cell culture medium and the enzymatic reaction is initiated by a short pulse of H_2O_2. To investigate the content of autophagosomes after genotoxic stress, we generated U2OS cells that constitutively expressed the construct APEX2-FLAG-LC3B. Therefore, WT U2OS cells were transfected with the respective construct and set under selection pressure. After non-transfected cells were removed, a single cell dilution was performed to obtain colonies that derived from single clones.

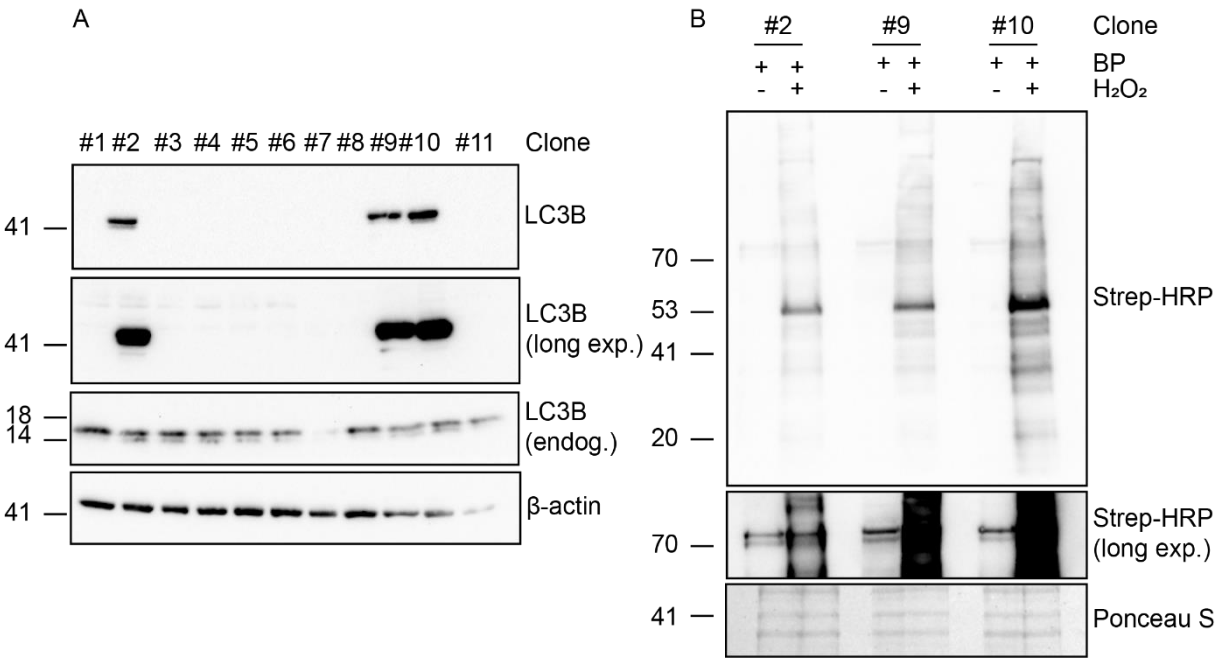

Figure 18: Generation of U2OS cells expressing APEX2-FLAG-LC3B. (A) After single cell dilution, eleven clones were tested for the construct by blotting for LC3B at the expected construct size ~45 kDa. Clones #2, #9 and #10 showed a signal, indicating the expression of the construct. **(B)** The functionality of the construct was tested in clones #2, #9 and #10 by blotting for biotin with streptavidin-HRP after induction with H_2O_2. Strep-HRP= streptavidin-horse radish peroxidase.

Ultimately, eleven clones were tested for the APEX2-FLAG-LC3B construct that has a molecular weight of about 45 kDa (Figure 18A). From the eleven clones, clones #2, #9 and #10 showed a band of the expected size indicating that the construct was expressed. The functionality of the construct was tested with the respective clones and biotinylation could be detected, where H_2O_2 had been added to the cells in combination with BP (Figure 18B). As clone #10 showed strongest biotinylation, it was selected for MS-based proteomics studies and cultivated in SILAC media for metabolic labeling.

APEX2 is particularly suitable, if attached to a protein with a defined localization. To this end, the fusion construct APEX2-FLAG-LC3B was used to characterize the content of autophagosomes in a MS-based SILAC approach after exposure to ETO (Figure 19). SILAC U2OS cells that express APEX2-FLAG-LC3B were treated with BafA in the last two hours of the ETO treatment or the DMSO control to prevent the turnover of autophagosomal content and to accumulate autophagosomes (Figure 19A). Biotinylation was induced in cells of the SILAC label 'medium' and 'heavy' and was omitted in cells labeled with 'light' amino acids, which served as a non-biotinylated control. Afterwards, cells were collected and mixed in a 1:1:1 ratio based on cell numbers and were solubilized using a dounce homogenizer. Different centrifugation steps enabled to purify a fraction rich in autophagosomes. As APEX2-FLAG-LC3B faces not only the autophagosomal lumen, but also the cytoplasm by residing in the inner and the outer autophagosomal lipid bilayer, identification of *in vitro* biotinylated cytoplasmic non-cargo proteins is possible. These proteins are considered as contaminants and were removed by enzymatic degradation using proteinase K (ProtK). The two lipid bilayers of the autophagosome protect the cargo proteins from degradation by ProtK. To avoid further downstream degradation, ProtK is inactivated by addition of PMSF, before biotinylated cargo proteins were pulled down using streptavidin and identified via LC-MS/MS (Figure 19B). Inputs of the samples of the different SILAC conditions were taken before combining and expression of the construct, functional biotinylation and DDR activation were checked (Figure 19C). Almost no signal was detected in the unbound fraction, which could indicate for efficient pulldown, but might also represent the low levels of proteins in general. In total 904 protein groups were identified in four biological replicates of which 381 could be quantified in two out of four experiments (Figure 19D). These 381 protein groups were used for further analysis. 128 of the 381 quantified protein groups were significantly enriched after ETO treatment, whereas 4 protein groups were significantly enriched after DMSO treatment and 249 protein groups showed no significant changes upon the treatments. Protein groups that were significantly enriched after ETO treatment had been associated with autophagy before (Figure 19E). Among them, the bait protein LC3B, SARs such as SQSTM1 and PHB2, proteins associated with autophagy such as LAMP1 and RAB7A and known cargo proteins such as the subunits of

the TRiQ/CCTchaperonin complex were identified, indicating that the approach led to successful enrichment and detection of autophagosomal cargo.

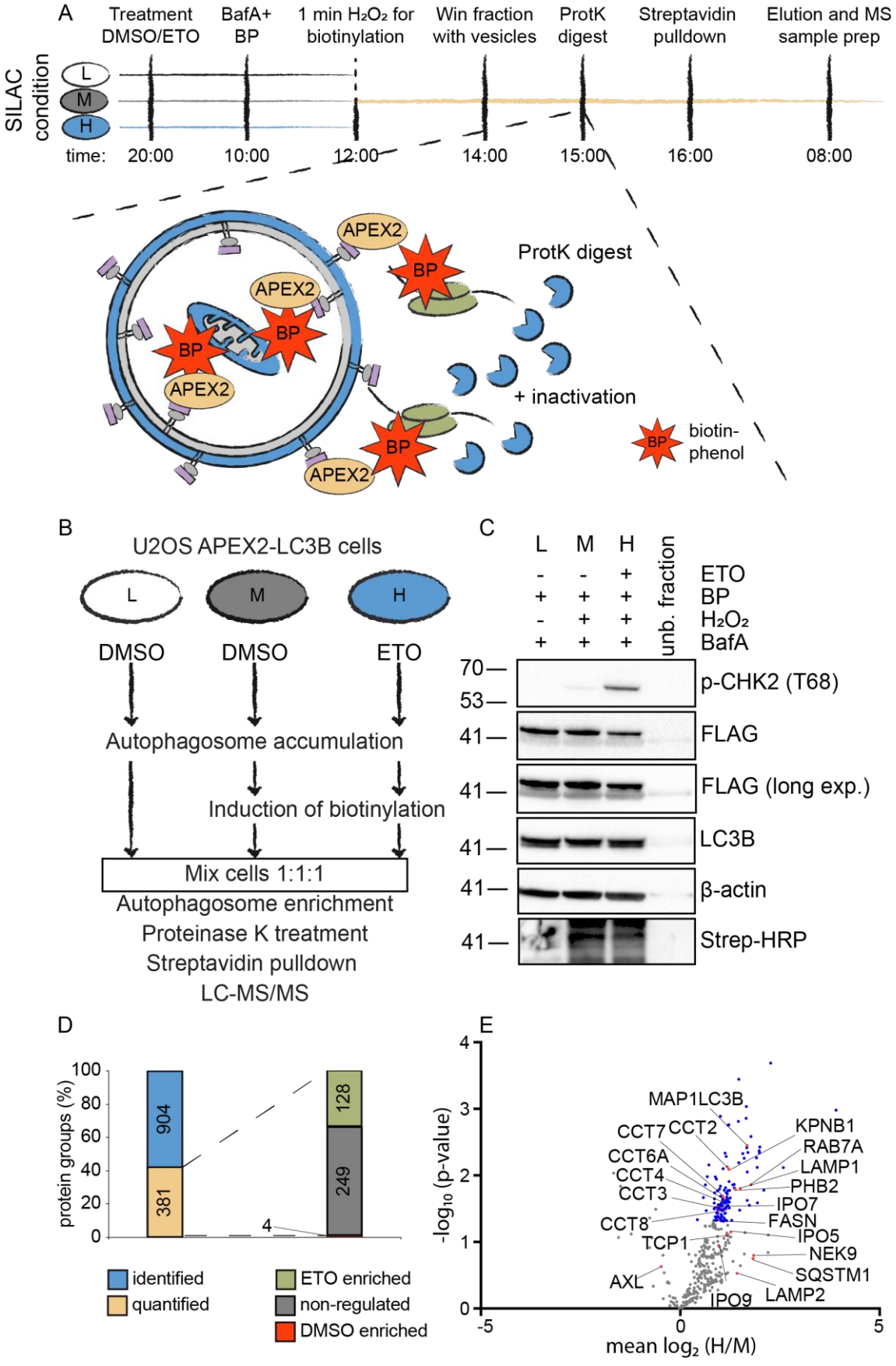

Figure 19: APEX2-based proximity biotinylation for identification of DNA damage-induced autophagic cargo. (A) A schematic highlighting the most important steps during autophagosome content profiling including biotinlyation induction, autophagosome enrichment and ProtK digest to remove unwanted cytoplasmic 'contaminants'. Note that biotinylation is not induced in the 'light' condition indicated by a dotted line. The number of horizontal lines indicates combining of the three samples, which takes place after biotinylation induction. **(B)** The SILAC-based workflow of the experiment. 'Heavy' labelled cells were treated for 16h with 10 µM ETO, whereas 'medium' and 'light' labelled cells were treated with DMSO. BafA was added to cells of all SILAC conditions in the last two hours of the treatment at 200 nM final concentration. Biotinylation was induced in 'medium' and 'heavy' labelled cells. Cells of the different SILAC conditions were mixed in a 1:1:1 ratio after biotinylation induction and before enrichment of autophagosomes **(C)** Inputs were analyzed by Western blotting to confirm DDR activation by blotting for p-CHK2 (T68) and biotinylation by using Strep-HRP. **(D)** Quantitative analysis of the dataset. 904 protein groups were identified overall in the 4 experiments of which 381 could be quantified in 2 out of 4 experiments. These 381 protein groups were used for further analysis in which 128 were significantly enriched after ETO treatment, 4 protein groups were significantly enriched after DMSO treatment and 249 protein groups showed no significant changes **(E)** Volcano plot showing comparison of ETO- to DMSO-induced autophagic cargo. Blue hits have a p-value that is significantly different from the mean and are enriched ≥ 1.3-fold. Hits in red are known to be degraded through autophagy or are proteins associated with autophagy. L: light, M: medium, H: heavy, BP: biotinphenol, Strep-HRP: streptavidin-horseradish peroxidase. P-value = 0.05, fold change ≥ 1.3, n=4.

6.4 COMPUTATIONAL ANALYSIS OF THE APEX2-FLAG-LC3B DATASET

Next, the APEX2-FLAG-LC3B dataset was analyzed with different bioinformatic tools to assess its quality and to identify putative autophagosomal cargo. Gene Ontology (GO) term analysis was performed with all 904 protein groups identified in four independent experiments using PANTHER (Figure 20A). Protein groups can comprise proteins that were not unambiguously identified by unique peptides, but share common peptides and are therefore quantified together. The dataset was compared with a previously published APEX2-LC3B dataset from the Behrends group comprising 994 BafA-sensitive protein groups and which is the only dataset with a comparable workflow [45]. The section 'cellular component' showed an enrichment for a set of genes with the associated GO term 'receptor complex', which included plasma membrane proteins such as integrins and ephrins. These genes were also found in other GO terms such as 'integral component of plasma membrane' or 'plasma membrane region'. The enriched GO terms 'lysosome' and 'cytoplasmic vesicle lumen' overlapped in genes for cathepsins. The section 'molecular function' showed a strong enrichment for a set of genes with the associated GO term 'cysteine-type endopeptidase activity' or 'ubiquitin-like protein ligase activity', which included several deubiquitylating enzymes or E3 ubiquitin-protein ligases, respectively. The section 'biological process' showed enrichment for GO terms similar to terms from the section 'cellular component' including the respective set of genes such as MTOR, HEXB, RAB7A and RAB14 in 'lysosome organization'.

A protein-protein interaction (PPI) hub analysis was performed that addressed the question, which proteins would most commonly interact with the protein groups in the dataset. For the PPI hub analysis all protein groups were used that could be quantified in at least 2 out of 4 experiments. These were 381 protein groups, which were extended by the proteins within the quantified protein groups, which led to 445 proteins in total. Among the top ten most commonly interacting hits, five of the six hATG8s were listed (Figure 20B). Other proteins indicated as common protein hubs were SLC2A4, 14-3-3 proteins, the 14-3-3 binding protein ARRB2 and ACTB. For visualization purposes, the clustergram indicates the interaction of the top 300 hits from the dataset with the associated hATG8s (Figure 20C). About a third of all quantified protein groups has been reported to interact with the indicated hATG8s.

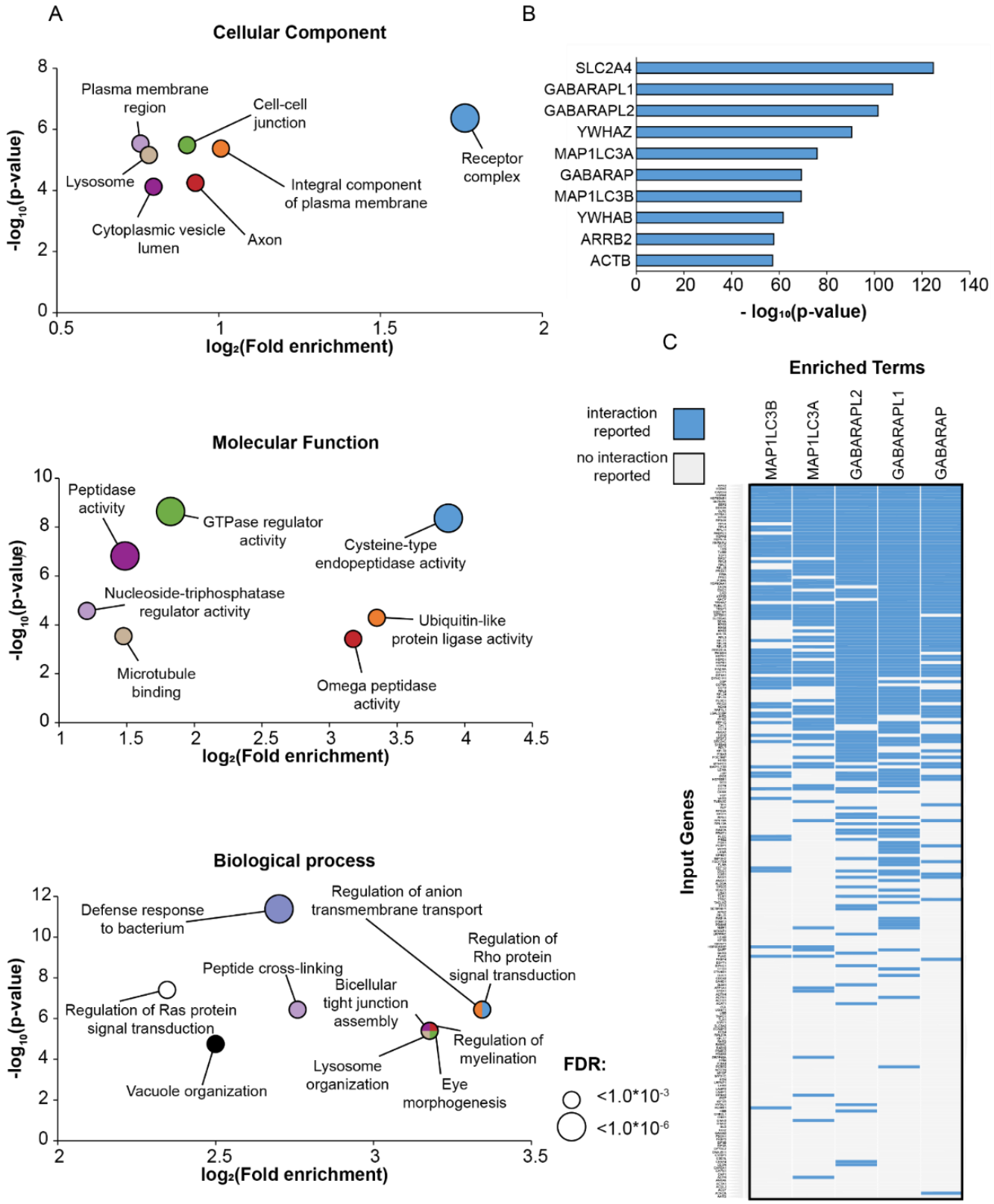

Figure 20: Bioinformatic analysis of the autophagosomal content after ETO treatment. (A) GO term analysis using PANTHER and a previously published dataset as background [45]. Redundant terms and terms with low enrichment or low significance were excluded for visualization. **(B)** Proteins that have been most commonly connected to the dataset by PPI hub analysis using enrichR [297]. **(C)** Clustergram to visualize the interactions of associated hATG8s to the top 300 ETO-induced hits of the dataset.

To get a more informative picture of the ETO-induced autophagic cargo, a cluster analysis was performed on the 128 significantly enriched proteins groups of the dataset. The 128 protein groups were extended by the quantified proteins within the protein groups, which led to 163 proteins in total. In the end, nine clusters of a minimum of three proteins could be identified (Figure 21). 72 proteins could not cluster among each other or be assigned to any of the other nine clusters and were therefore removed from further analysis. Cluster 1 and cluster 2 are the biggest clusters identified with 27 and 21 proteins, respectively. Cluster 3, cluster 4 and cluster 5 are of a medium size with 12, 9 and 8 proteins. The remaining clusters consists of either 4 or 3 proteins. The protein clusters were analyzed by GO term enrichment-, Reactome- and KEGG-analysis. Most of the clusters were associated with terms that could clearly be connected to autophagy or autophagic cargo. Interestingly, cluster 1 represents an exception as chromatin-associated proteins with largely nuclear localization assemble it. Taken together, the systematic analysis of autophagy cargo after DNA damage indicates that nuclear proteins could be potential autophagosomal cargo.

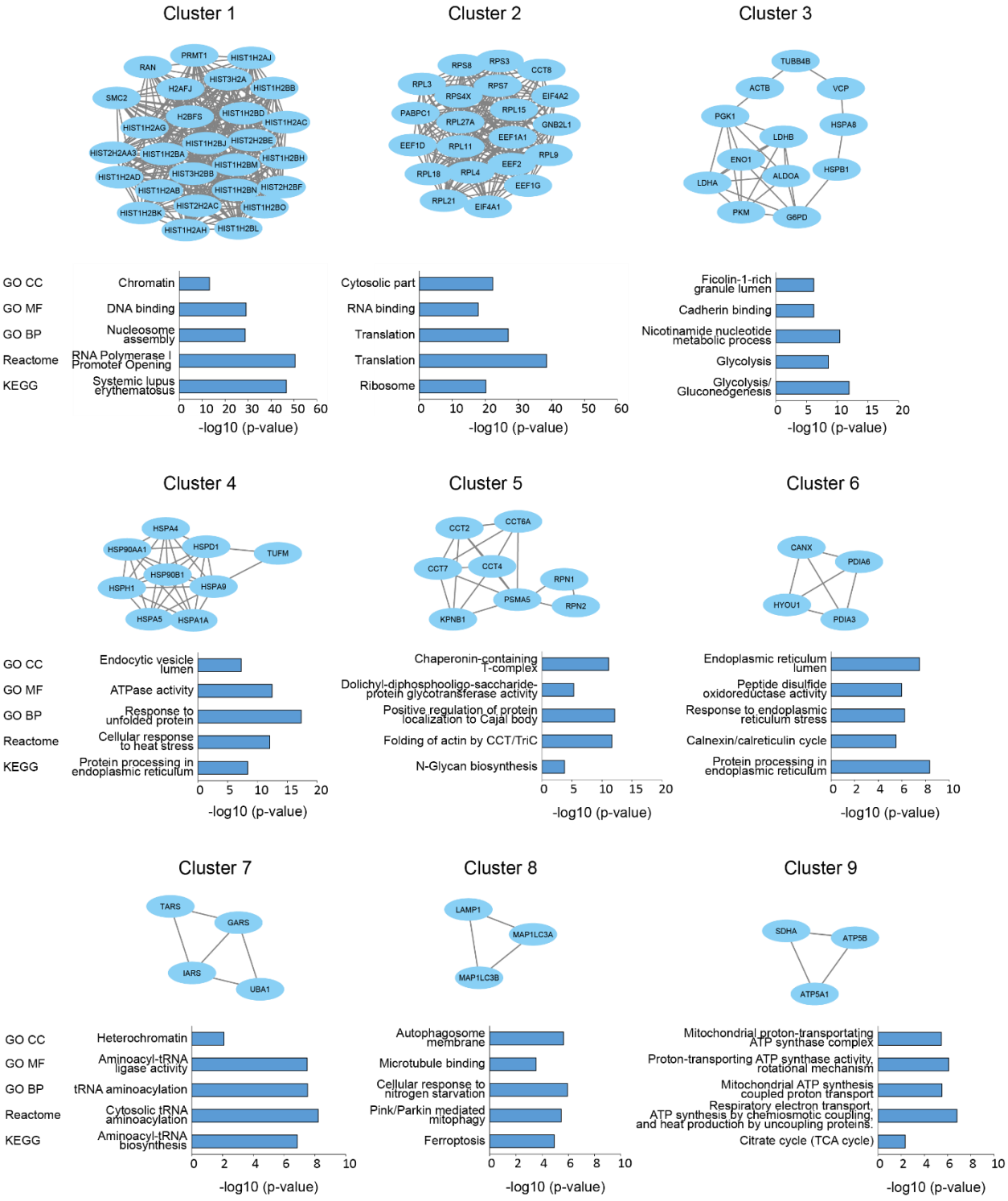

ACSL3 ACTG1 AHCY AHNAK2 ANXA1 CAD CAPZA1 CCT3 CFL1 CKAP4 CLTC COPA DDX39A DDX39B DYNC1H1 EEF1A1P5 EPRS ESYT1 FASN FDXR FKBP9 FSCN1 GANAB GAPDH GDI2 GFPT1 GSTP1 HADHA HIST1H2BC HMGCS1 HSD17B4 HSP90AB1 IMPDH2 IPO7 LASP1 LMNA MAP1LC3B2 MTHFD1 NAP1L1 NME1 NME1-NME2 NME2 NME2P1 P4HB PAICS PC PCBP2 PCBP3 PCCA PFN1 PHB2 PPIA PPIB PPP2R1A PRDX1 RAB1A RAB7A S100A9 SCAMP3 SERPINH1 SRSF3 ST13 ST13P4 ST13P5 STAT1 TAGLN2 TFRC TRAP1 VCL VPS35 WDR1 YWHAZ

Figure 21: Cluster analysis of ETO-induced autophagic cargo identified by autophagosome content profiling. For the cluster analysis only the significantly enriched protein groups were considered (128 protein groups in total, p≥0.5, fold change ≥1.3). The analysis was extended by the proteins in all protein groups. This procedure extended the total amount of proteins analyzed for cluster analysis from 128 to 163. These 163 proteins were analyzed using StringDB at a threshold of 0.7. The network was processed further using Cytoscape and the Cluster viz app. The mcode algorithm was used to generate the protein cluster. Proteins that were not associated to any of the clusters are listed below. GO term, Reactome and KEGG analysis was performed using enrichR.

6.5 VALIDATION OF AUTOPHAGOSOMAL TARGET PROTEINS

To confirm that the proteins identified by autophagosomal content profiling are degraded by autophagy, a ProtK protection assay can be performed. The assay resembles the protocol for autophagosome content profiling, but instead of subjecting the autophagosome-rich fraction to LC-MS/MS-based analysis, samples are treated with different combinations of ProtK and Triton X-100 before they are subjected for Western blotting (Figure 22A). Triton X-100 disrupts the autophagosomal membranes and releases the cargo. The combined treatment of Triton X-100 with ProtK causes the degradation of all proteins in the autophagosome-rich fraction. Triton X-100 alone causes no degradation. ProtK alone results in the hydrolysis of cytoplasmic proteins outside the autophagosome or proteins that are localized on the autophagosomal surface such as cytoplasmic parts of the transmembrane protein ATG9A. Proteins within the autophagosome such as SAR p62 are protected from ProtK by the two lipid bilayers as outlined for the autophagosomal content profiling (Figure 19A).

A ProtK protection assay was performed with WT U2OS cells that were treated with ETO to trigger DNA damage-induced autophagy (Figure 22B). Blotting for ATG9A with an antibody that recognizes a cytoplasmic epitope led to no signal in ProtK-treated samples. Blotting for p62 resulted in a faint band in ProtK-treated samples, indicating that p62 was protected by lipid bilayers. The same is true for LC3B, which shows an enrichment for LC3B-II. RPS10, a component of the 40S ribosomal subunit was not identified in our dataset as autophagosomal cargo and was therefore used as a negative control. It was shown in yeast that DNA damage-induced autophagy led to the degradation of RNR1, the orthologue of human RRM1 [206]. RRM1 was quantified in two out of four experiments of the autophagosome content profiling approach, but showed no significant enrichment after ETO treatment (Figure 22C). RRM1 showed a signal in ProtK-treated samples indicating that it is regulated by autophagy and confirming the results of the previous study (Figure 22B). From the autophagosome content profiling after ETO treatment a set of proteins was selected for confirmation by ProtK assay (Figure 22D). Some of the proteins were of particular interest as they have been described as proteins of nuclear localization (Figure 22C). From ten proteins tested in the ProtK protection assay only the histone variant histone H2A could not be validated.

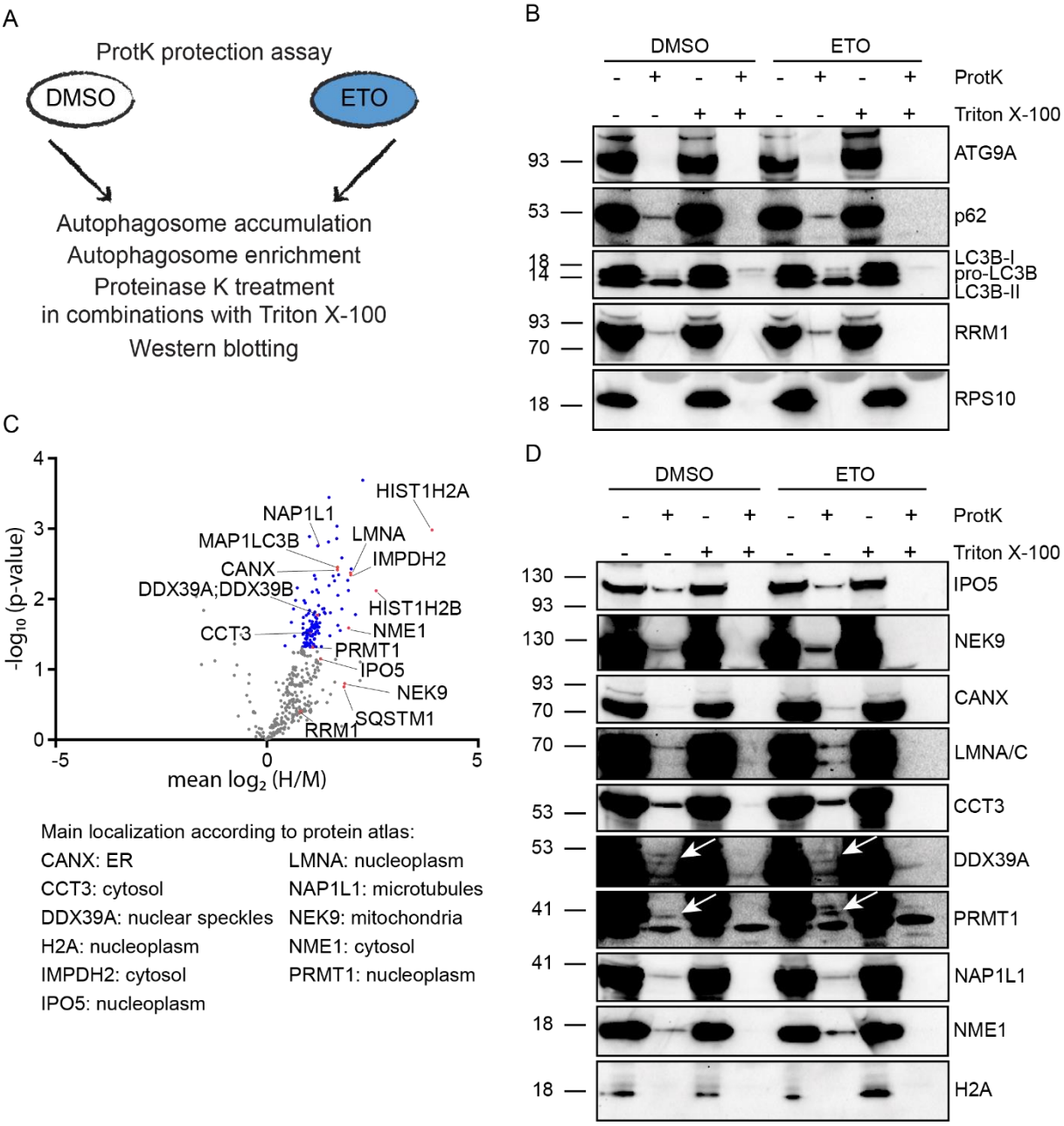

Figure 22: ProtK protection assay to validate selected hits from autophagosome content profiling. (A) General workflow for ProtK protection assay. **(B)** ProtK protection assay confirms regulation of p62, LC3B and RRM1 by autophagy. **(C)** Volcano plot from Figure 19, but with proteins highlighted that were chosen for validation. The cellular localization of the proteins of interest is listed according to protein atlas. **(D)** ProtK protection assay for the validation of selected target proteins. White arrows indicate the bands for DDX39A and PRMT1.

To confirm the results from the ProtK protection assay, whole cell lysates were generated from U2OS cells that were treated with ETO and BafA and analyzed by Western blotting (Figure 23A). Autophagy activation was monitored by blotting for LC3B and p62 and DDR activation was confirmed by blotting for p-CHK2 (T68). Protein levels of some of the potential cargo proteins were assessed, but no change could be detected that would resemble the signal of p62 that is degraded upon ETO-induced autophagy. As some of the proteins such as Lamin A (LMNA) are known to have a long half-live, the experiment was repeated in a similar set-up with exposure of the cells to ETO for up to 24h (Figure 23B). The protein levels of the potentially autophagy-regulated hits seemed to remain stable.

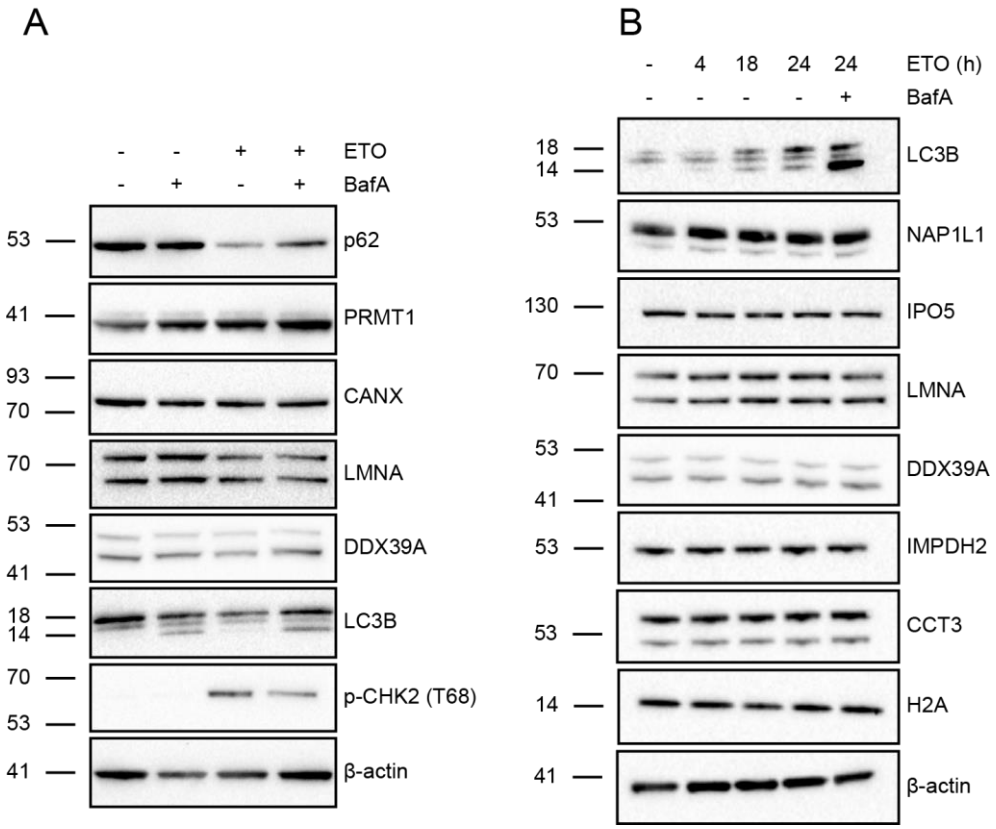

Figure 23: Autophagy inhibition by BafA to validate target proteins. (A) Whole cell lysates of U2OS cells that were treated for 16h with 10 µM ETO were analyzed via Western blotting. In the last 4h of the treatment, 200 nM BafA was added. **(B)** As in (A), but for indicated time points.

Taken together, autophagosomal content profiling after ETO treatment led to the identification of potential cargo proteins with nuclear localization. Using ProtK protection assay most of the proteins could be validated suggesting a previously unrecognized role for autophagy in the regulation of proteins of the nucleus. However, analyzing whole cell extracts with a block in the autophagy pathway did not allow confirming those results.

7 DISCUSSION

In this study, two main aspects of DNA damage-induced autophagy were investigated. The first aspect includes the signaling events that occur during DNA damage-induced autophagy in U2OS and RPE-1 cells. Therefore, different p-sites that are commonly described in literature to indicate mTORC1 activity were compared after genotoxic or starvation stress. Further, the role of the DDR kinases in DNA damage-induced autophagy was assessed. Therefore, U2OS and RPE-1 cells that expressed the tandem-LC3B assay were treated with respective DDR kinase inhibitors and the effect on CPT-induced autophagy was monitored. The second aspect involves the identification of target proteins of autophagy after DNA damage in U2OS cells. To study the autophagosomal cargo after DNA damage in a systematic manner, a recently developed MS-based proteomics approach was established [45]. The data was analyzed using different bioinformatic tools to obtain insights into classes of proteins that are degraded. In a last step, several of the identified DNA damage-induced cargo proteins were selected for validation using different assays.

7.1 DNA DAMAGE INDUCES AUTOPHAGY

Exposure of U2OS cells to CPT or ETO induced autophagy as assessed by the LC3B conversion assay and tandem-LC3B assay. The semi-quantitative analysis of the LC3B conversion assay indicates that the autophagy-inducing treatments CPT and ETO show a significant difference compared to basal autophagy, when used in combination with the autophagy inhibitor BafA (Figure 12). The difference between starvation-induced autophagy and basal autophagy is not significant in the LC3B conversion assay. This does not mean that starvation does not induce autophagy. Most probably, the significance is not given as short periods of starvation can already stimulate autophagy potently, which leads to a fast conversion of LC3B-I to LC3B-II, but simultaneously to a quick degradation of the lipidated form [298]. Hence, the signal of LC3B-II might not be strong enough for a significant difference compared to basal autophagy even though BafA was used in the last two hours of the starvation treatment. Proof of that can be found, when the degradation of the SAR p62 is monitored (Figure 12). Here, BafA-inhibited basal autophagy shows significantly different protein levels of p62 when compared to the autophagy-inducing treatments CPT, ETO and starvation without BafA treatment. In line, starvation treatment led to a strong dephosphorylation of the mTORC1-regulated site p-p70S6K (T389), which is used as a read-out for mTORC1 activity [193].

The quantitative tandem-LC3B assay allowed to compare the effect of particular DNA damage treatments on autophagy activation. In the experiments presented here, topoisomerase inhibitors I and II, CPT and ETO, respectively, caused the strongest activation of autophagy compared to treatments with UV, IR, CIS and HU (Figure 13C). The genotoxicity of the different treatments was not assessed. Hence, one cannot draw the conclusion that the DNA lesions caused by CPT and ETO, mostly DSBs, initiate autophagy strongest compared to other types of damage such as inter-strand crosslinks that are evoked by CIS. IR that also causes DSBs such as CPT and ETO treatment did not show a strong activation of autophagy. However, the

activation was measured after 16h of recovery. Therefore, the treatments are not easily comparable. The same is true for the UV treatment that causes bulky DNA lesions. HU that leads to replication fork collapse after prolonged treatment showed the weakest effect among the different DNA damaging treatments. The question arises whether the treatments used cause autophagy by the same or different signaling pathways. IR can damage mitochondrial DNA which results in a perturbed electron transport chain that leads to increased ROS concentrations inside the cell [299]. Hence, IR might induce autophagy by ROS production and genotoxic stress. The signaling pathways that lead to autophagy activation after ROS are based on the ROS-sensitive DDR kinase ATM that activates LKB1-AMPK-TSC2 or CHK2-Beclin 1 [153,175,176].

7.2 SIGNALING EVENTS IN DNA DAMAGE-INDUCED AUTOPHAGY

mTORC1 is the main regulator of autophagy. Its activity can be assessed by blotting for mTORC1-regulated p-sites such as p-p70S6K (T389) or p-ULK1 (S757) [300]. U2OS cells that were starved for 4h showed a strong reduction of p-p70S6K (T389) and p-ULK1 (S757) (Figure 12A and Figure 24B). Interestingly, DNA damage did not cause the dephosphorylation of p-p70S6K (T389). This is in contrast to previous publications that report mTORC1-dependent activation of autophagy after genotoxic stress in MEFs [193,203]. Similarly, the PPM1D-dependent dephosphorylation of ULK1 at S637 (S638 in humans) that was reported as a requirement for DNA damage-induced autophagy in MEFs, was not reproducible in U2OS cells (Figure 12A) [191]. This could indicate that the signaling pathways that lead to autophagy after DNA damage differ from primary to cancer cells. In line, ETO treatment was unable to inactivate mTORC1 in the breast cancer cell line MCF-7 as assessed by blotting for the direct and indirect mTORC1-regulated sites on 4EBP1 and S6K, respectively [153]. Activation of AMPK after genotoxic stress has also been observed in MEFs, but not in MCF-7 cells [153,193]. In U2OS cells, CPT was unable to promote further phosphorylation of AMPK on T172 compared to non-stressed conditions, whereas starvation did (Figure 24A and Figure 24B). This was different from RPE-1 cells that showed AMPK activation after CPT treatment. The activation of AMPK under non-stressed conditions could be indicative for the relatively high levels of basal replication stress present in U2OS cells. Contrary, the activation of the checkpoint kinase CHK2 was functional and showed no increased phosphorylation levels under non-perturbed conditions (Figure 24A).

Taken together, the signaling events during DNA damage-induced autophagy were mostly studied in MEFs [191,193,203]. These pathways are based on mTORC1 inactivation via LKB1-AMPK-TSC2 or the direct dephosphorylation of ULK1 by PPM1D. A corner stone in DNA damage-induced autophagy is the tumor suppressor p53 that controls many ATG genes and members of the DDR after genotoxic stress [155]. Hence, the p53 status in cancer cells will have a crucial impact on DNA damage-induced autophagy and its underlying signaling events.

7.3 INVESTIGATING THE ROLE OF THE DDR KINASES IN DNA DAMAGE-INDUCED AUTOPHAGY

The role of the DDR kinases in autophagy activation after DNA damage was studied in U2OS and RPE-1 cells. U2OS cells that expressed the tandem-LC3B assay were treated with a respective inhibitor before autophagy was induced by CPT treatment (Figure 16A). As the PIKKs ATM, ATR and DNA-PKcs share many substrates one could have expected that their individual inhibition might show only mild effects on autophagy activation due to their partial redundancy. However, inhibition of ATM and DNA-PKcs showed a strong effect, whereas the inhibition of ATR had a mild, yet significant effect on DNA damage-induced autophagy. Similar results were obtained in RPE-1 cells expressing tandem-LC3B (Figure 16B). Given that the ATM-CHK2 and the ATR-CHK1 axis had already been connected to DNA damage-induced autophagy before, it was unexpected to see that inhibition of CHK1 or CHK2 showed no effect on the activation of autophagy after CPT [166,172]. The study that revealed a role for the ATR-CHK1 axis in DNA damage-induced autophagy was triggered after strong UV and MMS treatments that led to ACD. Similar to our study, sub-lethal doses with CPT or DOX were also tested, which did not trigger ATR-CHK1-mediated autophagy [166]. Of note, the study used the same ATR inhibitor in a similar concentration to our study, whereas the inhibitors for ATM, CHK1 and CHK2 were different. Most of the experiments conducted including the respective inhibitors were performed in HeLa cells that are known to have a diminished p53 function [301,302]. The study that revealed a role for the ATM-CHK2 axis in DNA damage-induced autophagy was triggered after CIS and ETO treatments that were in similar concentration and duration compared to our study [172]. Most of the experiments were conducted in cancer cell lines from liver or lung epithelium. The inhibitors used for ATR and CHK1 inhibition were different compared to our study, but the inhibitors used for ATM and CHK2 inhibition were the same. The ATM inhibitor was used in the same concentration, whereas CHK2 was inhibited in a twofold higher concentration. The results from both studies were validated in a single experiment each including the short hairpin RNA-mediated knockdown of CHK1 or CHK2, respectively [166,172].

The experiments to assess the role of the DDR kinases in DNA damage-induced autophagy were repeated using a similar approach by the Stolz lab (Figure 16C). In stark contrast to our data in U2OS and RPE-1 cells, inhibition of ATM and DNA-PKcs had no influence on DNA damage-induced autophagy (Figure 16C). Further, ATR and CHK1 inhibition had strong effects on DNA damage-induced autophagy. This would indicate that DNA damage-induced autophagy is mediated by the ATR-CHK1 signaling axis. This had been reported before, but exclusively for strong and lethal DNA damage treatments and explicitly not for similar sub-lethal CPT treatments as performed here [166]. Further, the time-course experiment in RPE-1 cells revealed that CPT induced autophagy at a later time point, around 17h-18h, compared to U2OS cells that showed robust CPT-induced autophagy activation from 6h on (Figure 13). This was confirmed by our data obtained from RPE-1 cells expressing tandem-LC3B, where shorter treatments with CPT did not induce autophagy (Figure 15B). The differences between

the two cell lines in regard of autophagy activation after DNA damage might rely on the slight different treatments, but also on the relatively instable genome of U2OS cells.

Overall, the experiments performed on the role of the DDR kinases in autophagy have been inconclusive. Knockdown of the respective kinases using siRNA showed no effect on the conversion of LC3B or the protein levels of p62 upon autophagy activation by CPT treatment (Figure 17). It is unlikely that effects on autophagy were not detectable due to insufficient knockdown efficiency as these were confirmed and DDR signaling was perturbed. However, it is possible that the effects are only detectable when using more quantitative assays than Western blotting or that minimal DDR signaling suffices to trigger autophagy. It is also plausible that commonly used DDR kinase inhibitors have off-target effects that could influence autophagy. The inhibitors for ATM (KU-55933) and DNA-PKcs (NU7741) that were used in this study have been shown to inhibit the PtdIns3K VPS34, which explains the strong inhibition observed in my data [303,304]. Conversely, these effects are absent in the analogous assay performed by the Stolz lab. Lastly, the effect of ATR inhibition was consistent in both assays, but its knockdown did not affect LC3B conversion nor p62 levels.

7.4 CHARACTERIZATION OF THE AUTOPHAGOSOMAL CONTENT AFTER DNA DAMAGE

Autophagosome content profiling based on the APEX2-FLAG-LC3B construct was used to systematically identify ETO-induced autophagic protein cargo. Among the enriched proteins several are known to be regulated by autophagy such as the subunits of the TRiQ/CCT chaperonin complex, but also proteasomal and ribosomal subunits [305]. Three different types of bioinformatic analysis suggest that the dataset is of good quality and represents *bona fide* autophagic cargo or at least proteins in proximity of the bait protein LC3B.

First, several of the terms derived from the GO enrichment analysis could be associated to autophagy (Figure 20A). The proteins behind the terms were often of lysosomal localization such cathepsins or LAMP1. Although these proteins might not be expected inside of autophagosomes, they might represent proteins from enriched autolysosomes due to incomplete inhibition by BafA. Further, the enriched receptor complex and plasma membrane-related terms consist mostly of integrins, which are associated with focal adhesions (FAs). FAs are large macromolecular assemblies that consist additionally to integrins of scaffolding and signaling proteins such as Vinculin (VCL) and Focal adhesion kinase 1. They connect the actin cytoskeleton to the extracellular matrix to provide traction [306]. FAs are known to be assembled and disassemble during cell migration [307]. Degradation of FAs is mediated by different autophagy pathways dependent or independent of SARs such p62 or NBR1 [308,309].

Second, the PPI hub analysis indicated that the most common proteins that are supposed to interact with the proteins in the dataset are the hATG8s (Figure 20B). About a third of the proteins included in the analysis have been associated with the autophagy marker proteins before.

Third, the cluster analysis performed on the enriched proteins after ETO treatment revealed nine clusters that are mostly comprised of proteins that are known to be degraded by autophagy (Figure 21). This includes ribosomal subunits and cytoplasmic tRNA ligases (cluster 2 and cluster 7), proteins involved in glycolysis (cluster 3), different chaperones and subunits of the TRiQ/CCT chaperonin complex (cluster 4 and cluster 5), mitochondrial and ER proteins (cluster 9 and cluster 6) as well as ATG proteins (cluster 8) [305,310–317]. The exception were histones and proteins with nuclear association in cluster 1, although single studies report that CMA can regulate histones H3-H4 and other nuclear proteins such as CHK1 [168,318]. The cluster analysis enabled the identification of well characterized targets of autophagy. However, room for improvement remains. Many proteins that were enriched could not be associated with any of these clusters. One of these proteins was PHB2, a known SAR that is localized at the inner mitochondrial membrane (IMM) and that mediates mitophagy by direct interaction with hATG8s after disruption of the outer mitochondrial membrane [317]. This might also explain why proteins of the mitochondrial electron transport chain, which reside in the IMM were identified (cluster 9). Hence, PHB2 could have been clustered either within cluster 9 or with the ATG cluster 8. Moreover, some proteins such as the TRiQ/CCT chaperonin complex subunit CCT8 was not associated with its respective protein complex members in cluster 5, but was connected with cluster 2 that represents mostly ribosomal subunits. Further, proteins that were not significantly enriched such as p62 or Serine/threonine-protein kinase Nek9 (NEK9) were excluded from the analysis although their association with autophagy is apparent. This could indicate that the statistical test applied is too stringent and that also proteins that do not show a significant change compared to control cells could be target proteins of autophagy.

7.5 VALIDATION OF POTENTIAL CARGO PROTEINS OF DNA DAMAGE-INDUCED AUTOPHAGY

The ProtK protection assay was used to validate selected proteins from the autophagosome content profiling experiment after ETO treatment (Figure 22A). To validate the assay, endogenous LC3B, the SAR p62 and a previously reported DNA damage-induced protein target in yeast, RRM1, were validated, first [206]. All three proteins were resistant towards treatment with ProtK indicating their protection by autophagosomal membranes (Figure 22B). Despite their enrichment in the MS-based experiment towards cells treated with ETO, the protein levels of all three proteins seemed to be similar in the ProtK protection assay when compared to cells treated with DMSO (Figure 22C). As U2OS cells initiate autophagy significantly from 6h CPT treatment on, one can assume that ETO treatment does the same at a similar time point. Hence, U2OS cells that were treated for 16h with ETO initiated DNA damage-induced autophagy already for about 10h, before autophagosomes were purified from whole cell extracts. Further, BafA was applied only in the last two hours of the ETO treatment to accumulate autophagosomes. Hence, the autophagosomal content identified by APEX2-FLAG-LC3B proximity biotinylation represents cargo that was captured after DNA damage-induced autophagy was active for approximately 8h. Accordingly, protein levels of autophagy-regulated target proteins must have been downregulated for about 8h, before

BafA treatment would have partially rescued the turnover, which might result in the missing accumulation of autophagosomal cargo in the ProtK protection assay (Figure 22D).

Among the proteins identified by autophagosomal content profiling after ETO treatment, several were of nuclear localization or had been reported to function partially inside the nucleus (Figure 22C). Using the ProtK protection assay, several of the candidate proteins were validated (Figure 22D). This included the nuclear lamina protein LMNA and LMNC that had been reported to be degraded by autophagy in cells that undergo oncogene-induced senescence, but also during DNA damage-induced micronucleophagy [225,319,320]. Other proteins of the nuclear envelope such as LMNB1 or proteins that were described as mediators of autophagy-dependent degradation of lamins such as SMURF2 or UBE2I were not identified by the autophagosome content profiling approach [225,320,321]. The protein arginine N-methyltransferase 1 (PRMT1) was also validated by ProtK protection assay. Among the target proteins of PRMT1 are histones and potentially the lamins LMNA and LMNC [322,323]. Whether PRMT1 is selectively degraded by autophagy or eventually engulfed as a bystander next to parts of the nuclear envelope after DNA damage remains to be determined. Of note, PRMT1 is the homologue of *Caenorhabditis elegans epg-11*, which has been implicated into the autophagic removal of P granules, ribonucleoprotein aggregates formed in the germline [324,325]. Calnexin (CANX) that was also validated as a cargo protein has recently been associated to mediate the selective autophagy of procollagen in collaboration with the reticulophagy receptor FAM134B [316]. CANX resides in the ER, which is associated with the outer face of the nuclear lamina and could therefore be degraded together with parts of the nuclear envelope or associated to MN after DNA damage.

The nucleoside diphosphate kinase A (NME1) has also been validated using ProtK protection assay, which confirmed its lysosomal regulation that had been reported earlier [326]. NME1 is diverse in its catalytic activities as it possesses 3’-5’ exonuclease activity and can phosphorylate as a protein and nucleoside kinase different types of substrates [327]. It is considered a metastasis suppressor as mutants without functional 3’-5’ exonuclease activity lose their ability to suppress metastasis in xenograft models [328,329]. NME1 is involved in the Granzyme A-mediated cell death pathway, where it is part of the ER-associated protein complex SET composed of the 3’-5’ exonuclease TREX1 and other proteins [330,331]. Upon Granzyme A-mediated activation of the complex, NME1 and TREX1 work in concert to cause lethal DNA damage inside the nucleus [331]. Intriguingly, upon rupture of the nuclear envelope of MN, TREX1 has recently been implicated in limiting the CGAS-mediated immune response by NME1-independent degradation of the micronucleated DNA [332].

Among the top hits of the MS-based dataset are the histone variants histone H2A and H2B that are known to dimerize before assembling to a nucleosome with other histones such as the histone dimer H3-H4 [333]. Histones H3 and H4 were also identified by MS, but only in one of the four replicates H3 was quantified. Interestingly, histone H2A could not be validated by the ProtK protection assay suggesting that H2A was not protected by autophagosomal

membranes. Whether this means that H2A is not a cargo, but rather a LC3B proximal protein on the autophagosomal surface requires further investigation. However, the developers of autophagosome content profiling described recently some proteins as ProtK-indigestable due to their RNA- or lipid-binding conformation, which included histones, ribosomal and proteasomal subunits [264]. They excluded these proteins from their further analysis and designated them as contaminants, but noted that this could be erroneous. Notably, after their translation at ER-resident ribosomes histones are bound by dedicated histone chaperones that ensure their proper folding and import to the nucleus. The histone chaperone that binds the H2A-H2B dimer is NAP1L1 that could be validated as a ProtK protected cargo protein (Figure 22D) [334,335]. Several reports indicate that the nuclear import of histone H2A-H2B is mediated by an interplay of the histone dimer with NAP1L1 and different importins such as KPNB1, IPO5, IPO4 and IPO9 and the GTP-binding nuclear protein Ran [336–338]. These and other proteins associated to the nuclear import and export machinery were identified by autophagosome content profiling after ETO treatment. Some interactions between importins and hATG8s had been reported earlier [261]. Finally, IPO5 was selected for validation using ProtK protection assay (Figure 22D).

NEK9 has recently been described as an selective autophagy adaptor for MYH9 to regulate primary cilium biogenesis [339]. Its LIR-based interaction with hATG8s had been reported before [261,340]. Following studies revealed that NEK9 can phosphorylate hATG8s to change their affinities to the SARs p62 and NBR1 [341]. Despite its description as an autophagy adaptor that is not degraded upon autophagy activation, NEK9 was validated as an ETO-induced autophagy cargo using the ProtK protection assay (Figure 22D). Whether NEK9 can be degraded by ETO-induced autophagy or turns out to be a proximal protein of LC3B that escaped ProtK digestion requires further studies.

Validation of the cargo proteins over the whole cell lysate was not successful under the conditions tested (Figure 23). Presumably, the long half-live of some of the proteins did not allow their validation via Western blotting. The generation of KO cells as outlined within the introduction would allow examining the protein levels independent of chemical or siRNA-mediated inhibition of autophagy. Fluorescence-microscopy experiments to indicate the co-localization of cargo proteins with ATG marker proteins such as LC3B or LAMP1 are frequently used in literature to show their regulation by autophagy. Similarly, selective types of autophagy could be discriminated by examining the co-localization with SARs.

7.6 CONCLUDING REMARKS

The GO term analysis of the autophagosome content profiling dataset points into the direction of ETO-induced degradation of FAs, which are known targets of autophagy [308]. FA turnover plays a role in the motility of cells, but also during metastasis [307,309]. In line, ETO-induced autophagy led to the degradation of NME1 that has been described as a metastasis suppressor [326,329,342]. Hence, autophagy-mediated degradation of NME1 would favor metastasis simultaneously to FA turnover. Autophagy has been connected to metastasis in various

cancers [343,344]. It would be of major clinical interest to investigate potential roles of ETO-based chemotherapy on autophagy-mediated metastasis.

The cluster analysis did not recognize a FA-associated cluster as only few proteins that are associated with FA, such as VCL and Fascin, were significantly enriched and considered for analysis. Nevertheless, a cluster of nuclear proteins was identified suggesting the regulation of proteins with nuclear localization or function by autophagy. Removal of nuclear proteins by autophagy has not been in the scope of the autophagy field as it is considered a cytoplasmic process. Single publications report CMA of nuclear proteins or regulation of nuclear envelope proteins by autophagy and recently CGAS was identified as SARs for the removal of MN. Given that histones and other chromatin-associated proteins such as the histone chaperone NAP1L1 were identified in the dataset, the autophagosomes enriched after ETO treatment might have contained MN or nuclear blebs derived from damaged nuclei.

Intriguingly, recent studies report the proteasomal degradation of histones after genotoxic stress, which has positive effects on DNA repair in yeast [345,346]. Of note, NAP1L1 is part of a protein family of histone chaperones that are conserved in eukaryotes [347]. Interestingly, a family member in yeast, Vps75 that in contrast to the other members of the family binds preferentially H3-H4, was originally discovered in a genomic screen for vacuolar sorting proteins [348–350]. Its deletion had effects on vacuolar morphology and protein sorting suggesting a role outside the nucleus. Hence, as CMA of H3-H4 has been reported in cells devoid of the histone chaperone NASP, it would be of great interest to investigate a role for NAP1L1 in selective degradation of H2A-H2B after genotoxic stress [318].

PTMs play a major role in the regulation of selective types of autophagy [31,32,351]. In accordance, a recent study revealed that NEK9 can phosphorylate hATG8s that changes their affinities to the SARs p62 and NBR1 [341]. Hence, it would be tempting to speculate that ETO treatment would induce the NEK9-mediated switch to a selective form of hATG8-dependent autophagy. Of note, a MS-based study reported the interaction of NEK9 with the histone chaperone NAP1L1 [261].

8 MATERIAL AND METHODS

8.1 LIST OF CONSUMABLES, MACHINES AND SOFTWARE

Table 1: List of general consumables, machines and software used.

General solutions or chemicals	
Item	**Supplier**
Acetic acid	Sigma Aldrich
Acetone	Sigma Aldrich
Acetonitrile (ACN)	Sigma Aldrich
Ethanol	Sigma Aldrich
Formic acid	Sigma Aldrich
Methanol	Sigma Aldrich
RNase free water	Sigma Aldrich
Sodium chloride (NaCl)	Sigma Aldrich
Trifluoroacetic acid (TFA)	Sigma Aldrich
Cell culture	
Item	**Supplier/Composition**
0.05% Trypsin-EDTA	Gibco
Fetal bovine serum (FBS)	Gibco
100 U/ml Penicillin/Streptomycin	Gibco
L-glutamine	Gibco
ATM inhibitor KU-55933	Selleckchem
ATR inhibitor VE-821	Selleckchem
Bailomycin A	Sigma Aldrich
Biotin-phenol	Sigma Aldrich
Campthecin	Sigma Aldrich
CHK1 inhibitor CHIR-124	Selleckchem
CHK2 inhibitor BML-277	Selleckchem
Cisplatin	Sigma Aldrich
Dialyzed FBS (10,000 molecular weight cut-off)	Sigma Aldrich
Dimethyl sulfoxide (DMSO)	Sigma Aldrich
D-MEM for SILAC without lysine and arginine	Life Technologies
DNA-PKcs inhibitor NU7441	Selleckchem
Dulbecco's Modified Eagle Medium (D-MEM)	Gibco
Dulbecco's Phosphate-Buffered Saline (D-PBS)	Gibco
Earle's Balanced Salt Solution	Life Technologies
Etoposide	Sigma Aldrich
G418	Invivogen
Hydrogenperoxide	Sigma Aldrich
Hydroxyurea	Sigma Aldrich
Hygromycin	Invivogen
L-arginine (Arg0)	Cambridge Isotope Laboratories
L-arginine- U-^{13}C6 99% (Arg6)	Cambridge Isotope Laboratories
L-arginine-U-^{13}C6-^{15}N4 99% (Arg10)	Cambridge Isotope Laboratories

L-lysine (Lys0)	Cambridge Isotope Laboratories
L-lysine- U-^{13}C6-^{15}N2 99% (Lys8)	Cambridge Isotope Laboratories
L-lysine-4,4,5,5,-D4 96–98% (Lys4)	Cambridge Isotope Laboratories
Puromycin	Invivogen
Quenching solution	1 mM sodium azide, 10 mM sodium ascorbate and 5 mM Trolox in DPBS

Transfection

Item	Supplier
Linear polyethylenimine transfection (PEI, HCl Max, 40000)	Polysciences, Inc.
Lipofectamine RNAiMAX	Life Technologies
Opti-MEM with GlutaMAX	Gibco

Cell lysis

Item	Supplier/Composition
1 mM sodium orthovanadate	Sigma Aldrich
5 mM sodium fluoride	Sigma Aldrich
5 mM β-glycerophosphate	Sigma Aldrich
Complete protease inhibitor cocktail tablets	Roche Diagnostics
Dithiothreitol (DTT)	Sigma Aldrich
Modified RIPA buffer	50 mM Tris-HCl pH 7.5, 150 mM NaCl, 1 mM EDTA, 1% NP-40, 0.1% Sodium-deoxycholate
N-ethylmaleimide (NEM)	Sigma Aldrich
NuPAGE LDS Sample Buffer (4×) (LDS SB)	Thermo Fisher Scientific
QuickStart Bradford 1 × Dye Protein Reagent	BioRad
RIPA buffer	50 mM Tris-HCl, pH 7.4, 1% Triton X-100, 0.5% Sodium Deoxycholate, 0.1% SDS • 150mM NaCl

Autophagosome fractionation

Item	Supplier/Composition
Homogenization solution I	10 mM KCl,1.5 mM $MgCl_2$, 10 mM HEPES-KOH and 1 mM DTT pH 7.5
Homogenization solution II	75 mM KCl, 22.5 mM $MgCl_2$, 220 mM HEPES-KOH and 0.5 mM DTT pH 7.5
30 mg/ml proteinase K	New England Biolabs
PMSF	Sigma Aldrich
Dounco homogenizer 1mL, Pistill B	Faust Lab Science
Triton X-100	Sigma Aldrich

Pulldowns

Item	Supplier
High Capacity NeutrAvidin™ Agarose	Thermo Scientific

SDS-PAGE & Western blotting

Item	Supplier/Composition
0.45 µm nitrocellulose	Sigma Aldrich
Blocking buffer	10% skimmed milk solution in PBS-T
Blocking buffer Strep-HRP	3% BSA in PBS-T
Bovine serum albumin (BSA)	Sigma Aldrich
Colloidal Blue Staining Kit	Life Technologies
NuPAG MOPS SDS Running Buffer (20X)	Thermo Fisher Scientific

NuPAGE Bis-Tris gels 4-12%	Thermo Fisher Scientific
PBS-T	1x PBS, 0.1% Tween-20
Ponceau S	Sigma Aldrich
Ponceau S solution	0.1% (w/v) Ponceau S, 5% acetic acid
Primary antibody solution	5% BSA, 0.06% sodium azide
Secondary antibody solution	5% skimmed mild in PBS-T
SuperSignal West Pico Chemiluminescent Substrate	Thermo Scientific
Strep-HRP solution	1% BSA in PBS-T
Transfer buffer	25 mM Tris, 192 mM Glycine, 20% (v/v) methanol, pH 8.3

Flow cytometry

Item	Supplier
Annexin V Pacific Blue™ Ready Flow Conjugate	Thermo Scientific

Mass spectrometry

In-gel digestion

Item	Supplier/Composition
Chloroacetamide (CAA)	Sigma Aldrich
Sequencing grade Trypsin (0.5 µg/µl in 50 mM acetic acid)	Sigma Aldrich
Buffer B	80% ACN, 0.5% acetic acid
Destaining solution	50% Ethanol, 50 mM ABC buffer pH 8.0
Digestion buffer	25 mM ABC buffer pH 8.0
Peptide extraction buffer	30% ACN, 3% TFA

Stage tipping

Item	Supplier/Composition
Buffer A	0.1% formic acid
Buffer A*	5% ACN, 0.1% TFA
Buffer B	80% ACN, 0.1% formic acid
C18 elution buffer	50% ACN, 0.1% formic acid
C18 Empore 47 mm extraction disks	CDS Analytical

Table 2: List of antibodies used.

Antibodies

anti-	Product number	Supplier	Dilution	Origin
anti-mouse-HRP		Jackson ImmunoResearch Laboratories	1:5000	rabbit
anti-rabbit-HRP		Jackson ImmunoResearch Laboratories	1:5000	mouse
ATG9A	ab108338	Abcam	1:1000	rabbit
ATM	2873	Cell Signaling	1:1000	rabbit
ATR	13934	Cell Signaling	1:1000	rabbit
CANX	2679	Cell Signaling	1:1000	rabbit
CASP3	9662	Cell Signaling	1:1000	rabbit
CCT3	NBP1-79040	Novus Biologicals	1:1000	rabbit
DDX39A	SAB2700315	Sigma	1:1000	rabbit

DNA-PKcs	4602	Cell Signaling	1:1000	rabbit
FLAG M2	F1804	Sigma	1:1000	mouse
H2A	3636	Cell Signaling	1:1000	mouse
IMPDH2	36281	Cell Signaling	1:1000	rabbit
IPO5	PA5-30076	Thermo Fisher Scientific	1:1000	rabbit
LMNA/C	4777	Cell Signaling	1:1000	mouse
MAP1LC3B	NB100-2220	Novus Biologicals	1:500	rabbit
NAP1L1	14898-1-AP	Proteintech	1:1000	rabbit
NEK9	MA5-25650	Thermo Fisher Scientific	1:1000	mouse
NME1	TA801245S	OriGene	1:1000	mouse
p-AMPK (T172)	2531	Cell Signaling	1:1000	rabbit
PARP1	sc-8007	Santa Cruz Biotechnology	1:1000	mouse
p-CHK1 (S345)	2341	Cell Signaling	1:1000	rabbit
p-CHK2 (T68)	2661S	Cell Signaling	1:1000	rabbit
p-p70S6K (T389)	9205	Cell Signaling	1:1000	rabbit
PRMT1	2449	Cell Signaling	1:1000	rabbit
p-ULK (S638)	14205	Cell Signaling	1:1000	rabbit
p-ULK (S757)	6888T	Cell Signaling	1:1000	rabbit
RPS10	ab151550	Abcam	1:1000	rabbit
RRM1	8637	Cell Signaling	1:1000	rabbit
SQSTM1/p62	88588	Cell Signaling	1:1000	mouse
Strep-HRP	21130	Thermo Scientific	1:5000	
β-actin	A2228	Sigma	1:10,000	mouse

Table 3: List of plasmids and siRNA used.

Plasmids, siRNAs	
Item	**Supplier**
ATM	Dharmacon Pool
ATR	Dharmacon Pool
Control	Dharmacon Pool
DNA-PKcs	Dharmacon Pool
pcDNA-53-DEST-LC3B-FLAG-APEX2	unknown

Table 4: List of software used.

Software	
Item	**Developer**
Adobe Illustrator CC2021	Adobe
Cytoscape version 3.8.2	Ideker lab
Graphpad Prism 9	Prism
MaxQuant v1.5.2.8	Mann/Cox lab
Microsoft Excel	Microsoft
Perseus 1.6.14.0	Mann/Cox lab
R studio 3.4.4.	R studio PBC

Table 5: List of machines used.

Machines	
Item	**Supplier**
BD LSRFortessa SORP	BD Biosciences
ChemiDoc imaging system	BioRad
Easy-LC-1000	Thermo Fisher Scientific
NuPage Novex Gel System	Thermo Fisher Scientific
Q Exactive Plus	Thermo Fisher Scientific
Thermo Scientific 3311 Forma Steri-Cult CO2 Incubator	Eppendorf
Thermoshaker	Eppendorf
UV-C irradiator	Inhouse built
Vacufuge Plus	Eppendorf

8.2 CELL CULTURE

8.2.1 CULTIVATION OF CELLS

U2OS cells were obtained from ATCC and cultivated in D-MEM medium. RPE-1 cells were obtained from the Roukos lab and were cultivated in D-MEM F12 medium. Both media were supplemented with 10% fetal bovine serum, L-glutamine, penicillin and streptomycin. U2OS cells stably expressing mCherry-eGFP-LC3B (tandem-LC3B) were cultivated in D-MEM additionally supplemented with 1 µg/ml puromycin. RPE-1 cells stably expressing RFP-GFP-LC3B (tandem-LC3B) were obtained from the Dikic lab and cultivated in D-MEM F12 additionally supplemented with 1 µg/ml puromycin and 0.02 mg/ml hygromycin. U2OS cells stably expressing APEX2-FLAG-LC3B were cultivated in D-MEM additionally supplemented with 0.5 mg/ml G418. For SILAC, U2OS cells were cultivated in media containing isotope-labelled or isotope-free L-arginine and L-lysine, L-arginine (Arg0), L-lysine (Lys0), L-arginine- U-^{13}C6 99% (Arg6), L-lysine-4,4,5,5,-D4 96–98% (Lys4), L-arginine-U-^{13}C6-^{15}N4 99% (Arg10), L-lysine- U-^{13}C6-^{15}N2 99% (Lys8) (Cambridge Isotope Laboratories) as described previously [282]. Passaging of the cells included two washing steps with PBS and trypsinization with 0.05% trypsin for 3 min at 37°C. Afterwards, cells were collected in cultivation medium and centrifuged at 250 *x g* for 5 min, before plated according to the intended confluence. All cells were cultivated in a humidified incubator with 5% CO_2 at 37°C.

8.2.2 TRANSFECTION OF CELLS

For DNA transfection of cells in a 6-well plate, cells were grown to a confluence of 80% in 1 ml complete D-MEM. Next 2.5 µg of plasmid DNA were re-suspended in 150 µl Opti-MEM. 7.5 µl polyethylenimine (PEI) were added to the mix. The reaction tube was vortexed and incubated for 15 min at RT. The mix was added dropwise to the cells. A medium exchange was performed 6 to 12h later. Similarly, for siRNA transfection, 4 µl of siRNA (10 µM) and 5 µl siRNAMax were

each diluted in 100 µl Opti-MEM. The mixtures were combined, mixed by gentle pipetting, and incubated for 5 min at RT. Afterward, they were added to the cells for 6 hours before the medium was replaced with fresh D-MEM.The cells were used for experiments 48 to 72 hours after DNA or siRNA transfection, respectively. Transfection volumes in other culture dish sizes were scaled according to the surface area.

8.2.3 GENERATION OF U2OS CELLS STABLY EXPRESSING APEX2-FLAG-LC3B

U2OS cells were transfected with the respective expression vector. 48h post transfection, cells were seeded sparsely and selection pressure was applied by adding 0.5 mg/ml G418 for one week. The medium was replaced daily to keep selection pressure and remove dead cells. A dilution series was conducted to obtain single cells, which allowed growing cell populations from one clone. The functionality of the construct was checked by induction of biotinylation on a Western blot.

8.3 CELL-BASED ASSAYS

8.3.1 TANDEM-LC3B ASSAY

Cells expressing the tandem-LC3B assay were treated according to the experimental setup. Treatments ended at the same time so that cells were collected simultaneously with trypsin. Trypsin was inactivated by cultivation medium, and then two washes with PBS followed before the measurement by flow cytometry using a BD LSRFortessa SORP.

8.3.2 ANNEXIN V ASSAY

The Annexin V assay was performed according to the manufacturer's instructions before cells were collected and analyzed by flow cytometry using a BD LSRFortessa SORP.

8.3.3 PROTEINASE K PROTECTION ASSAY

Cells were harvested by scraping in PBS supplemented with protease inhibitors and collected in reaction tube. After a centrifugation step at 250 *x g* for 5 min at 4°C, the pellet was resuspended in 500 µL homogenization buffer I. The reaction tube was centrifuged at 500 *x g* for 3 min at 4°C and the pellet was resuspended in 100 µL homogenization solution I and incubated for 20 min at 4°C using an overhead shaker. Cells were resuspended within the supernatant and transferred into a dounce homogenizer after a centrifugation step at 500 *x g* for 3 min at 4°C. The cells were homogenized with 70 strokes of tight fitting pestle B and subsequently transferred into a new reaction tube. One fifth of the total volume of the cell lysate of homogenization buffer II was added, followed by a centrifugation step at 600 *x g* for 10 min. The supernatant was transferred into a new reaction tube. The lysate was equally distributed to 4 different reaction tubes that were treated either with water or 30 µg/mL ProtK or 0.2 % Triton X-100 (supplemented with protease inhibitor) or a combination of ProtK and Triton X-100 for 30 min at 37°C. ProtK was inhibited by PMSF to a final concentration of 5 mM. 1x sample buffer was added to the samples and boiled for 5 min at 95°C.

8.4 PROTEIN BIOCHEMISTRY-RELATED METHODS

8.4.1 CELL LYSIS

Cells were washed twice using ice-cold PBS, and collected and lysed in RIPA buffer (50 mM Tris-HCl, pH 7.5, 150 mM NaCl, 0.1% SDS, 0.5% Deoxycholate, 1% Triton X-100) supplemented with protease inhibitors (Complete protease inhibitor cocktail tablets, Roche Diagnostics), 1mM sodium orthovanadate, 5mM β-glycerophosphate, 5mM sodium floride and 10 mM N-ethylmaleimide (from SIGMA). Afterwards, cell lysates were cleared from cell debris by high-speed centrifugation at 16,000 x g for 15 min. Protein concentration was determined using QuickStart Bradford Protein assay (BioRad) before adding 4x LDS sample buffer supplemented with 1 mM DTT.

8.4.2 IMMUNOBLOTTING

Proteins were resolved on 4-12% gradient SDS-PAGE gels (NuPAGE® Bis-Tris Precast Gels, Life Technologies) and transferred to 0.45 µm nitrocellulose membranes. Membranes were stained with Ponceau S solution (0.1% Ponceau S, 5% acetic acid) before blocking with 10% skimmed milk solution in PBS supplemented with 0.1% Tween-20. Primary antibodies were diluted according to the manufacturer's instructions in 5% BSA supplemented with 0.06% sodium azide and incubated over night at 4°C shaking. Secondary antibodies coupled to horseradish peroxidase (Jackson ImmunoResearch Laboratories) were used in a 1:5000 dilution of 5% skimmed milk in PBS-T and incubated with the membrane for 1h at room temperature. For immunodetection SuperSignal West Pico Chemiluminscent Substrate (Thermo Scientific) was used.

8.5 AUTOPHAGOSOME CONTENT PROFILING

8.5.1 PROXIMITY LABELING

APEX2-mediated biotinylation was induced according to the experimental setup by adding 500 mM BP for 2h at 37°C before addition of 1 mM H_2O_2 for 1min at RT. To enrich autophagosomes 200 nM BafA was applied simultaneously to the BP treatment. After induction of biotinylation, cells were washed three times with quenching solution and three times with PBS. Cells were trypsinized for 3 min at 37°C and collected in PBS. Cells were centrifuged at 250 *x g* for 5 min and washed two times more in PBS. The pellet was resuspended in 3 mL of PBS and cells were counted. Inputs were taken from each SILAC condition to check for biotinylation according to the respective treatment. Cells were mixed in a 1:1:1 ratio based on cell numbers.

8.5.2 PROTEINASE K DIGEST & STREPTAVIDIN PULLDOWN

All steps below were performed at 4°C. Cells were washed in 6 mL homogenization buffer I, centrifuged for 3 min at 500 *x g* and resuspended in 6 mL homogenization buffer I. Cells were incubated in an overhead shaker for 20 min. Afterwards, cells were centrifuged for 3 min at 500 *x g* and 5 mL of the supernatant were carefully removed. The remaining 1 mL was used to

resuspend the pellet and transfer it into a dounce homogenizer. Cells were dounced with 70 strokes of tight fitting pestle B and subsequently transferred into a new reaction tube. One fifth of the total volume of the cell lysate of homogenization buffer II was added, followed by a centrifugation step at 600 *x g* for 10 min. The supernatant was transferred into a new reaction tube. Per mL lysate 30 µg ProtK were added including 1 mM $CaCl_2$ and incubated for 30 min at 4°C. ProtK was inactivated by application of PMSF to a final concentration of 5 mM. Cell lysated were cleared by centrifugation at 17,000 *x g* for 15 min. The pellet was resuspend in RIPA buffer for 30 min prior to centrifugation at 20,000 *x g* for 15 min. The autophagosome-rich fraction was incubated overnight with 30 µL pre-equilibrated NeutrAvidin beads. Beads were washed 4x times with RIPA buffer. Proteins were eluted by boiling in 3x sample buffer supplemented with 1 mM DTT for 20 min at 95°C.

8.6 MS-BASED PROTEOMICS

8.6.1 IN-GEL DIGESTION

Prior to resolving proteins on 4-12% gradient SDS-PAGE gels (NuPAGE® Bis-Tris Precast Gels, Life Technologies), samples with sample buffer were incubated for 30 min in the dark with 4.5 mM CAA. Gels were stained with the Colloidal Blue Staining Kit. Lanes were cut into 4-5 gel pieces and subsequently washed four times with destaining buffer and twice with ethanol before in-gel digestion with 0.625 µg trypsin in digestion buffer was performed overnight at 37°C. In-gel digestion was stopped by incubation with peptide extraction buffer for 20 min at RT. The supernatant was collected in a new reaction tube. Subsequently peptides were extracted from the gel pieces by 20 min incubations with peptide extraction buffer, buffer B and ACN, respectively and supernatant were collected in the same reaction tube corresponding to the initial gel piece. Peptides were vacuum concentrated at 45°C to reduce the sample volume to 100 µL. Samples were acidified to pH 2 using TFA, when necessary.

8.6.2 DESALTING AND CONCENTRATION OF PEPTIDES

Peptide purification was performed by the use of stop-and-go-extraction tips (StageTips) [352]. Therefore, two disks from a C_{18} 47 mm extraction disk were cut out with the help of a 17-gauge Hamilton syringe and pressed into a 200 µl pipette tip. The StageTips were washed consecutively by different centrifugation steps at 500 *x g* with 25 µL methanol, 25 µL buffer B and twice with 25 µL buffer A. Afterwards, the acidified sample was loaded to the C_{18} material and washed with 50 µL buffer A. Peptides were eluted into a 96-well plate by placing the StageTips into a rack and passing 50 µL elution buffer through the C_{18} material by centrifugation at 300 *x g*. The volume was reduced to 4.5-5 µL by vacuum concentration at 45°C. Finally, 1 µl of buffer A* was added to the samples.

8.6.3 MS ANALYSIS

Peptide fractions were loaded via UHPLC to a C_{18} reversed phase chromatography nanospray column and eluted with a linear ACN gradient containing 0.1% formic acid. The MS was

operated in data-dependent mode automatically switching between MS and MS_2 acquisition. MS spectra (*m*/*z* 300-1650) were acquired in the Orbitrap mass analyzer with a resolution of 70,000 at *m*/*z* = 200, after accumulation of ions to a target value of 3e6 estimated based on predictive automatic gain control from the previous full scan. The ten most intense ions were isolated using the quadrupole mass filter (maximum injection time 120 ms, isolation window 2.6 *m*/*z*, AGC target 1e5) and subsequently fragmented in the higher-energy C-trap dissociation (HCD) cell [353]. MS_2 spectra were acquired in the Orbitrap mass analyzer with a resolution of 35,000 at *m*/*z* = 200. Peptides with unassigned charge states, as well as with charge states <+2, were excluded from fragmentation.

8.6.4 MS PEPTIDE IDENTIFICATION

Raw data files were analyzed using MaxQuant (version 1.5.2.8) [274]. 95,057 human protein sequences obtained from the UniProtKB released in May 2018 using Andromeda search engine [275]. Spectra were searched with a mass tolerance of 6 ppm in MS mode, 20 ppm in HCD MS_2 mode, strict trypsin specificity and allowing up to two miscleavages. Cysteine carbamidomethylation was searched as a fixed modification, whereas protein N-terminal acetylation and methionine oxidation were searched as variable modifications. Potential contaminants and reverse identifications were filtered from the dataset based on a posterior error probability (PEP) ratio to arrive at a false discovery rate of below 1% estimated using a target-decoy approach [354]. Match between runs and re-quantify functions were switched on.

8.6.5 DATA PROCESSING AND VISUALIZATION

Statistical analysis was performed using the R software environment, the Graphpad Prism software and Microsoft excel. Statistical significance was calculated using two-sided ANOVA followed by Tukey's post hoc test or Welch test. Functional protein interaction network analysis was performed using interaction data from the STRING database [355]. Only interactions with a score higher 0.7 are represented in the networks. Cytoscape version 3.8.2 was used for visualization of protein interaction networks [356]. Cluster analysis was performed using the mcode algorithm within "stringApp" in cytoscape. GO term enrichment analysis was carried out using PANTHER and p-values were calculated by binomial statistics [357]. Perseus (v1.6.14.0) was used for the visualization of MS data [374, 543].

9 APPENDIX I

9.1 SUPPLEMENTARIES

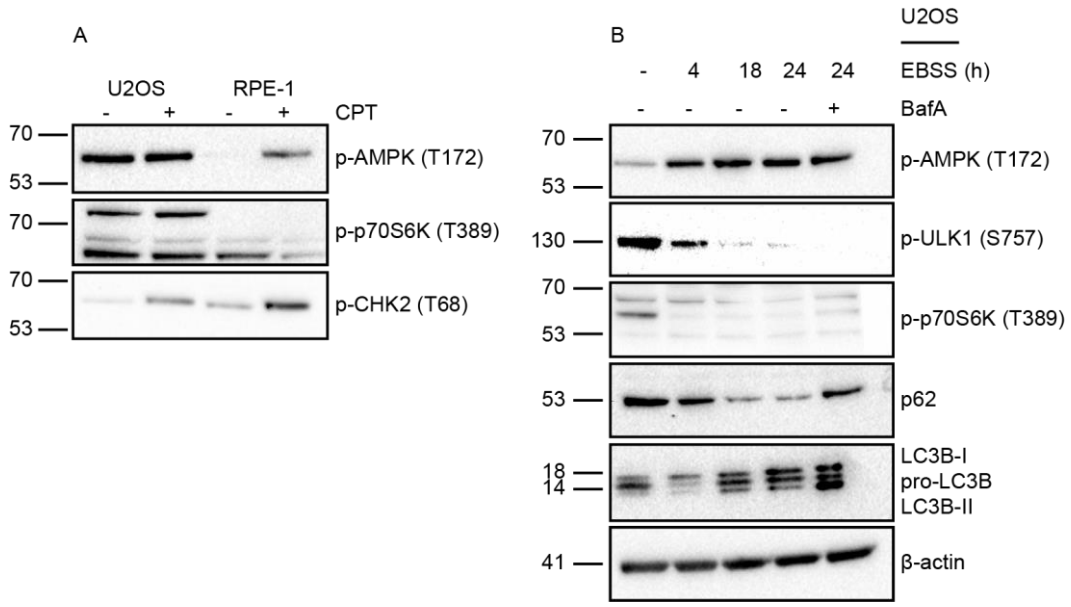

Figure 24: ATG signaling events in cancer and non-cancerous cells. **(A)** p-AMPK (T172) was assessed after CPT treatment. mTORC1 activity was assessed by blotting for p-p70S6K (T389). U2OS cells were treated with or without 10 µM CPT for 16h. RPE-1 cells were treated with or without 2 µM CPT for 18h. **(B)** U2OS cells were treated for indicated time points with starvation medium. 200 nM BafA was used in the last 4h of the EBSS treatment where indicated.

9.2 LIST OF ABBREVIATIONS

Abbreviation	Term
ABC	Ammonium bicarbonate
ACD	Autophagic cell death
ACN	Acetonitril
ADP	Adenosine diphosphate
AIM	ATG8-family interacting motif
AMP	Adenosine monophosphate
AMPK	AMP-activated protein kinase
APEX2	Ascorbate peroxidase 2
ATG	Autophagy-related
ATG8	Autophagy-related protein 8
ATM	Ataxia telangiectasia mutated
ATP	Adenosine triphosphate
ATR	Ataxia telangiectasia and Rad3-related protein
BafA	Bafilomycin A_1
BER	Base excision repair
BP	Biotin-phenol
BRCA1	Breast cancer type 1 susceptibility protein
BRCA2	Breast cancer type 2 susceptibility protein
C18	Octadodecyl alkane chains

Appendix I: 9.2 List of abbreviations

CAA	Chloroacetamide
CANX	Calnexin
CC	Cellular compartment
CCT	Chaperonin containing tailless complex polypeptide 1
CDKN1A	Cyclin-dependent kinase inhibitor 1
CHK1	Serine/threonine-protein kinase Chk1
CHK2	Serine/threonine-protein kinase Chk2
CHX	Cycloheximide
CIS	Cisplatin
CMA	Chaperone-mediated autophagy
CPT	Camptothecin
C-terminus	Carboxy-terminus
DDR	DNA damage response
DKO	Double knockout
DNA	Deoxyribonucleic acid
DNA-PK	DNA-dependent protein kinase
DNA-PKcs	DNA-dependent protein kinase catalytic subunit
DNS	Desoxyribonukleinsäure
dNTP	Deoxynucleotide triphosphate
DOX	Doxorubicin
DSB	Double strand break
DTT	Dithiothreitol
e.g.	exempli gratia
E1	Ubiquitin-activating enzyme
E2	Ubiquitin-conjugating enzyme
E3	Ubiquitin-ligating enzyme
EBSS	Earle's Balanced Salt Solution
eGFP	enhanced GFP
ER	Endoplasmic reticulum
ETO	Etoposide
EXO1	Exonuclease 1
FA	Focal adhesion
FDR	False discovery rate
GABARAP	γ-aminobutyric acid receptor-associated protein
GFP	Green fluorescent protein
GO	Gene Ontology
GTA	Genotoxin-induced Targeted Autophagy
Gy	Gray
H2O2	Hydrogen peroxide
hATG8s	human ATG8 proteins
HEPES	4-(2-hydroxyethyl)-1-piperazineethanesulfonic acid
HR	Homologous recombination
HSPA8	Heat shock cognate 71 kDa protein
HU	Hydroxyurea
ICL	Inter-strand crosslink
ICLR	Inter-strand crosslink repair

Appendix I: 9.2 List of abbreviations

IMB	Institute of Molecular Biology
IMM	Inner mitochondrial membrane
IR	Ionizing radiation
K	Lysine
KEGG	Kyoto Encyclopedia of Genes and Genomes
KO	Knockout
LAMP2A	Lysosome-associated membrane glycoprotein 2A
LC-MS/MS	Liquid chromatography and tandem mass spectrometry
LFQ	Label-free quantification
LIR	LC3 interacting regions
LKB1	Liver kinase B1
m/z	Mass to charge
M1	Amino-terminal methionine
MAP1LC3	Microtubule-associated proteins 1A/1B light chain 3
MCF-7	Michigan Cancer Foundation - 7
MEFs	Mouse embryonic fibroblasts
MF	Molecular function
MMR	Mismatch repair
MMR	DNA mismatch-repair
MMS	Methyl methanesulfonate
MN	Micronuclei
MRN	MRE11-RAD50-NBS1
mRNA	Messenger RNA
MS	Mass spectrometry
MS/MS	Tandem MS
mTOR	mechanistic Target Of Rapamycin
mTORC1	mechanistic Target Of Rapamycin Complex 1
N	Number of biological replicates
NAD+	Nicotinamide adenine dinucleotide
NEK9	Serine/threonine-protein kinase Nek9
NEM	N-ethylmaleimide
NER	Nucleotide excision repair
NHEJ	Non-homologous end joining
NME1	Nucleoside diphosphate kinase A
NOXA	Phorbol-12-myristate-13-acetate-induced protein 1
PARP	Poly (ADP-ribose) polymerase
PBS	Phosphate buffered saline
PCNA	Proliferating cell nuclear antigen
PCR	Polymerase chain reaction
PE	Phosphatidylethanolamine
PEI	Polyethylenimine
PEP	Posterior error probability
PI3K	Phosphatidylinositol-3-kinase
PIK3C3	Phosphatidylinositol 3-kinase catalytic subunit 3
PIKKs	Phosphatidylinositol 3-kinase-related kinases
PMSF	Phenylmethylsulfonyl fluoride

Appendix I: 9.2 List of abbreviations

POLδ	DNA polymerase δ
POLε	DNA polymerase ε
PPI	Protein-protein interaction
PRMT1	Protein arginine N-methyltransferase 1
ProtK	Proteinase K
PtdIns	Phosphatidylinositol
PtdIns3K	Phosphatidylinositol 3-kinase
PtdIns3P	Phosphatidylinositol-3-phosphate
PTM	Posttranslational modification
R	Arginine
RB	Retinoblastoma protein
RFP	Red fluorescent protein
RIPA	Radioimmunoprecipitation assay buffer
RNA	Ribonucleic acid
RNR	Ribonucleotide reductase
RNS	Reactive nitrogen species
ROS	Reactive oxygen species
RPA	Replication protein A
RPE-1	human retinal pigment epithelial-1 cells
RT	Room temperature
S	Substrate
S6Ks	RPS6 ribosomal protein kinases
SAR	Selective autophagy receptor
SDS-PAGE	Sodium dodecyl sulfate polyacrylamide gel electrophoresis
SILAC	Stable isotope labeling with amino acids in cell culture
siRNA	Short interfering RNA
SQSTM1	Sequestosome-1
SSBs	DNA single strand breaks
ssDNA	Single stranded DNA
ssDNA	single-stranded DNA
StageTips	Stop-and-go-extraction tips
SUMO	Small ubiquitin-related modifier
TDP1	Tyrosyl DNA phosphodiesterase 1
TDP2	Tyrosyl DNA phosphodiesterase 2
TEM	Transmission electron microscopy
TEX264	Testis-expressed protein 264
TOP1	Topoisomerase 1
TOP1cc	Topoisomerase 1 cleavage complex
TOP2	Topoisomerase 2
TP53	Cellular tumor antigen p53
TRiQ	Tailless complex polypeptide 1 ring complex
U2OS	Human Bone Osteosarcoma Epithelial Cells
Ub	Ubiquitin
UBL	Ubiquitin-like
ULK1	Uncoordinated-51-like kinase 1
UPS	Ubiquitin-proteasome system

Appendix I: 9.2 List of abbreviations

UV	Ultraviolet
V-ATPase	Vacuolar H^+-translocating ATPase
VCP	Valosin-containing protein
WIPI	WD repeat domain phosphoinositide-interacting protein
WT	Wild type
XRCC5	X-ray repair cross-complementing protein 5
XRCC6	X-ray repair cross-complementing protein 6

10 REFERENCES

10.1 REFERENCES ACCORDING TO APPEARANCE

[1] I. Dikic, Proteasomal and Autophagic Degradation Systems, Annu. Rev. Biochem. 86 (2017) 193–224. https://doi.org/10.1146/annurev-biochem-061516-044908.

[2] N. Mizushima, M. Komatsu, Autophagy: Renovation of Cells and Tissues, Cell. 147 (2011) 728–741. https://doi.org/10.1016/J.CELL.2011.10.026.

[3] A. Ciechanover, Proteolysis: From the lysosome to ubiquitin and the proteasome, Nat. Rev. Mol. Cell Biol. 6 (2005) 79–86. https://doi.org/10.1038/nrm1552.

[4] C. Pohl, I. Dikic, Cellular quality control by the ubiquitin-proteasome system and autophagy, Science (80-.). 366 (2019) 818–822. https://doi.org/10.1126/science.aax3769.

[5] R. Yau, M. Rape, The increasing complexity of the ubiquitin code, Nat. Cell Biol. 18 (2016) 579–586. https://doi.org/10.1038/ncb3358.

[6] C. Hoege, B. Pfander, G.L. Moldovan, G. Pyrowolakis, S. Jentsch, RAD6-dependent DNA repair is linked to modification of PCNA by ubiquitin and SUMO, Nature. 419 (2002) 135–141. https://doi.org/10.1038/nature00991.

[7] C. Doil, N. Mailand, S. Bekker-Jensen, P. Menard, D.H. Larsen, R. Pepperkok, J. Ellenberg, S. Panier, D. Durocher, J. Bartek, J. Lukas, C. Lukas, RNF168 Binds and Amplifies Ubiquitin Conjugates on Damaged Chromosomes to Allow Accumulation of Repair Proteins, Cell. 136 (2009) 435–446. https://doi.org/10.1016/j.cell.2008.12.041.

[8] F. Huang, X. Zeng, W. Kim, M. Balasubramani, A. Fortian, S.P. Gygi, N.A. Yates, A. Sorkin, Lysine 63-linked polyubiquitination is required for EGF receptor degradation, Proc. Natl. Acad. Sci. U. S. A. 110 (2013) 15722–15727. https://doi.org/10.1073/pnas.1308014110.

[9] B.E. Riley, S.E. Kaiser, T.A. Shaler, A.C.Y. Ng, T. Hara, M.S. Hipp, K. Lage, R.J. Xavier, K.Y. Ryu, K. Taguchi, M. Yamamoto, K. Tanaka, N. Mizushima, M. Komatsu, R.R. Kopito, Ubiquitin accumulation in autophagy-deficient mice is dependent on the Nrf2-mediated stress response pathway: A potential role for protein aggregation in autophagic substrate selection, J. Cell Biol. 191 (2010) 537–552. https://doi.org/10.1083/jcb.201005012.

[10] M. Polajnar, M.S. Dietz, M. Heilemann, C. Behrends, Expanding the host cell ubiquitylation machinery targeting cytosolic Salmonella, EMBO Rep. 18 (2017) 1572–1585. https://doi.org/10.15252/embr.201643851.

[11] Y. Nibe, S. Oshima, M. Kobayashi, C. Maeyashiki, Y. Matsuzawa, K. Otsubo, H. Matsuda, E. Aonuma, Y. Nemoto, T. Nagaishi, R. Okamoto, K. Tsuchiya, T. Nakamura, S. Nakada, M. Watanabe, Novel polyubiquitin imaging system, PolyUb-FC, reveals that K33-linked polyubiquitin is recruited by SQSTM1/p62, Autophagy. 14 (2018) 347–358.

https://doi.org/10.1080/15548627.2017.1407889.

[12] T.M. Durcan, M.Y. Tang, J.R. Pérusse, E.A. Dashti, M.A. Aguileta, G. McLelland, P. Gros, T.A. Shaler, D. Faubert, B. Coulombe, E.A. Fon, USP8 regulates mitophagy by removing K6-linked ubiquitin conjugates from parkin, EMBO J. 33 (2014) 2473–2491. https://doi.org/10.15252/embj.201489729.

[13] A. Lilienbaum, Relationship between the proteasomal system and autophagy, Int. J. Biochem. Mol. Biol. 4 (2013) 1–26.

[14] N. Mizushima, B. Levine, A.M. Cuervo, D.J. Klionsky, Autophagy fights disease through cellular self-digestion, Nature. 451 (2008) 1069–1075. https://doi.org/10.1038/nature06639.

[15] D.J. Klionsky, G. Petroni, R.K. Amaravadi, E.H. Baehrecke, A. Ballabio, P. Boya, J.M. Bravo-San Pedro, K. Cadwell, F. Cecconi, A.M.K. Choi, M.E. Choi, C.T. Chu, P. Codogno, M.I. Colombo, A.M. Cuervo, V. Deretic, I. Dikic, Z. Elazar, E. Eskelinen, G.M. Fimia, D.A. Gewirtz, D.R. Green, M. Hansen, M. Jäättelä, T. Johansen, G. Juhász, V. Karantza, C. Kraft, G. Kroemer, N.T. Ktistakis, S. Kumar, C. Lopez-Otin, K.F. Macleod, F. Madeo, J. Martinez, A. Meléndez, N. Mizushima, C. Münz, J.M. Penninger, R.M. Perera, M. Piacentini, F. Reggiori, D.C. Rubinsztein, K.M. Ryan, J. Sadoshima, L. Santambrogio, L. Scorrano, H. Simon, A.K. Simon, A. Simonsen, A. Stolz, N. Tavernarakis, S.A. Tooze, T. Yoshimori, J. Yuan, Z. Yue, Q. Zhong, L. Galluzzi, F. Pietrocola, Autophagy in major human diseases, EMBO J. (2021) e108863. https://doi.org/10.15252/embj.2021108863.

[16] L. Galluzzi, E.H. Baehrecke, A. Ballabio, P. Boya, J.M. Bravo-San Pedro, F. Cecconi, A.M. Choi, C.T. Chu, P. Codogno, M.I. Colombo, A.M. Cuervo, J. Debnath, V. Deretic, I. Dikic, E.-L. Eskelinen, G.M. Fimia, S. Fulda, D.A. Gewirtz, D.R. Green, M. Hansen, J.W. Harper, M. Jäättelä, T. Johansen, G. Juhasz, A.C. Kimmelman, C. Kraft, N.T. Ktistakis, S. Kumar, B. Levine, C. Lopez-Otin, F. Madeo, S. Martens, J. Martinez, A. Melendez, N. Mizushima, C. Münz, L.O. Murphy, J.M. Penninger, M. Piacentini, F. Reggiori, D.C. Rubinsztein, K.M. Ryan, L. Santambrogio, L. Scorrano, A.K. Simon, H.-U. Simon, A. Simonsen, N. Tavernarakis, S.A. Tooze, T. Yoshimori, J. Yuan, Z. Yue, Q. Zhong, G. Kroemer, Molecular definitions of autophagy and related processes., EMBO J. 36 (2017) 1811–1836. https://doi.org/10.15252/embj.201796697.

[17] S. Shimizu, T. Kanaseki, N. Mizushima, T. Mizuta, S. Arakawa-Kobayashi, C.B. Thompson, Y. Tsujimoto, Role of Bcl-2 family proteins in a non-apoptotic programmed cell death dependent on autophagy genes, Nat. Cell Biol. 6 (2004) 1221–1228. https://doi.org/10.1038/ncb1192.

[18] S. Arakawa, M. Tsujioka, T. Yoshida, H. Tajima-Sakurai, Y. Nishida, Y. Matsuoka, I. Yoshino, Y. Tsujimoto, S. Shimizu, Role of Atg5-dependent cell death in the embryonic development of Bax/Bak double-knockout mice, Cell Death Differ. 24 (2017) 1598–1608. https://doi.org/10.1038/cdd.2017.84.

[19] S. Pattingre, A. Tassa, X. Qu, R. Garuti, H.L. Xiao, N. Mizushima, M. Packer, M.D. Schneider, B. Levine, Bcl-2 antiapoptotic proteins inhibit Beclin 1-dependent autophagy, Cell. 122 (2005) 927–939. https://doi.org/10.1016/j.cell.2005.07.002.

[20] S.K. Bhutia, R. Dash, S.K. Das, B. Azab, Z.Z. Su, S.G. Lee, S. Grant, A. Yacoub, P. Dent, D.T. Curiel, D. Sarkar, P.B. Fisher, Mechanism of autophagy to apoptosis switch triggered in prostate cancer cells by antitumor cytokine melanoma differentiation-associated gene 7/interleukin-24, Cancer Res. 70 (2010) 3667–3676. https://doi.org/10.1158/0008-5472.CAN-09-3647.

[21] M. Haller, A.K. Hock, E. Giampazolias, A. Oberst, D.R. Green, J. Debnath, K.M. Ryan, K.H. Vousden, S.W.G. Tait, Ubiquitination and proteasomal degradation of ATG12 regulates its proapoptotic activity, Autophagy. 10 (2014) 2269–2278. https://doi.org/10.4161/15548627.2014.981914.

[22] N. Mizushima, T. Yoshimori, B. Levine, Y. Kong, J.M. Shelton, J.A. Richardson, V. Le, B. Levine, B.A. Rothermel, J.A. Hill, J. Yuan, Methods in mammalian autophagy research., Cell. 140 (2010) 313–26. https://doi.org/10.1016/j.cell.2010.01.028.

[23] R. Huang, Y. Xu, W. Wan, X. Shou, J. Qian, Z. You, B. Liu, C. Chang, T. Zhou, J. Lippincott-Schwartz, W. Liu, xxDeacetylation of nuclear LC3 drives autophagy initiation under starvation, Mol. Cell. 57 (2015) 456–467. https://doi.org/10.1016/j.molcel.2014.12.013.

[24] H. Nakatogawa, Y. Ichimura, Y. Ohsumi, Atg8, a Ubiquitin-like Protein Required for Autophagosome Formation, Mediates Membrane Tethering and Hemifusion, Cell. 130 (2007) 165–178. https://doi.org/10.1016/j.cell.2007.05.021.

[25] N. Mizushima, T. Noda, T. Yoshimori, Y. Tanaka, T. Ishii, M.D. George, D.J. Klionsky, M. Ohsumi, Y. Ohsumi, A protein conjugation system essential for autophagy, Nature. 395 (1998) 395–398. https://doi.org/10.1038/26506.

[26] N. Mizushima, The ATG conjugation systems in autophagy, Curr. Opin. Cell Biol. 63 (2020) 1–10. https://doi.org/10.1016/j.ceb.2019.12.001.

[27] T. Shpilka, H. Weidberg, S. Pietrokovski, Z. Elazar, Atg8: An autophagy-related ubiquitin-like protein family, Genome Biol. 12 (2011) 1–11. https://doi.org/10.1186/gb-2011-12-7-226.

[28] H. Weidberg, E. Shvets, T. Shpilka, F. Shimron, V. Shinder, Z. Elazar, LC3 and GATE-16/GABARAP subfamilies are both essential yet act differently in autophagosome biogenesis, EMBO J. 29 (2010) 1792–1802. https://doi.org/10.1038/emboj.2010.74.

[29] V. Kirkin, History of the Selective Autophagy Research: How Did It Begin and Where Does It Stand Today?, J. Mol. Biol. (2019). https://doi.org/10.1016/J.JMB.2019.05.010.

[30] A. Ordureau, J.A. Paulo, J. Zhang, H. An, K.N. Swatek, J.R. Cannon, Q. Wan, D. Komander, J.W. Harper, Global Landscape and Dynamics of Parkin and USP30-Dependent Ubiquitylomes in iNeurons during Mitophagic Signaling, Mol. Cell. 77 (2020) 1124–1142.e10. https://doi.org/10.1016/j.molcel.2019.11.013.

[31] P. Wild, H. Farhan, D.G. McEwan, S. Wagner, V. V Rogov, N.R. Brady, B. Richter, J. Korac, O. Waidmann, C. Choudhary, V. Dötsch, D. Bumann, I. Dikic, Phosphorylation of the autophagy receptor optineurin restricts Salmonella growth., Science. 333 (2011) 228–33. https://doi.org/10.1126/science.1205405.

[32] B. Richter, D.A. Sliter, L. Herhaus, A. Stolz, C. Wang, P. Beli, G. Zaffagnini, P. Wild, S. Martens, S.A. Wagner, R.J. Youle, I. Dikic, Phosphorylation of OPTN by TBK1 enhances its binding to Ub chains and promotes selective autophagy of damaged mitochondria., Proc. Natl. Acad. Sci. U. S. A. 113 (2016) 4039–44. https://doi.org/10.1073/pnas.1523926113.

[33] J. Korac, V. Schaeffer, I. Kovacevic, A.M. Clement, B. Jungblut, C. Behl, J. Terzic, I. Dikic, Ubiquitin-independent function of optineurin in autophagic clearance of protein aggregates, J. Cell Sci. 126 (2013) 580–592. https://doi.org/10.1242/jcs.114926.

[34] O. Akinduro, K. Sully, A. Patel, D.J. Robinson, A. Chikh, G. McPhail, K.M. Braun, M.P. Philpott, C.A. Harwood, C. Byrne, R.F.L. O'Shaughnessy, D. Bergamaschi, Constitutive Autophagy and Nucleophagy during Epidermal Differentiation, J. Invest. Dermatol. 136 (2016) 1460–1470. https://doi.org/10.1016/J.JID.2016.03.016.

[35] A. Khaminets, T. Heinrich, M. Mari, P. Grumati, A.K. Huebner, M. Akutsu, L. Liebmann, A. Stolz, S. Nietzsche, N. Koch, M. Mauthe, I. Katona, B. Qualmann, J. Weis, F. Reggiori, I. Kurth, C.A. Hübner, I. Dikic, Regulation of endoplasmic reticulum turnover by selective autophagy, Nature. 522 (2015) 354–358. https://doi.org/10.1038/nature14498.

[36] G. Zaffagnini, S. Martens, Mechanisms of Selective Autophagy, JMB. (2016). https://doi.org/10.1016/j.jmb.2016.02.004.

[37] V. Kirkin, V. V. Rogov, A Diversity of Selective Autophagy Receptors Determines the Specificity of the Autophagy Pathway, Mol. Cell. 76 (2019) 268–285. https://doi.org/10.1016/J.MOLCEL.2019.09.005.

[38] A. Khaminets, C. Behl, I. Dikic, Ubiquitin-Dependent And Independent Signals In Selective Autophagy, Trends Cell Biol. 26 (2016) 6–16. https://doi.org/10.1016/j.tcb.2015.08.010.

[39] D. Gatica, V. Lahiri, D.J. Klionsky, Cargo recognition and degradation by selective autophagy, Nat. Cell Biol. 20 (2018) 233–242. https://doi.org/10.1038/s41556-018-0037-z.

[40] C. Demetriades, M. Plescher, A.A. Teleman, Lysosomal recruitment of TSC2 is a universal response to cellular stress, Nat. Commun. 7 (2016) 10662. https://doi.org/10.1038/ncomms10662.

[41] L. Murrow, J. Debnath, Autophagy as a Stress-Response and Quality-Control Mechanism: Implications for Cell Injury and Human Disease, Annu. Rev. Pathol. Mech. Dis. 8 (2013) 105–137. https://doi.org/10.1146/annurev-pathol-020712-163918.

[42] T. Juretschke, P. Beli, Causes and consequences of DNA damage-induced autophagy, Matrix Biol. (2021). https://doi.org/10.1016/j.matbio.2021.02.004.

[43] R. Krick, Y. Muehe, T. Prick, S. Bremer, P. Schlotterhose, E.-L. Eskelinen, J. Millen, D.S. Goldfarb, M. Thumm, Piecemeal Microautophagy of the Nucleus Requires the Core Macroautophagy Genes, Mol. Biol. Cell. 19 (2008) 4492–4505. https://doi.org/10.1091/mbc.E08-04-0363.

[44] Y. Sakai, A. Koller, L.K. Rangell, G.A. Keller, S. Subramani, Peroxisome degradation by microautophagy in Pichia pastoris: Identification of specific steps and morphological intermediates, J. Cell Biol. 141 (1998) 625–636. https://doi.org/10.1083/jcb.141.3.625.

[45] F. Le Guerroué, F. Eck, J. Jung, T. Starzetz, M. Mittelbronn, M. Kaulich, C. Behrends, Autophagosomal Content Profiling Reveals an LC3C-Dependent Piecemeal Mitophagy Pathway, Mol. Cell. 68 (2017) 786–796.e6. https://doi.org/10.1016/J.MOLCEL.2017.10.029.

[46] S. Schuck, Microautophagy - distinct molecular mechanisms handle cargoes of many sizes, J. Cell Sci. 133 (2020). https://doi.org/10.1242/jcs.246322.

[47] C. Park, A.M. Cuervo, Selective Autophagy: Talking with the UPS, Cell Biochem. Biophys. 67 (2013) 3–13. https://doi.org/10.1007/s12013-013-9623-7.

[48] S. Kaushik, A.M. Cuervo, The coming of age of chaperone-mediated autophagy, Nat. Rev. Mol. Cell Biol. 19 (2018) 365–381. https://doi.org/10.1038/s41580-018-0001-6.

[49] D.H. Kim, D.D. Sarbassov, S.M. Ali, R.R. Latek, K.V.P. Guntur, H. Erdjument-Bromage, P. Tempst, D.M. Sabatini, GβL, a positive regulator of the rapamycin-sensitive pathway required for the nutrient-sensitive interaction between raptor and mTOR, Mol. Cell. 11 (2003) 895–904. https://doi.org/10.1016/S1097-2765(03)00114-X.

[50] T.R. Peterson, M. Laplante, C.C. Thoreen, Y. Sancak, S.A. Kang, W.M. Kuehl, N.S. Gray, D.M. Sabatini, DEPTOR Is an mTOR Inhibitor Frequently Overexpressed in Multiple Myeloma Cells and Required for Their Survival, Cell. 137 (2009) 873–886. https://doi.org/10.1016/j.cell.2009.03.046.

[51] K. Thedieck, P. Polak, M.L. Kim, K.D. Molle, A. Cohen, P. Jenö, C. Arrieumerlou, M.N. Hall, PRAS40 and PRR5-Like Protein Are New mTOR Interactors that Regulate Apoptosis, PLoS One. 2 (2007) e1217. https://doi.org/10.1371/journal.pone.0001217.

[52] K. Hara, Y. Maruki, X. Long, K. ichi Yoshino, N. Oshiro, S. Hidayat, C. Tokunaga, J. Avruch, K. Yonezawa, Raptor, a binding partner of target of rapamycin (TOR), mediates TOR action, Cell. 110 (2002) 177–189. https://doi.org/10.1016/S0092-8674(02)00833-4.

[53] C. Betz, M.N. Hall, Where is mTOR and what is it doing there?, J. Cell Biol. 203 (2013) 563–574. https://doi.org/10.1083/jcb.201306041.

[54] M.N. Corradetti, K.L. Guan, Upstream of the mammalian target of rapamycin: Do all roads pass through mTOR?, Oncogene. 25 (2006) 6347–6360. https://doi.org/10.1038/sj.onc.1209885.

[55] Y. Ma, Y. Vassetzky, S. Dokudovskaya, mTORC1 pathway in DNA damage response, Biochim. Biophys. Acta - Mol. Cell Res. 1865 (2018) 1293–1311. https://doi.org/10.1016/j.bbamcr.2018.06.011.

[56] M. Laplante, D.M. Sabatini, An Emerging Role of mTOR in Lipid Biosynthesis, Curr. Biol. 19 (2009) R1046–R1052. https://doi.org/10.1016/j.cub.2009.09.058.

[57] I. Ben-Sahra, J.J. Howell, J.M. Asara, B.D. Manning, Stimulation of de novo pyrimidine synthesis by growth signaling through mTOR and S6K1, Science (80-.). 339 (2013) 1323–1328. https://doi.org/10.1126/science.1228792.

[58] P.E. Burnett, R.K. Barrow, N.A. Cohen, S.H. Snyder, D.M. Sabatini, RAFT1 phosphorylation of the translational regulators p70 S6 kinase and 4E-BP1, Proc. Natl. Acad. Sci. U. S. A. 95 (1998) 1432–1437. https://doi.org/10.1073/pnas.95.4.1432.

[59] I. Papandreou, A.L. Lim, K. Laderoute, N.C. Denko, Hypoxia signals autophagy in tumor cells via AMPK activity, independent of HIF-1, BNIP3, and BNIP3L, Cell Death Differ. 15 (2008) 1572–1581. https://doi.org/10.1038/cdd.2008.84.

[60] H.-U. Simon, R. Friis, S.W.G. Tait, K.M. Ryan, Retrograde signaling from autophagy modulates stress responses., Sci. Signal. 10 (2017) eaag2791. https://doi.org/10.1126/scisignal.aag2791.

[61] B. Xiao, M.J. Sanders, E. Underwood, R. Heath, F. V. Mayer, D. Carmena, C. Jing, P.A. Walker, J.F. Eccleston, L.F. Haire, P. Saiu, S.A. Howell, R. Aasland, S.R. Martin, D. Carling, S.J. Gamblin, Structure of mammalian AMPK and its regulation by ADP, Nature. 472 (2011) 230–233. https://doi.org/10.1038/nature09932.

[62] D.M. Gwinn, D.B. Shackelford, D.F. Egan, M.M. Mihaylova, A. Mery, D.S. Vasquez, B.E. Turk, R.J. Shaw, AMPK Phosphorylation of Raptor Mediates a Metabolic Checkpoint, Mol. Cell. 30 (2008) 214–226. https://doi.org/10.1016/j.molcel.2008.03.003.

[63] C.C. Dibble, W. Elis, S. Menon, W. Qin, J. Klekota, J.M. Asara, P.M. Finan, D.J. Kwiatkowski, L.O. Murphy, B.D. Manning, TBC1D7 Is a Third Subunit of the TSC1-TSC2 Complex Upstream of mTORC1, Mol. Cell. 47 (2012) 535–546. https://doi.org/10.1016/j.molcel.2012.06.009.

[64] R.J. Shaw, M. Kosmatka, N. Bardeesy, R.L. Hurley, L.A. Witters, R.A. DePinho, L.C. Cantley, The tumor suppressor LKB1 kinase directly activates AMP-activated kinase and regulates apoptosis in response to energy stress, Proc. Natl. Acad. Sci. U. S. A. 101 (2004) 3329–3335. https://doi.org/10.1073/pnas.0308061100.

[65] A. Woods, S.R. Johnstone, K. Dickerson, F.C. Leiper, L.G.D. Fryer, D. Neumann, U. Schlattner, T. Wallimann, M. Carlson, D. Carling, LKB1 Is the Upstream Kinase in the AMP-Activated Protein Kinase Cascade, Curr. Biol. 13 (2003) 2004–2008. https://doi.org/10.1016/j.cub.2003.10.031.

[66] S.A. Hawley, A.E. Gadalla, G.S. Olsen, D. Grahame Hardie, The antidiabetic drug metformin activates the AMP-activated protein kinase cascade via an adenine nucleotide-independent mechanism, Diabetes. 51 (2002) 2420–2425. https://doi.org/10.2337/diabetes.51.8.2420.

[67] A. Woods, K. Dickerson, R. Heath, S.P. Hong, M. Momcilovic, S.R. Johnstone, M. Carlson, D. Carling, Ca2+/calmodulin-dependent protein kinase kinase-β acts upstream of AMP-activated protein kinase in mammalian cells, Cell Metab. 2 (2005) 21–33. https://doi.org/10.1016/j.cmet.2005.06.005.

[68] M. Momcilovic, S.P. Hong, M. Carlson, Mammalian TAK1 activates Snf1 protein kinase

in yeast and phosphorylates AMP-activated protein kinase in vitro, J. Biol. Chem. 281 (2006) 25336–25343. https://doi.org/10.1074/jbc.M604399200.

[69] F.A. Ross, C. MacKintosh, D.G. Hardie, AMP-activated protein kinase: a cellular energy sensor that comes in 12 flavours, FEBS J. 283 (2016) 2987–3001. https://doi.org/10.1111/febs.13698.

[70] I.G. Ganley, D.H. Lam, J. Wang, X. Ding, S. Chen, X. Jiang, ULK1·ATG13·FIP200 complex mediates mTOR signaling and is essential for autophagy, J. Biol. Chem. 284 (2009) 12297–12305. https://doi.org/10.1074/jbc.M900573200.

[71] M. Zachari, I.G. Ganley, The mammalian ULK1 complex and autophagy initiation, Essays Biochem. 61 (2017) 585–596. https://doi.org/10.1042/EBC20170021.

[72] C.A. Mercer, A. Kaliappan, P.B. Dennis, A novel, human Atg13 binding protein, Atg101, interacts with ULK1 and is essential for macroautophagy, Autophagy. 5 (2009) 649–662. https://doi.org/10.4161/auto.5.5.8249.

[73] C.H. Jung, C.B. Jun, S.-H. Ro, Y.-M. Kim, N.M. Otto, J. Cao, M. Kundu, D.-H. Kim, ULK-Atg13-FIP200 complexes mediate mTOR signaling to the autophagy machinery., Mol. Biol. Cell. 20 (2009) 1992–2003. https://doi.org/10.1091/mbc.E08-12-1249.

[74] E.J. Lee, C. Tournier, The requirement of uncoordinated 51-like kinase 1 (ULK1) and ULK2 in the regulation of autophagy, Autophagy. 7 (2011) 689–695. https://doi.org/10.4161/auto.7.7.15450.

[75] M. Kundu, T. Lindsten, C.Y. Yang, J. Wu, F. Zhao, J. Zhang, M.A. Selak, P.A. Ney, C.B. Thompson, Ulk1 plays a critical role in the autophagic clearance of mitochondria and ribosomes during reticulocyte maturation, Blood. 112 (2008) 1493–1502. https://doi.org/10.1182/blood-2008-02-137398.

[76] I. Koyama-Honda, E. Itakura, T.K. Fujiwara, N. Mizushima, Temporal analysis of recruitment of mammalian ATG proteins to the autophagosome formation site, Autophagy. 9 (2013) 1491–1499. https://doi.org/10.4161/auto.25529.

[77] E. Karanasios, S.A. Walker, H. Okkenhaug, M. Manifava, E. Hummel, H. Zimmermann, Q. Ahmed, M.C. Domart, L. Collinson, N.T. Ktistakis, Autophagy initiation by ULK complex assembly on ER tubulovesicular regions marked by ATG9 vesicles, Nat. Commun. 7 (2016) 1–17. https://doi.org/10.1038/ncomms12420.

[78] L.-C. Tábara, R. Escalante, VMP1 Establishes ER-Microdomains that Regulate Membrane Contact Sites and Autophagy, PLoS One. 11 (2016) e0166499. https://doi.org/10.1371/journal.pone.0166499.

[79] M. Tsukada, Y. Ohsumi, Isolation and characterization of autophagy-defective mutants of Saccharomyces cerevisiae, FEBS Lett. 333 (1993) 169–174. https://doi.org/10.1016/0014-5793(93)80398-E.

[80] B. Levine, D.J. Klionsky, Autophagy wins the 2016 Nobel Prizein Physiology or Medicine: Breakthroughs in baker's yeast fuel advances in biomedical research, Proc. Natl. Acad. Sci. U. S. A. 114 (2017) 201–205.

https://doi.org/10.1073/pnas.1619876114.

[81] M. Thumm, R. Egner, B. Koch, M. Schlumpberger, M. Straub, M. Veenhuis, D.H. Wolf, Isolation of autophagocytosis mutants of Saccharomyces cerevisiae, FEBS Lett. 349 (1994) 275–280. https://doi.org/10.1016/0014-5793(94)00672-5.

[82] T.M. Harding, K.A. Morano, S. V. Scott, D.J. Klionsky, Isolation and characterization of yeast mutants in the cytoplasm to vacuole protein targeting pathway, J. Cell Biol. 131 (1995) 591–602. https://doi.org/10.1083/jcb.131.3.591.

[83] N. Mizushima, T. Yoshimori, Y. Ohsumi, The Role of Atg Proteins in Autophagosome Formation, Annu. Rev. Cell Dev. Biol. 27 (2011) 107–132. https://doi.org/10.1146/annurev-cellbio-092910-154005.

[84] K. Søreng, T.P. Neufeld, A. Simonsen, Membrane Trafficking in Autophagy, Int. Rev. Cell Mol. Biol. 336 (2018) 1–92. https://doi.org/10.1016/BS.IRCMB.2017.07.001.

[85] E.L. Axe, S.A. Walker, M. Manifava, P. Chandra, H.L. Roderick, A. Habermann, G. Griffiths, N.T. Ktistakis, Autophagosome formation from membrane compartments enriched in phosphatidylinositol 3-phosphate and dynamically connected to the endoplasmic reticulum, J. Cell Biol. 182 (2008) 685–701. https://doi.org/10.1083/jcb.200803137.

[86] K. Suzuki, T. Kirisako, Y. Kamada, N. Mizushima, T. Noda, Y. Ohsumi, The pre-autophagosomal structure organized by concerted functions of APG genes is essential for autophagosome formation, EMBO J. 20 (2001) 5971–5981. https://doi.org/10.1093/emboj/20.21.5971.

[87] C.F. Bento, M. Renna, G. Ghislat, C. Puri, A. Ashkenazi, M. Vicinanza, F.M. Menzies, D.C. Rubinsztein, Mammalian Autophagy: How Does It Work?, Annu. Rev. Biochem. 85 (2016) 685–713. https://doi.org/10.1146/annurev-biochem-060815-014556.

[88] Y. Ohashi, S. Tremel, R.L. Williams, VPS34 complexes from a structural perspective, J. Lipid Res. 60 (2019) 229–241. https://doi.org/10.1194/jlr.R089490.

[89] T. Proikas-Cezanne, S. Waddell, A. Gaugel, T. Frickey, A. Lupas, A. Nordheim, WIPI-1α (WIPI49), a member of the novel 7-bladed WIPI protein family, is aberrantly expressed in human cancer and is linked to starvation-induced autophagy, Oncogene. 23 (2004) 9314–9325. https://doi.org/10.1038/sj.onc.1208331.

[90] A.C. Nascimbeni, P. Codogno, E. Morel, Local detection of PtdIns3P at autophagosome biogenesis membrane platforms, Autophagy. 13 (2017) 1602–1612. https://doi.org/10.1080/15548627.2017.1341465.

[91] T. Kotani, H. Kirisako, M. Koizumi, Y. Ohsumi, H. Nakatogawa, The Atg2-Atg18 complex tethers pre-autophagosomal membranes to the endoplasmic reticulum for autophagosome formation, Proc. Natl. Acad. Sci. U. S. A. 115 (2018) 10363–10368. https://doi.org/10.1073/pnas.1806727115.

[92] D.P. Valverde, S. Yu, V. Boggavarapu, N. Kumar, J.A. Lees, T. Walz, K.M. Reinisch, T.J. Melia, ATG2 transports lipids to promote autophagosome biogenesis., J. Cell Biol.

(2019) jcb.201811139. https://doi.org/10.1083/jcb.201811139.

[93] S. Maeda, C. Otomo, T. Otomo, The autophagic membrane tether ATG2A transfers lipids between membranes, Elife. 8 (2019). https://doi.org/10.7554/eLife.45777.

[94] C. Zhou, K. Ma, R. Gao, C. Mu, L. Chen, Q. Liu, Q. Luo, D. Feng, Y. Zhu, Q. Chen, Regulation of mATG9 trafficking by Src- and ULK1-mediated phosphorylation in basal and starvation-induced autophagy, Cell Res. 27 (2017) 184–201. https://doi.org/10.1038/cr.2016.146.

[95] D. Papinski, M. Schuschnig, W. Reiter, L. Wilhelm, C.A. Barnes, A. Maiolica, I. Hansmann, T. Pfaffenwimmer, M. Kijanska, I. Stoffel, S.S. Lee, A. Brezovich, J.H. Lou, B.E. Turk, R. Aebersold, G. Ammerer, M. Peter, C. Kraft, Early Steps in Autophagy Depend on Direct Phosphorylation of Atg9 by the Atg1 Kinase, Mol. Cell. 53 (2014) 471–483. https://doi.org/10.1016/j.molcel.2013.12.011.

[96] H.C. Dooley, M. Razi, H.E.J. Polson, S.E. Girardin, M.I. Wilson, S.A. Tooze, WIPI2 Links LC3 Conjugation with PI3P, Autophagosome Formation, and Pathogen Clearance by Recruiting Atg12–5-16L1, Mol. Cell. 55 (2014) 238–252. https://doi.org/10.1016/j.molcel.2014.05.021.

[97] S. Jentsch, H.D. Ulrich, Protein breakdown: Ubiquitous deja vu, Nature. 395 (1998) 321–323. https://doi.org/10.1038/26335.

[98] N. Mizushima, H. Sugita, T. Yoshimori, Y. Ohsumi, A new protein conjugation system in human: The counterpart of the yeast Apg12p conjugation system essential for autophagy, J. Biol. Chem. 273 (1998) 33889–33892. https://doi.org/10.1074/jbc.273.51.33889.

[99] T. Shintani, N. Mizushima, Y. Ogawa, A. Matsuura, T. Noda, Y. Ohsumi, Apg10p, a novel protein-conjugating enzyme essential for autophagy in yeast, EMBO J. 18 (1999) 5234–5241. https://doi.org/10.1093/emboj/18.19.5234.

[100] M. Skytte Rasmussen, S. Mouilleron, B. Kumar Shrestha, M. Wirth, R. Lee, K. Bowitz Larsen, Y. Abudu Princely, N. O'Reilly, E. Sjøttem, S.A. Tooze, T. Lamark, T. Johansen, ATG4B contains a C-terminal LIR motif important for binding and efficient cleavage of mammalian orthologs of yeast Atg8, Autophagy. 13 (2017) 834–853. https://doi.org/10.1080/15548627.2017.1287651.

[101] M. Li, Y. Hou, J. Wang, X. Chen, Z.M. Shao, X.M. Yin, Kinetics comparisons of mammalian Atg4 homologues indicate selective preferences toward diverse Atg8 substrates, J. Biol. Chem. 286 (2011) 7327–7338. https://doi.org/10.1074/jbc.M110.199059.

[102] I. Tamargo-Gómez, G.G. Martínez-García, M.F. Suárez, V. Rey, A. Fueyo, H. Codina-Martínez, G. Bretones, X.M. Caravia, E. Morel, N. Dupont, R. Cabo, C. Tomás-Zapico, S. Souquere, G. Pierron, P. Codogno, C. López-Otín, Á.F. Fernández, G. Mariño, ATG4D is the main ATG8 delipidating enzyme in mammalian cells and protects against cerebellar neurodegeneration, Cell Death Differ. 28 (2021) 2651–2672. https://doi.org/10.1038/s41418-021-00776-1.

[103] K.J. Kauffman, S. Yu, J. Jin, B. Mugo, N. Nguyen, A. O'Brien, S. Nag, A.H. Lystad, T.J. Melia, Delipidation of mammalian Atg8-family proteins by each of the four ATG4 proteases, Autophagy. 14 (2018) 992–1010. https://doi.org/10.1080/15548627.2018.1437341.

[104] S.P. Jackson, J. Bartek, The DNA-damage response in human biology and disease, Nature. 461 (2009) 1071–1078. https://doi.org/10.1038/nature08467.

[105] A. Tubbs, A. Nussenzweig, Endogenous DNA Damage as a Source of Genomic Instability in Cancer, Cell. 168 (2017) 644–656. https://doi.org/10.1016/j.cell.2017.01.002.

[106] N.P. Dantuma, H. van Attikum, Spatiotemporal regulation of posttranslational modifications in the DNA damage response., EMBO J. 35 (2016) 6–23. https://doi.org/10.15252/embj.201592595.

[107] A.N. Blackford, S.P. Jackson, ATM, ATR, and DNA-PK: The Trinity at the Heart of the DNA Damage Response, Mol. Cell. 66 (2017) 801–817. https://doi.org/10.1016/j.molcel.2017.05.015.

[108] H.C. Reinhardt, B. Schumacher, The p53 network: Cellular and systemic DNA damage responses in aging and cancer, Trends Genet. 28 (2012) 128–136. https://doi.org/10.1016/j.tig.2011.12.002.

[109] T. Shibue, K. Takeda, E. Oda, H. Tanaka, H. Murasawa, A. Takaoka, Y. Morishita, S. Akira, T. Taniguchi, N. Tanaka, Integral role of Noxa in p53-mediated apoptotic response, Genes Dev. 17 (2003) 2233–2238. https://doi.org/10.1101/gad.1103603.

[110] B.J. Aubrey, G.L. Kelly, A. Janic, M.J. Herold, A. Strasser, How does p53 induce apoptosis and how does this relate to p53-mediated tumour suppression?, Cell Death Differ. 25 (2018) 104–113. https://doi.org/10.1038/cdd.2017.169.

[111] T. Lindahl, D.E. Barnes, Repair of endogenous DNA damage, in: Cold Spring Harb. Symp. Quant. Biol., Cold Spring Harbor Laboratory Press, 2000: pp. 127–133. https://doi.org/10.1101/sqb.2000.65.127.

[112] T.A. Kunkel, D.A. Erie, DNA mismatch repair, Annu. Rev. Biochem. 74 (2005) 681–710. https://doi.org/10.1146/annurev.biochem.74.082803.133243.

[113] M.L. Hegde, T.K. Hazra, S. Mitra, Early steps in the DNA base excision/single-strand interruption repair pathway in mammalian cells, Cell Res. 18 (2008) 27–47. https://doi.org/10.1038/cr.2008.8.

[114] W.L. De Laat, N.G.J. Jaspers, J.H.J. Hoeijmakers, Molecular mechanism of nucleotide excision repair, Genes Dev. 13 (1999) 768–785. https://doi.org/10.1101/gad.13.7.768.

[115] M. McVey, Strategies for DNA interstrand crosslink repair: Insights from worms, flies, frogs, and slime molds, Environ. Mol. Mutagen. 51 (2010) 646–658. https://doi.org/10.1002/em.20551.

[116] S. Hashimoto, H. Anai, K. Hanada, Mechanisms of interstrand DNA crosslink repair and

human disorders, Genes Environ. 38 (2016). https://doi.org/10.1186/s41021-016-0037-9.

[117] W.D. Wright, S.S. Shah, W.D. Heyer, Homologous recombination and the repair of DNA double-strand breaks, J. Biol. Chem. 293 (2018) 10524–10535. https://doi.org/10.1074/jbc.TM118.000372.

[118] N.R. Pannunzio, G. Watanabe, M.R. Lieber, Nonhomologous DNA end-joining for repair of DNA double-strand breaks, J. Biol. Chem. 293 (2018) 10512–10523. https://doi.org/10.1074/jbc.TM117.000374.

[119] S. Nik-Zainal, H. Davies, J. Staaf, M. Ramakrishna, D. Glodzik, X. Zou, I. Martincorena, L.B. Alexandrov, S. Martin, D.C. Wedge, P. Van Loo, Y.S. Ju, M. Smid, A.B. Brinkman, S. Morganella, M.R. Aure, O.C. Lingjærde, A. Langerød, M. Ringnér, S.M. Ahn, S. Boyault, J.E. Brock, A. Broeks, A. Butler, C. Desmedt, L. Dirix, S. Dronov, A. Fatima, J.A. Foekens, M. Gerstung, G.K.J. Hooijer, S.J. Jang, D.R. Jones, H.Y. Kim, T.A. King, S. Krishnamurthy, H.J. Lee, J.Y. Lee, Y. Li, S. McLaren, A. Menzies, V. Mustonen, S. O'Meara, I. Pauporté, X. Pivot, C.A. Purdie, K. Raine, K. Ramakrishnan, F.G. Rodríguez-González, G. Romieu, A.M. Sieuwerts, P.T. Simpson, R. Shepherd, L. Stebbings, O.A. Stefansson, J. Teague, S. Tommasi, I. Treilleux, G.G. Van Den Eynden, P. Vermeulen, A. Vincent-Salomon, L. Yates, C. Caldas, L.V. t. Veer, A. Tutt, S. Knappskog, B.K.T. Tan, J. Jonkers, Å. Borg, N.T. Ueno, C. Sotiriou, A. Viari, P.A. Futreal, P.J. Campbell, P.N. Span, S. Van Laere, S.R. Lakhani, J.E. Eyfjord, A.M. Thompson, E. Birney, H.G. Stunnenberg, M.J. Van De Vijver, J.W.M. Martens, A.L. Børresen-Dale, A.L. Richardson, G. Kong, G. Thomas, M.R. Stratton, Landscape of somatic mutations in 560 breast cancer whole-genome sequences, Nature. 534 (2016) 47–54. https://doi.org/10.1038/nature17676.

[120] A.R. Venkitaraman, Cancer susceptibility and the functions of BRCA1 and BRCA2, Cell. 108 (2002) 171–182. https://doi.org/10.1016/S0092-8674(02)00615-3.

[121] P.S. Patel, A. Algouneh, R. Hakem, Exploiting synthetic lethality to target BRCA1/2-deficient tumors: where we stand, Oncogene. 40 (2021) 3001–3014. https://doi.org/10.1038/s41388-021-01744-2.

[122] S. Vyas, M. Chesarone-Cataldo, T. Todorova, Y.H. Huang, P. Chang, A systematic analysis of the PARP protein family identifies new functions critical for cell physiology, Nat. Commun. 4 (2013) 1–13. https://doi.org/10.1038/ncomms3240.

[123] H. Farmer, H. McCabe, C.J. Lord, A.H.J. Tutt, D.A. Johnson, T.B. Richardson, M. Santarosa, K.J. Dillon, I. Hickson, C. Knights, N.M.B. Martin, S.P. Jackson, G.C.M. Smith, A. Ashworth, Targeting the DNA repair defect in BRCA mutant cells as a therapeutic strategy, Nature. 434 (2005) 917–921. https://doi.org/10.1038/nature03445.

[124] P.C. Fong, D.S. Boss, T.A. Yap, A. Tutt, P. Wu, M. Mergui-Roelvink, P. Mortimer, H. Swaisland, A. Lau, M.J. O'Connor, A. Ashworth, J. Carmichael, S.B. Kaye, J.H.M. Schellens, J.S. de Bono, Inhibition of Poly(ADP-Ribose) Polymerase in Tumors from BRCA Mutation Carriers , N. Engl. J. Med. 361 (2009) 123–134. https://doi.org/10.1056/nejmoa0900212.

[125] E.F. Fang, M. Scheibye-Knudsen, K.F. Chua, M.P. Mattson, D.L. Croteau, V.A. Bohr,

Nuclear DNA damage signalling to mitochondria in ageing, Nat. Rev. Mol. Cell Biol. 17 (2016) 308–321. https://doi.org/10.1038/nrm.2016.14.

[126] F.W. Alt, Y. Zhang, F.L. Meng, C. Guo, B. Schwer, Mechanisms of programmed DNA lesions and genomic instability in the immune system, Cell. 152 (2013) 417–429. https://doi.org/10.1016/j.cell.2013.01.007.

[127] O. Huambachano, F. Herrera, A. Rancourt, M.S. Satoh, Double-stranded DNA binding domain of poly(ADP-ribose) polymerase-1 and molecular insight into the regulation of its activity, J. Biol. Chem. 286 (2011) 7149–7160. https://doi.org/10.1074/jbc.M110.175190.

[128] D. D'Amours, S. Desnoyers, I. D'Silva, G.G. Poirier, Poly(ADP-ribosyl)ation reactions in the regulation of nuclear functions, Biochem. J. 342 (1999) 249–268. https://doi.org/10.1042/0264-6021:3420249.

[129] S. Jungmichel, F. Rosenthal, M. Altmeyer, J. Lukas, M.O. Hottiger, M.L. Nielsen, Proteome-wide identification of poly(ADP-Ribosyl)ation targets in different genotoxic stress responses, Mol. Cell. 52 (2013) 272–285. https://doi.org/10.1016/j.molcel.2013.08.026.

[130] M.R. Lieber, The Mechanism of Double-Strand DNA Break Repair by the Nonhomologous DNA End-Joining Pathway, Annu. Rev. Biochem. 79 (2010) 181–211. https://doi.org/10.1146/annurev.biochem.052308.093131.

[131] T. Ruscetti, B.E. Lehnert, J. Halbrook, H. Le Trong, M.F. Hoekstra, D.J. Chen, S.R. Peterson, Stimulation of the DNA-dependent protein kinase by poly(ADP-ribose) polymerase, J. Biol. Chem. 273 (1998) 14461–14467. https://doi.org/10.1074/jbc.273.23.14461.

[132] Y. Ma, U. Pannicke, K. Schwarz, M.R. Lieber, Hairpin opening and overhang processing by an Artemis/DNA-dependent protein kinase complex in nonhomologous end joining and V(D)J recombination, Cell. 108 (2002) 781–794. https://doi.org/10.1016/S0092-8674(02)00671-2.

[133] S.A. Nick McElhinny, C.M. Snowden, J. McCarville, D.A. Ramsden, Ku Recruits the XRCC4-Ligase IV Complex to DNA Ends, Mol. Cell. Biol. 20 (2000) 2996–3003. https://doi.org/10.1128/mcb.20.9.2996-3003.2000.

[134] P. Schwertman, S. Bekker-Jensen, N. Mailand, Regulation of DNA double-strand break repair by ubiquitin and ubiquitin-like modifiers, Nat. Rev. Mol. Cell Biol. 17 (2016) 379–394. https://doi.org/10.1038/nrm.2016.58.

[135] A. Ray Chaudhuri, A. Nussenzweig, The multifaceted roles of PARP1 in DNA repair and chromatin remodelling, Nat. Rev. Mol. Cell Biol. 18 (2017) 610–621. https://doi.org/10.1038/nrm.2017.53.

[136] E.P. Mimitou, L.S. Symington, Nucleases and helicases take center stage in homologous recombination, Trends Biochem. Sci. 34 (2009) 264–272. https://doi.org/10.1016/j.tibs.2009.01.010.

[137] M. Li, X. Yu, Function of BRCA1 in the DNA Damage Response Is Mediated by ADP-Ribosylation, Cancer Cell. 23 (2013) 693–704. https://doi.org/10.1016/j.ccr.2013.03.025.

[138] P. Huertas, S.P. Jackason, Human CtIP mediates cell cycle control of DNA end resection and double strand break repair, J. Biol. Chem. 284 (2009) 9558–9565. https://doi.org/10.1074/jbc.M808906200.

[139] S. Gravel, J.R. Chapman, C. Magill, S.P. Jackson, DNA helicases Sgs1 and BLM promote DNA double-strand break resection, Genes Dev. 22 (2008) 2767–2772. https://doi.org/10.1101/gad.503108.

[140] H. Yang, Q. Li, J. Fan, W.K. Holloman, N.P. Pavletich, The BRCA2 homologue Brh2 nucleates RAD51 filament formation at a dsDNA-ssDNA junction, Nature. 433 (2005) 653–657. https://doi.org/10.1038/nature03234.

[141] E. Fanning, V. Klimovich, A.R. Nager, A dynamic model for replication protein A (RPA) function in DNA processing pathways, Nucleic Acids Res. 34 (2006) 4126–4137. https://doi.org/10.1093/nar/gkl550.

[142] L. Zou, S.J. Elledge, Sensing DNA damage through ATRIP recognition of RPA-ssDNA complexes, Science (80-.). 300 (2003) 1542–1548. https://doi.org/10.1126/science.1083430.

[143] S. Schlam-Babayov, A. Bensimon, M. Harel, T. Geiger, R. Aebersold, Y. Ziv, Y. Shiloh, Phosphoproteomics reveals novel modes of function and inter-relationships among PIKKs in response to genotoxic stress, EMBO J. 40 (2021) e104400. https://doi.org/10.15252/embj.2020104400.

[144] M.E. Ashour, R. Atteya, S.F. El-Khamisy, Topoisomerase-mediated chromosomal break repair: an emerging player in many games, Nat. Rev. Cancer. 15 (2015) 137–151. https://doi.org/10.1038/nrc3892.

[145] S.J. Froelich-Ammon, N. Osheroff, Topoisomerase poisons: Harnessing the dark side of enzyme mechanism, J. Biol. Chem. 270 (1995) 21429–21432. https://doi.org/10.1074/jbc.270.37.21429.

[146] J. Fielden, A. Ruggiano, M. Popović, K. Ramadan, DNA protein crosslink proteolysis repair: From yeast to premature ageing and cancer in humans, DNA Repair (Amst). 71 (2018) 198–204. https://doi.org/10.1016/j.dnarep.2018.08.025.

[147] Y. Pommier, Y. Sun, S.Y.N. Huang, J.L. Nitiss, Roles of eukaryotic topoisomerases in transcription, replication and genomic stability, Nat. Rev. Mol. Cell Biol. 17 (2016) 703–721. https://doi.org/10.1038/nrm.2016.111.

[148] S.W. Yang, A.B. Burgin, B.N. Huizenga, C.A. Robertson, K.C. Yao, H.A. Nash, A eukaryotic enzyme that can disjoin dead-end covalent complexes between DNA and type I topoisomerases, Proc. Natl. Acad. Sci. U. S. A. 93 (1996) 11534–11539. https://doi.org/10.1073/pnas.93.21.11534.

[149] L. Debéthune, G. Kohlhagen, A. Grandas, Y. Pommier, Processing of nucleopeptides

mimicking the topoisomerase I-DNA covalent complex by tyrosyl-DNA phosphodiesterase, Nucleic Acids Res. 30 (2002) 1198–1204. https://doi.org/10.1093/nar/30.5.1198.

[150] J. Fielden, K. Wiseman, I. Torrecilla, S. Li, S. Hume, S.-C. Chiang, A. Ruggiano, A. Narayan Singh, R. Freire, S. Hassanieh, E. Domingo, I. Vendrell, R. Fischer, B.M. Kessler, T.S. Maughan, S.F. El-Khamisy, K. Ramadan, TEX264 coordinates p97- and SPRTN-mediated resolution of topoisomerase 1-DNA adducts, Nat. Commun. 11 (2020) 1274. https://doi.org/10.1038/s41467-020-15000-w.

[151] R. Gao, M.J. Schellenberg, S.Y.N. Huang, M. Abdelmalak, C. Marchand, K.C. Nitiss, J.L. Nitiss, R.S. Williams, Y. Pommier, Proteolytic degradation of topoisomerase II (Top2) enables the processing of Top2·DNA and Top2·RNA covalent complexes by tyrosyl-DNA-phosphodiesterase 2 (TDP2), J. Biol. Chem. 289 (2014) 17960–17969. https://doi.org/10.1074/jbc.M114.565374.

[152] Y. Pommier, S. yin N. Huang, R. Gao, B.B. Das, J. Murai, C. Marchand, Tyrosyl-DNA-phosphodiesterases (TDP1 and TDP2), DNA Repair (Amst). 19 (2014) 114–129. https://doi.org/10.1016/j.dnarep.2014.03.020.

[153] A. Alexander, S.-L. Cai, J. Kim, A. Nanez, M. Sahin, K.H. MacLean, K. Inoki, K.-L. Guan, J. Shen, M.D. Person, D. Kusewitt, G.B. Mills, M.B. Kastan, C.L. Walker, ATM signals to TSC2 in the cytoplasm to regulate mTORC1 in response to ROS., Proc. Natl. Acad. Sci. U. S. A. 107 (2010) 4153–8. https://doi.org/10.1073/pnas.0913860107.

[154] J. Zhang, D.N. Tripathi, J. Jing, A. Alexander, J. Kim, R.T. Powell, R. Dere, J. Tait-Mulder, J.-H. Lee, T.T. Paull, R.K. Pandita, V.K. Charaka, T.K. Pandita, M.B. Kastan, C.L. Walker, ATM functions at the peroxisome to induce pexophagy in response to ROS, Nat. Cell Biol. 17 (2015) 1259–1269. https://doi.org/10.1038/ncb3230.

[155] D. Kenzelmann Broz, S.S. Mello, K.T. Bieging, D. Jiang, R.L. Dusek, C.A. Brady, A. Sidow, L.D. Attardi, Global genomic profiling reveals an extensive p53-regulated autophagy program contributing to key p53 responses, Genes Dev. 27 (2013) 1016–1031. https://doi.org/10.1101/gad.212282.112.

[156] L. Shang, S. Chen, F. Du, S. Li, L. Zhao, X. Wang, Nutrient starvation elicits an acute autophagic response mediated by Ulk1 dephosphorylation and its subsequent dissociation from AMPK., Proc. Natl. Acad. Sci. U. S. A. 108 (2011) 4788–93. https://doi.org/10.1073/pnas.1100844108.

[157] H. Zhang, M. Bosch-Marce, L.A. Shimoda, S.T. Yee, H.B. Jin, J.B. Wesley, F.J. Gonzalez, G.L. Semenza, Mitochondrial autophagy is an HIF-1-dependent adaptive metabolic response to hypoxia, J. Biol. Chem. 283 (2008) 10892–10903. https://doi.org/10.1074/jbc.M800102200.

[158] T.L.M. Thurston, M.P. Wandel, N. Von Muhlinen, Á. Foeglein, F. Randow, Galectin 8 targets damaged vesicles for autophagy to defend cells against bacterial invasion, Nature. 482 (2012) 414–418. https://doi.org/10.1038/nature10744.

[159] D. Petkova, P. Verlhac, A. Rozières, J. Baguet, M. Claviere, C. Kretz-Remy, R. Mahieux, C. Viret, M. Faure, Distinct Contributions of Autophagy Receptors in Measles Virus

Replication, Viruses. 9 (2017) 123. https://doi.org/10.3390/v9050123.

[160] R. Vanzo, J. Bartkova, J.M. Merchut-Maya, A. Hall, J. Bouchal, L. Dyrskjøt, L.B. Frankel, V. Gorgoulis, A. Maya-Mendoza, M. Jäättelä, J. Bartek, Autophagy role(s) in response to oncogenes and DNA replication stress, Cell Death Differ. (2019) 1–20. https://doi.org/10.1038/s41418-019-0403-9.

[161] H.M. Shen, P. Codogno, Autophagic cell death: Loch Ness monster or endangered species?, Autophagy. 7 (2011) 457–465. https://doi.org/10.4161/auto.7.5.14226.

[162] L. Galluzzi, I. Vitale, S.A. Aaronson, J.M. Abrams, D. Adam, P. Agostinis, E.S. Alnemri, L. Altucci, I. Amelio, D.W. Andrews, M. Annicchiarico-Petruzzelli, A. V. Antonov, E. Arama, E.H. Baehrecke, N.A. Barlev, N.G. Bazan, F. Bernassola, M.J.M. Bertrand, K. Bianchi, M. V. Blagosklonny, K. Blomgren, C. Borner, P. Boya, C. Brenner, M. Campanella, E. Candi, D. Carmona-Gutierrez, F. Cecconi, F.K.-M. Chan, N.S. Chandel, E.H. Cheng, J.E. Chipuk, J.A. Cidlowski, A. Ciechanover, G.M. Cohen, M. Conrad, J.R. Cubillos-Ruiz, P.E. Czabotar, V. D'Angiolella, T.M. Dawson, V.L. Dawson, V. De Laurenzi, R. De Maria, K.-M. Debatin, R.J. DeBerardinis, M. Deshmukh, N. Di Daniele, F. Di Virgilio, V.M. Dixit, S.J. Dixon, C.S. Duckett, B.D. Dynlacht, W.S. El-Deiry, J.W. Elrod, G.M. Fimia, S. Fulda, A.J. García-Sáez, A.D. Garg, C. Garrido, E. Gavathiotis, P. Golstein, E. Gottlieb, D.R. Green, L.A. Greene, H. Gronemeyer, A. Gross, G. Hajnoczky, J.M. Hardwick, I.S. Harris, M.O. Hengartner, C. Hetz, H. Ichijo, M. Jäättelä, B. Joseph, P.J. Jost, P.P. Juin, W.J. Kaiser, M. Karin, T. Kaufmann, O. Kepp, A. Kimchi, R.N. Kitsis, D.J. Klionsky, R.A. Knight, S. Kumar, S.W. Lee, J.J. Lemasters, B. Levine, A. Linkermann, S.A. Lipton, R.A. Lockshin, C. López-Otín, S.W. Lowe, T. Luedde, E. Lugli, M. MacFarlane, F. Madeo, M. Malewicz, W. Malorni, G. Manic, J.-C. Marine, S.J. Martin, J.-C. Martinou, J.P. Medema, P. Mehlen, P. Meier, S. Melino, E.A. Miao, J.D. Molkentin, U.M. Moll, C. Muñoz-Pinedo, S. Nagata, G. Nuñez, A. Oberst, M. Oren, M. Overholtzer, M. Pagano, T. Panaretakis, M. Pasparakis, J.M. Penninger, D.M. Pereira, S. Pervaiz, M.E. Peter, M. Piacentini, P. Pinton, J.H.M. Prehn, H. Puthalakath, G.A. Rabinovich, M. Rehm, R. Rizzuto, C.M.P. Rodrigues, D.C. Rubinsztein, T. Rudel, K.M. Ryan, E. Sayan, L. Scorrano, F. Shao, Y. Shi, J. Silke, H.-U. Simon, A. Sistigu, B.R. Stockwell, A. Strasser, G. Szabadkai, S.W.G. Tait, D. Tang, N. Tavernarakis, A. Thorburn, Y. Tsujimoto, B. Turk, T. Vanden Berghe, P. Vandenabeele, M.G. Vander Heiden, A. Villunger, H.W. Virgin, K.H. Vousden, D. Vucic, E.F. Wagner, H. Walczak, D. Wallach, Y. Wang, J.A. Wells, W. Wood, J. Yuan, Z. Zakeri, B. Zhivotovsky, L. Zitvogel, G. Melino, G. Kroemer, Molecular mechanisms of cell death: recommendations of the Nomenclature Committee on Cell Death 2018, Cell Death Differ. 25 (2018) 486–541. https://doi.org/10.1038/s41418-017-0012-4.

[163] J. Nassour, R. Radford, A. Correia, J.M. Fusté, B. Schoell, A. Jauch, R.J. Shaw, J. Karlseder, Autophagic cell death restricts chromosomal instability during replicative crisis, Nature. 565 (2019) 659–663. https://doi.org/10.1038/s41586-019-0885-0.

[164] P. Puustinen, A. Keldsbo, E. Corcelle-Termeau, K. Ngoei, S.L. Sønder, T. Farkas, K. Kaae Andersen, J.S. Oakhill, M. Jäättelä, DNA-dependent protein kinase regulates lysosomal AMP-dependent protein kinase activation and autophagy, Autophagy. (2020). https://doi.org/10.1080/15548627.2019.1710430.

[165] T.-Y. Chen, B.-M. Huang, T.K. Tang, Y.-Y. Chao, X.-Y. Xiao, P.-R. Lee, L.-Y. Yang, C.-Y. Wang, Genotoxic stress-activated DNA-PK-p53 cascade and autophagy cooperatively induce ciliogenesis to maintain the DNA damage response, Cell Death Differ. (2021) 1–15. https://doi.org/10.1038/s41418-020-00713-8.

[166] M. Liu, T. Zeng, X. Zhang, C. Liu, Z. Wu, L. Yao, C. Xie, H. Xia, Q. Lin, L. Xie, D. Zhou, X. Deng, H.-L. Chan, T.-J. Zhao, H.-R. Wang, ATR/Chk1 signaling induces autophagy through sumoylated RhoB-mediated lysosomal translocation of TSC2 after DNA damage, Nat. Commun. 9 (2018) 4139. https://doi.org/10.1038/s41467-018-06556-9.

[167] V. V Eapen, D.P. Waterman, A. Bernard, N. Schiffmann, E. Sayas, R. Kamber, B. Lemos, G. Memisoglu, J. Ang, A. Mazella, S.G. Chuartzman, R.J. Loewith, M. Schuldiner, V. Denic, D.J. Klionsky, J.E. Haber, A pathway of targeted autophagy is induced by DNA damage in budding yeast., Proc. Natl. Acad. Sci. U. S. A. 114 (2017) E1158–E1167. https://doi.org/10.1073/pnas.1614364114.

[168] C. Park, Y. Suh, A.M. Cuervo, Regulated degradation of Chk1 by chaperone-mediated autophagy in response to DNA damage, Nat. Commun. 6 (2015) 6823. https://doi.org/10.1038/ncomms7823.

[169] D. Edifizi, H. Nolte, S. Brodesser, M. Krüger, B.R. Schumacher, Multilayered Reprogramming in Response to Persistent DNA Damage in C. elegans, CellReports. 20 (2017) 2026–2043. https://doi.org/10.1016/j.celrep.2017.08.028.

[170] A. Mesquita, J. Glenn, A. Jenny, Differential activation of eMI by distinct forms of cellular stress, Autophagy. (2020) 1–13. https://doi.org/10.1080/15548627.2020.1783833.

[171] P. Groth, S. Ausländer, M.M. Majumder, N. Schultz, F. Johansson, E. Petermann, T. Helleday, Methylated DNA Causes a Physical Block to Replication Forks Independently of Damage Signalling, O6-Methylguanine or DNA Single-Strand Breaks and Results in DNA Damage, J. Mol. Biol. 402 (2010) 70–82. https://doi.org/10.1016/j.jmb.2010.07.010.

[172] Y. Chen, J. Wu, G. Liang, G. Geng, F. Zhao, P. Yin, S. Nowsheen, C. Wu, Y. Li, L. Li, W. Kim, Q. Zhou, J. Huang, J. Liu, C. Zhang, G. Guo, M. Deng, X. Tu, X. Gao, Z. Liu, Y. Chen, Z. Lou, K. Luo, J. Yuan, CHK2-FOXK axis promotes transcriptional control of autophagy programs, Sci. Adv. 6 (2020) eaax5819. https://doi.org/10.1126/sciadv.aax5819.

[173] G.P. Sapkota, M. Deak, A. Kieloch, N. Morrice, A.A. Goodarzi, C. Smythe, Y. Shiloh, S.P. Lees-Miller, D.R. Alessi, Ionizing radiation induces ataxia telangiectasia mutated kinase (ATM)-mediated phosphorylation of LKB1/STK11 at Thr-366, Biochem. J. 368 (2002) 507–516. https://doi.org/10.1042/BJ20021284.

[174] L. Luo, W. Huang, R. Tao, N. Hu, Z.X. Xiao, Z. Luo, ATM and LKB1 dependent activation of AMPK sensitizes cancer cells to etoposide-induced apoptosis, Cancer Lett. 328 (2013) 114–119. https://doi.org/10.1016/j.canlet.2012.08.034.

[175] Q. Guo, S. Wang, S. Zhang, H. Xu, X. Li, Y. Guan, F. Yi, T. Zhou, B. Jiang, N. Bai, M. Ma, Z. Wang, Y. Feng, W. Guo, X. Wu, G. Zhao, G. Fan, S. Zhang, C. Wang, L. Cao, B.P. O'Rourke, S. Liu, P. Wang, S. Han, X. Song, L. Cao, ATM-CHK2-Beclin 1 axis promotes

autophagy to maintain ROS homeostasis under oxidative stress, EMBO J. 39 (2020). https://doi.org/10.15252/embj.2019103111.

[176] J.-H. Lee, M.R. Mand, C.-H. Kao, Y. Zhou, S.W. Ryu, A.L. Richards, J.J. Coon, T.T. Paull, ATM directs DNA damage responses and proteostasis via genetically separable pathways., Sci. Signal. 11 (2018) eaan5598. https://doi.org/10.1126/scisignal.aan5598.

[177] J.A. Muñoz-Gámez, J.M. Rodríguez-Vargas, R. Quiles-Pérez, R. Aguilar-Quesada, D. Martín-Oliva, G. De Murcia, J.M. De Murcia, A. Almendros, M. Ruiz De Almodóvar, F.J. Oliver, PARP-1 is involved in autophagy induced by DNA damage, Autophagy. 5 (2009) 61–74. https://doi.org/10.4161/auto.5.1.7272.

[178] J.M. Rodríguez-Vargas, M.J. Ruiz-Magaña, C. Ruiz-Ruiz, J. Majuelos-Melguizo, A. Peralta-Leal, M.I. Rodríguez, J.A. Muñoz-Gámez, M.R. de Almodóvar, E. Siles, A.L. Rivas, M. Jäättela, F.J. Oliver, ROS-induced DNA damage and PARP-1 are required for optimal induction of starvation-induced autophagy, Cell Res. 22 (2012) 1181–1198. https://doi.org/10.1038/cr.2012.70.

[179] J.M. Rodríguez-Vargas, M.I. Rodríguez, J. Majuelos-Melguizo, Á. García-Diaz, A. González-Flores, A. López-Rivas, L. Virág, G. Illuzzi, V. Schreiber, F. Dantzer, F.J. Oliver, Autophagy requires poly(adp-ribosyl)ation-dependent AMPK nuclear export, Cell Death Differ. 23 (2016) 2007–2018. https://doi.org/10.1038/cdd.2016.80.

[180] Y. Kobayashi, Y. Furukawa-Hibi, C. Chen, Y. Horio, K. Isobe, K. Ikeda, N. Motoyama, SIRT1 is critical regulator of FOXO-mediated transcription in response to oxidative stress., Int. J. Mol. Med. 16 (2005) 237–243. https://doi.org/10.3892/ijmm.16.2.237.

[181] R. Huang, Y. Xu, W. Wan, X. Shou, J. Qian, Z. You, B. Liu, C. Chang, T. Zhou, J. Lippincott-Schwartz, W. Liu, Deacetylation of Nuclear LC3 Drives Autophagy Initiation under Starvation, Mol. Cell. 57 (2015) 456–466. https://doi.org/10.1016/j.molcel.2014.12.013.

[182] N.L. Price, A.P. Gomes, A.J.Y. Ling, F. V. Duarte, A. Martin-Montalvo, B.J. North, B. Agarwal, L. Ye, G. Ramadori, J.S. Teodoro, B.P. Hubbard, A.T. Varela, J.G. Davis, B. Varamini, A. Hafner, R. Moaddel, A.P. Rolo, R. Coppari, C.M. Palmeira, R. De Cabo, J.A. Baur, D.A. Sinclair, SIRT1 is required for AMPK activation and the beneficial effects of resveratrol on mitochondrial function, Cell Metab. 15 (2012) 675–690. https://doi.org/10.1016/j.cmet.2012.04.003.

[183] C. Cantó, K.J. Menzies, J. Auwerx, NAD+ Metabolism and the Control of Energy Homeostasis: A Balancing Act between Mitochondria and the Nucleus, Cell Metab. 22 (2015) 31–53. https://doi.org/10.1016/j.cmet.2015.05.023.

[184] C. Éthier, M. Tardif, L. Arul, G.G. Poirier, PARP-1 Modulation of mTOR Signaling in Response to a DNA Alkylating Agent, PLoS One. 7 (2012) e47978. https://doi.org/10.1371/journal.pone.0047978.

[185] H. Yamaguchi, S. Arakawa, T. Kanaseki, T. Miyatsuka, Y. Fujitani, H. Watada, Y. Tsujimoto, S. Shimizu, Golgi membrane-associated degradation pathway in yeast and mammals., EMBO J. 35 (2016) 1991–2007.

https://doi.org/10.15252/embj.201593191.

[186] Y. Nishida, S. Arakawa, K. Fujitani, H. Yamaguchi, T. Mizuta, T. Kanaseki, M. Komatsu, K. Otsu, Y. Tsujimoto, S. Shimizu, Discovery of Atg5/Atg7-independent alternative macroautophagy, Nature. 461 (2009) 654–658. https://doi.org/10.1038/nature08455.

[187] S. Shimizu, Biological Roles of Alternative Autophagy., Mol. Cells. 41 (2018) 50–54. https://doi.org/10.14348/molcells.2018.2215.

[188] S. Honda, S. Arakawa, Y. Nishida, H. Yamaguchi, E. Ishii, S. Shimizu, Ulk1-mediated Atg5-independent macroautophagy mediates elimination of mitochondria from embryonic reticulocytes, Nat. Commun. 5 (2014) 4004. https://doi.org/10.1038/ncomms5004.

[189] H. Yamaguchi, S. Honda, S. Torii, K. Shimizu, K. Katoh, K. Miyake, N. Miyake, N. Fujikake, H.T. Sakurai, S. Arakawa, S. Shimizu, Wipi3 is essential for alternative autophagy and its loss causes neurodegeneration, Nat. Commun. 11 (2020) 5311. https://doi.org/10.1038/s41467-020-18892-w.

[190] S. Torii, H. Yamaguchi, A. Nakanishi, S. Arakawa, S. Honda, K. Moriwaki, H. Nakano, S. Shimizu, Identification of a phosphorylation site on Ulk1 required for genotoxic stress-induced alternative autophagy, Nat. Commun. 11 (2020) 1–19. https://doi.org/10.1038/s41467-020-15577-2.

[191] S. Torii, T. Yoshida, S. Arakawa, S. Honda, A. Nakanishi, S. Shimizu, Identification of PPM1D as an essential Ulk1 phosphatase for genotoxic stress-induced autophagy., EMBO Rep. 17 (2016) 1552–1564. https://doi.org/10.15252/embr.201642565.

[192] M. Nagata, S. Arakawa, H. Yamaguchi, S. Torii, H. Endo, M. Tsujioka, S. Honda, Y. Nishida, A. Konishi, S. Shimizu, Dram1 regulates DNA damage-induced alternative autophagy, Cell Stress. 2 (2018) 55–65. https://doi.org/10.15698/cst2018.03.127.

[193] Z. Feng, H. Zhang, A.J. Levine, S. Jin, The coordinate regulation of the p53 and mTOR pathways in cells, Proc. Natl. Acad. Sci. U. S. A. 102 (2005) 8204–8209. https://doi.org/10.1073/pnas.0502857102.

[194] Z. Feng, W. Hu, E. De Stanchina, A.K. Teresky, S. Jin, S. Lowe, A.J. Levine, The regulation of AMPK β1, TSC2, and PTEN expression by p53: Stress, cell and tissue specificity, and the role of these gene products in modulating the IGF-1-AKT-mTOR pathways, Cancer Res. 67 (2007) 3043–3053. https://doi.org/10.1158/0008-5472.CAN-06-4149.

[195] E. Tasdemir, M.C. Maiuri, L. Galluzzi, I. Vitale, M. Djavaheri-Mergny, M. D'Amelio, A. Criollo, E. Morselli, C. Zhu, F. Harper, U. Nannmark, C. Samara, P. Pinton, J.M. Vicencio, R. Carnuccio, U.M. Moll, F. Madeo, P. Paterlini-Brechot, R. Rizzuto, G. Szabadkai, G. Pierron, K. Blomgren, N. Tavernarakis, P. Codogno, F. Cecconi, G. Kroemer, Regulation of autophagy by cytoplasmic p53, Nat. Cell Biol. 10 (2008) 676–687. https://doi.org/10.1038/ncb1730.

[196] E. Morselli, E. Tasdemir, M.C. Maiuri, L. Galluzzi, O. Kepp, A. Criollo, J.M. Vicencio, T. Soussi, G. Kroemer, Mutant p53 protein localized in the cytoplasm inhibits autophagy,

Cell Cycle. 7 (2008) 3056–3061. https://doi.org/10.4161/cc.7.19.6751.

[197] E. Morselli, S. Shen, C. Ruckenstuhl, M.A. Bauer, G. Mariño, L. Galluzzi, A. Criollo, M. Michaud, M.C. Maiuri, T. Chano, F. Madeo, G. Kroemer, p53 inhibits autophagy by interacting with the human ortholog of yeast Atg17, RB1CC1/FIP200, Cell Cycle. 10 (2011) 2763–2769. https://doi.org/10.4161/cc.10.16.16868.

[198] J.-H. Chen, P. Zhang, W.-D. Chen, D.-D. Li, X.-Q. Wu, R. Deng, L. Jiao, X. Li, J. Ji, G.-K. Feng, Y.-X. Zeng, J.-W. Jiang, X.-F. Zhu, ATM-mediated PTEN phosphorylation promotes PTEN nuclear translocation and autophagy in response to DNA-damaging agents in cancer cells., Autophagy. 11 (2015) 239–52. https://doi.org/10.1080/15548627.2015.1009767.

[199] G. Napolitano, A. Ballabio, TFEB at a glance, J. Cell Sci. 129 (2016) 2475–2481. https://doi.org/10.1242/jcs.146365.

[200] J.A. Martina, Y. Chen, M. Gucek, R. Puertollano, MTORC1 functions as a transcriptional regulator of autophagy by preventing nuclear transport of TFEB, Autophagy. 8 (2012) 903–914. https://doi.org/10.4161/auto.19653.

[201] J.A. Martina, R. Puertollano, Rag GTPases mediate amino acid-dependent recruitment of TFEB and MITF to lysosomes, J. Cell Biol. 200 (2013) 475–491. https://doi.org/10.1083/jcb.201209135.

[202] J.A. Martina, H.I. Diab, L. Lishu, L. Jeong-A, S. Patange, N. Raben, R. Puertollano, The nutrient-responsive transcription factor TFE3 promotes autophagy, lysosomal biogenesis, and clearance of cellular debris, Sci. Signal. 7 (2014) ra9-ra9. https://doi.org/10.1126/scisignal.2004754.

[203] E. Jeong, O.A. Brady, J.A. Martina, M. Pirooznia, I. Tunc, R. Puertollano, The transcription factors TFE3 and TFEB amplify p53 dependent transcriptional programs in response to DNA damage, Elife. 7 (2018). https://doi.org/10.7554/eLife.40856.

[204] J. Füllgrabe, G. Ghislat, D.-H. Cho, D.C. Rubinsztein, Transcriptional regulation of mammalian autophagy at a glance, J. Cell Sci. 129 (2016) 3059–3066. https://doi.org/10.1242/JCS.188920.

[205] S. Björklund, L. Thelander, S. Skog, B. Tribukait, S-Phase-Specific Expression of Mammalian Ribonucleotide Reductase R1 and R2 Subunit mRNAs, Biochemistry. 29 (1990) 5452–5458. https://doi.org/10.1021/bi00475a007.

[206] M. Dyavaiah, J.P. Rooney, S. V. Chittur, Q. Lin, T.J. Begley, Autophagy-Dependent Regulation of the DNA Damage Response Protein Ribonucleotide Reductase 1, Mol. Cancer Res. 9 (2011) 462–475. https://doi.org/10.1158/1541-7786.MCR-10-0473.

[207] V. Domkin, L. Thelander, A. Chabes, Yeast DNA damage-inducible Rnr3 has a very low catalytic activity strongly stimulated after the formation of a cross-talking Rnr1/Rnr3 complex, J. Biol. Chem. 277 (2002) 18574–18578. https://doi.org/10.1074/jbc.M201553200.

[208] J. Yue, H. Lu, J. Liu, M. Berwick, Z. Shen, Filamin-A as a marker and target for DNA

damage based cancer therapy, DNA Repair (Amst). 11 (2012) 192–200. https://doi.org/10.1016/j.dnarep.2011.10.019.

[209] G. Hewitt, B. Carroll, R. Sarallah, C. Correia-Melo, M. Ogrodnik, G. Nelson, E.G. Otten, D. Manni, R. Antrobus, B.A. Morgan, T. von Zglinicki, D. Jurk, A. Seluanov, V. Gorbunova, T. Johansen, J.F. Passos, V.I. Korolchuk, SQSTM1/p62 mediates crosstalk between autophagy and the UPS in DNA repair, Autophagy. 12 (2016) 1917–1930. https://doi.org/10.1080/15548627.2016.1210368.

[210] Y. Wang, N. Zhang, L. Zhang, R. Li, W. Fu, K. Ma, X. Li, L. Wang, J. Wang, H. Zhang, W. Gu, W.G. Zhu, Y. Zhao, Autophagy Regulates Chromatin Ubiquitination in DNA Damage Response through Elimination of SQSTM1/p62, Mol. Cell. 63 (2016) 34–48. https://doi.org/10.1016/j.molcel.2016.05.027.

[211] A. Sharma, T. Alswillah, K. Singh, P. Chatterjee, B. Willard, M. Venere, M.K. Summers, A. Almasan, USP14 regulates DNA damage repair by targeting RNF168-dependent ubiquitination, Autophagy. 14 (2018) 1976–1990. https://doi.org/10.1080/15548627.2018.1496877.

[212] E.Y. Liu, N. Xu, J. O'Prey, L.Y. Lao, S. Joshi, J.S. Long, M. O'Prey, D.R. Croft, F. Beaumatin, A.D. Baudot, M. Mrschtik, M. Rosenfeldt, Y. Zhang, D.A. Gillespie, K.M. Ryan, Loss of autophagy causes a synthetic lethal deficiency in DNA repair, Proc. Natl. Acad. Sci. 112 (2015) 773–778. https://doi.org/10.1073/pnas.1409563112.

[213] H. Zhang, J.M. Barceló, B. Lee, G. Kohlhagen, D.B. Zimonjic, N.C. Popescu, Y. Pommier, Human mitochondrial topoisomerase I, Proc. Natl. Acad. Sci. U. S. A. 98 (2001) 10608–10613. https://doi.org/10.1073/pnas.191321998.

[214] X. Ren, L. Zhang, Y. Zhang, L. Mao, H. Jiang, Mitochondria response to camptothecin and hydroxycamptothecine-induced apoptosis in Spodoptera exigua cells, Pestic. Biochem. Physiol. 140 (2017) 97–104. https://doi.org/10.1016/j.pestbp.2017.07.003.

[215] N. Sen, B.B. Das, A. Ganguly, T. Mukherjee, G. Tripathi, S. Bandyopadhyay, S. Rakshit, T. Sen, H.K. Majumder, Camptothecin induced mitochondrial dysfunction leading to programmed cell death in unicellular hemoflagellate Leishmania donovani, Cell Death Differ. 11 (2004) 924–936. https://doi.org/10.1038/sj.cdd.4401435.

[216] S.-C. Chiang, M. Meagher, N. Kassouf, M. Hafezparast, P.J. McKinnon, R. Haywood, S.F. El-Khamisy, Mitochondrial protein-linked DNA breaks perturb mitochondrial gene transcription and trigger free radical–induced DNA damage, Sci. Adv. 3 (2017) e1602506. https://doi.org/10.1126/sciadv.1602506.

[217] Y.A. Valentin-Vega, K.H. Maclean, J. Tait-Mulder, S. Milasta, M. Steeves, F.C. Dorsey, J.L. Cleveland, D.R. Green, M.B. Kastan, Mitochondrial dysfunction in ataxia-telangiectasia., Blood. 119 (2012) 1490–500. https://doi.org/10.1182/blood-2011-08-373639.

[218] Y. Qi, Q. Qiu, X. Gu, Y. Tian, Y. Zhang, ATM mediates spermidine-induced mitophagy via PINK1 and Parkin regulation in human fibroblasts, Sci. Rep. 6 (2016) 24700. https://doi.org/10.1038/srep24700.

[219] Y. Tomioka, T. Kotani, H. Kirisako, Y. Oikawa, Y. Kimura, H. Hirano, Y. Ohsumi, H. Nakatogawa, TORC1 inactivation stimulates autophagy of nucleoporin and nuclear pore complexes, J. Cell Biol. 219 (2020). https://doi.org/10.1083/jcb.201910063.

[220] C.W. Lee, F. Wilfling, P. Ronchi, M. Allegretti, S. Mosalaganti, S. Jentsch, M. Beck, B. Pfander, Selective autophagy degrades nuclear pore complexes, Nat. Cell Biol. 22 (2020) 159–166. https://doi.org/10.1038/s41556-019-0459-2.

[221] K. Mochida, Y. Oikawa, Y. Kimura, H. Kirisako, H. Hirano, Y. Ohsumi, H. Nakatogawa, Receptor-mediated selective autophagy degrades the endoplasmic reticulum and the nucleus, Nature. 522 (2015) 359–362. https://doi.org/10.1038/nature14506.

[222] D. Mijaljica, M. Prescott, R.J. Devenish, A Late Form of Nucleophagy in Saccharomyces cerevisiae, PLoS One. 7 (2012) e40013. https://doi.org/10.1371/journal.pone.0040013.

[223] S. Chandra, P.J. Mannino, D.J. Thaller, N.R. Ader, M.C. King, T.J. Melia, C.P. Lusk, Atg39 selectively captures inner nuclear membrane into lumenal vesicles for delivery to the autophagosome, J. Cell Biol. 220 (2021). https://doi.org/10.1083/jcb.202103030.

[224] K. Bartsch, K. Knittler, C. Borowski, S. Rudnik, M. Damme, K. Aden, M.E. Spehlmann, N. Frey, P. Saftig, A. Chalaris, B. Rabe, Absence of RNase H2 triggers generation of immunogenic micronuclei removed by autophagy, Hum. Mol. Genet. 26 (2017) 3960–3972. https://doi.org/10.1093/hmg/ddx283.

[225] Z. Dou, C. Xu, G. Donahue, T. Shimi, J.-A. Pan, J. Zhu, A. Ivanov, B.C. Capell, A.M. Drake, P.P. Shah, J.M. Catanzaro, M. Daniel Ricketts, T. Lamark, S.A. Adam, R. Marmorstein, W.-X. Zong, T. Johansen, R.D. Goldman, P.D. Adams, S.L. Berger, Autophagy mediates degradation of nuclear lamina, Nature. 527 (2015) 105–109. https://doi.org/10.1038/nature15548.

[226] Z. Dou, A. Ivanov, P.D. Adams, S.L. Berger, Mammalian autophagy degrades nuclear constituents in response to tumorigenic stress, Autophagy. 12 (2016) 1416–1417. https://doi.org/10.1080/15548627.2015.1127465.

[227] S. Rello-Varona, D. Lissa, S. Shen, M. Niso-Santano, L. Senovilla, G. Mariño, I. Vitale, M. Jemaà, F. Harper, G. Pierron, M. Castedo, G. Kroemer, Autophagic removal of micronuclei, Cell Cycle. 11 (2012) 170–176. https://doi.org/10.4161/cc.11.1.18564.

[228] Y.Y. Lan, D. Londoño, R. Bouley, M.S. Rooney, N. Hacohen, Dnase2a Deficiency Uncovers Lysosomal Clearance of Damaged Nuclear DNA via Autophagy, Cell Rep. 9 (2014) 180–192. https://doi.org/10.1016/j.celrep.2014.08.074.

[229] Y.Y. Lan, J.M. Heather, T. Eisenhaure, C.S. Garris, D. Lieb, R. Raychowdhury, N. Hacohen, Extranuclear DNA accumulates in aged cells and contributes to senescence and inflammation, Aging Cell. 18 (2019). https://doi.org/10.1111/acel.12901.

[230] X. Gui, H. Yang, T. Li, X. Tan, P. Shi, M. Li, F. Du, Z.J. Chen, Autophagy induction via STING trafficking is a primordial function of the cGAS pathway, Nature. 567 (2019) 262–266. https://doi.org/10.1038/s41586-019-1006-9.

[231] S.M. Harding, J.L. Benci, J. Irianto, D.E. Discher, A.J. Minn, R.A. Greenberg, Mitotic progression following DNA damage enables pattern recognition within micronuclei, Nature. 548 (2017) 466–470. https://doi.org/10.1038/nature23470.

[232] K.J. Mackenzie, P. Carroll, C.-A. Martin, O. Murina, A. Fluteau, D.J. Simpson, N. Olova, H. Sutcliffe, J.K. Rainger, A. Leitch, R.T. Osborn, A.P. Wheeler, M. Nowotny, N. Gilbert, T. Chandra, M.A.M. Reijns, A.P. Jackson, cGAS surveillance of micronuclei links genome instability to innate immunity, Nature. 548 (2017) 461–465. https://doi.org/10.1038/nature23449.

[233] M. Zhao, F. Wang, J. Wu, Y. Cheng, Y. Cao, X. Wu, M. Ma, F. Tang, Z. Liu, H. Liu, B. Ge, CGAS is a micronucleophagy receptor for the clearance of micronuclei, Autophagy. (2021) 1–17. https://doi.org/10.1080/15548627.2021.1899440.

[234] Y. Fujiwara, A. Furuta, H. Kikuchi, S. Aizawa, Y. Hatanaka, C. Konya, K. Uchida, A. Yoshimura, Y. Tamai, K. Wada, T. Kabuta, Discovery of a novel type of autophagy targeting RNA, Autophagy. 9 (2013) 403–409. https://doi.org/10.4161/auto.23002.

[235] Y. Fujiwara, H. Kikuchi, S. Aizawa, A. Furuta, Y. Hatanaka, C. Konya, K. Uchida, K. Wada, T. Kabuta, Direct uptake and degradation of DNA by lysosomes, Autophagy. 9 (2013) 1167–1171. https://doi.org/10.4161/auto.24880.

[236] K. Hase, Y. Fujiwara, H. Kikuchi, S. Aizawa, F. Hakuno, S.I. Takahashi, K. Wada, T. Kabuta, RNautophagy/DNautophagy possesses selectivity for RNA/DNA substrates, Nucleic Acids Res. 43 (2015) 6439–6449. https://doi.org/10.1093/nar/gkv579.

[237] S. Aizawa, V.R. Contu, Y. Fujiwara, K. Hase, H. Kikuchi, C. Kabuta, K. Wada, T. Kabuta, Lysosomal membrane protein SIDT2 mediates the direct uptake of DNA by lysosomes, Autophagy. 13 (2017) 218–222. https://doi.org/10.1080/15548627.2016.1248019.

[238] S. Aizawa, Y. Fujiwara, V.R. Contu, K. Hase, M. Takahashi, H. Kikuchi, C. Kabuta, K. Wada, T. Kabuta, Lysosomal putative RNA transporter SIDT2 mediates direct uptake of RNA by lysosomes, Autophagy. 12 (2016) 565–578. https://doi.org/10.1080/15548627.2016.1145325.

[239] Y. Fujiwara, K. Hase, K. Wada, T. Kabuta, An RNautophagy/DNautophagy receptor, LAMP2C, possesses an arginine-rich motif that mediates RNA/DNA-binding, Biochem. Biophys. Res. Commun. 460 (2015) 281–286. https://doi.org/10.1016/j.bbrc.2015.03.025.

[240] K. Hase, V.R. Contu, C. Kabuta, R. Sakai, M. Takahashi, N. Kataoka, F. Hakuno, S.I. Takahashi, Y. Fujiwara, K. Wada, T. Kabuta, Cytosolic domain of SIDT2 carries an arginine-rich motif that binds to RNA/DNA and is important for the direct transport of nucleic acids into lysosomes, Autophagy. (2020). https://doi.org/10.1080/15548627.2020.1712109.

[241] K. Ma, W. Fu, M. Tang, C. Zhang, T. Hou, R. Li, X. Lu, Y. Wang, J. Zhou, X. Li, L. Zhang, L. Wang, Y. Zhao, W.-G. Zhu, PTK2-mediated degradation of ATG3 impedes cancer cells susceptible to DNA damage treatment, Autophagy. 13 (2017) 579–591. https://doi.org/10.1080/15548627.2016.1272742.

[242] D. Maskey, S. Yousefi, I. Schmid, I. Zlobec, A. Perren, R. Friis, H.-U. Simon, ATG5 is induced by DNA-damaging agents and promotes mitotic catastrophe independent of autophagy, Nat. Commun. 4 (2013) 2130. https://doi.org/10.1038/ncomms3130.

[243] D.J. Klionsky, A.K. Abdel-Aziz, S. Abdelfatah, M. Abdellatif, A. Abdoli, S. Abel, H. Abeliovich, M.H. Abildgaard, Y.P. Abudu, A. Acevedo-Arozena, I.E. Adamopoulos, K. Adeli, T.E. Adolph, A. Adornetto, E. Aflaki, G. Agam, A. Agarwal, B.B. Aggarwal, M. Agnello, P. Agostinis, J.N. Agrewala, A. Agrotis, P. V Aguilar, S.T. Ahmad, Z.M. Ahmed, U. Ahumada-Castro, S. Aits, S. Aizawa, Y. Akkoc, T. Akoumianaki, H.A. Akpinar, A.M. Al-Abd, L. Al-Akra, A. Al-Gharaibeh, M.A. Alaoui-Jamali, S. Alberti, E. Alcocer-Gómez, C. Alessandri, M. Ali, M.A. Alim Al-Bari, S. Aliwaini, J. Alizadeh, E. Almacellas, A. Almasan, A. Alonso, G.D. Alonso, N. Altan-Bonnet, D.C. Altieri, É.M.C. Álvarez, S. Alves, C. Alves da Costa, M.M. Alzaharna, M. Amadio, C. Amantini, C. Amaral, S. Ambrosio, A.O. Amer, V. Ammanathan, Z. An, S.U. Andersen, S.A. Andrabi, M. Andrade-Silva, A.M. Andres, S. Angelini, D. Ann, U.C. Anozie, M.Y. Ansari, P. Antas, A. Antebi, Z. Antón, T. Anwar, L. Apetoh, N. Apostolova, T. Araki, Y. Araki, K. Arasaki, W.L. Araújo, J. Araya, C. Arden, M.-A. Arévalo, S. Arguelles, E. Arias, J. Arikkath, H. Arimoto, A.R. Ariosa, D. Armstrong-James, L. Arnauné-Pelloquin, A. Aroca, D.S. Arroyo, I. Arsov, R. Artero, D.M.L. Asaro, M. Aschner, M. Ashrafizadeh, O. Ashur-Fabian, A.G. Atanasov, A.K. Au, P. Auberger, H.W. Auner, L. Aurelian, R. Autelli, L. Avagliano, Y. Ávalos, S. Aveic, C.A. Aveleira, T. Avin-Wittenberg, Y. Aydin, S. Ayton, S. Ayyadevara, M. Azzopardi, M. Baba, J.M. Backer, S.K. Backues, D.-H. Bae, O.-N. Bae, S.H. Bae, E.H. Baehrecke, A. Baek, S.-H. Baek, S.H. Baek, G. Bagetta, A. Bagniewska-Zadworna, H. Bai, J. Bai, X. Bai, Y. Bai, N. Bairagi, S. Baksi, T. Balbi, C.T. Baldari, W. Balduini, A. Ballabio, M. Ballester, S. Balazadeh, R. Balzan, R. Bandopadhyay, S. Banerjee, S. Banerjee, Á. Bánréti, Y. Bao, M.S. Baptista, A. Baracca, C. Barbati, A. Bargiela, D. Barilà, P.G. Barlow, S.J. Barmada, E. Barreiro, G.E. Barreto, J. Bartek, B. Bartel, A. Bartolome, G.R. Barve, S.H. Basagoudanavar, D.C. Bassham, R.C. Bast, A. Basu, H. Batoko, I. Batten, E.E. Baulieu, B.L. Baumgarner, J. Bayry, R. Beale, I. Beau, F. Beaumatin, L.R.G. Bechara, G.R. Beck, M.F. Beers, J. Begun, C. Behrends, G.M.N. Behrens, R. Bei, E. Bejarano, S. Bel, C. Behl, A. Belaid, N. Belgareh-Touzé, C. Bellarosa, F. Belleudi, M. Belló Pérez, R. Bello-Morales, J.S. de O. Beltran, S. Beltran, D.M. Benbrook, M. Bendorius, B.A. Benitez, I. Benito-Cuesta, J. Bensalem, M.W. Berchtold, S. Berezowska, D. Bergamaschi, M. Bergami, A. Bergmann, L. Berliocchi, C. Berlioz-Torrent, A. Bernard, L. Berthoux, C.G. Besirli, S. Besteiro, V.M. Betin, R. Beyaert, J.S. Bezbradica, K. Bhaskar, I. Bhatia-Kissova, R. Bhattacharya, S. Bhattacharya, S. Bhattacharyya, M.S. Bhuiyan, S.K. Bhutia, L. Bi, X. Bi, T.J. Biden, K. Bijian, V.A. Billes, N. Binart, C. Bincoletto, A.B. Birgisdottir, G. Bjorkoy, G. Blanco, A. Blas-Garcia, J. Blasiak, R. Blomgran, K. Blomgren, J.S. Blum, E. Boada-Romero, M. Boban, K. Boesze-Battaglia, P. Boeuf, B. Boland, P. Bomont, P. Bonaldo, S.R. Bonam, L. Bonfili, J.S. Bonifacino, B.A. Boone, M.D. Bootman, M. Bordi, C. Borner, B.C. Bornhauser, G. Borthakur, J. Bosch, S. Bose, L.M. Botana, J. Botas, C.M. Boulanger, M.E. Boulton, M. Bourdenx, B. Bourgeois, N.M. Bourke, G. Bousquet, P. Boya, P. V Bozhkov, L.H.M. Bozi, T.O. Bozkurt, D.E. Brackney, C.H. Brandts, R.J. Braun, G.H. Braus, R. Bravo-Sagua, J.M. Bravo-San Pedro, P. Brest, M.-A. Bringer, A. Briones-Herrera, V.C. Broaddus, P. Brodersen, J.L. Brodsky, S.L. Brody, P.G. Bronson, J.M. Bronstein, C.N. Brown, R.E. Brown, P.C. Brum, J.H. Brumell, N. Brunetti-Pierri, D. Bruno, R.J. Bryson-Richardson, C. Bucci, C. Buchrieser, M. Bueno, L.E. Buitrago-Molina, S. Buraschi, S. Buch, J.R. Buchan, E.M. Buckingham, H. Budak, M. Budini, G. Bultynck,

F. Burada, J.R. Burgoyne, M.I. Burón, V. Bustos, S. Büttner, E. Butturini, A. Byrd, I. Cabas, S. Cabrera-Benitez, K. Cadwell, J. Cai, L. Cai, Q. Cai, M. Cairó, J.A. Calbet, G.A. Caldwell, K.A. Caldwell, J.A. Call, R. Calvani, A.C. Calvo, M. Calvo-Rubio Barrera, N.O.S. Camara, J.H. Camonis, N. Camougrand, M. Campanella, E.M. Campbell, F.-X. Campbell-Valois, S. Campello, I. Campesi, J.C. Campos, O. Camuzard, J. Cancino, D. Candido de Almeida, L. Canesi, I. Caniggia, B. Canonico, C. Cantí, B. Cao, M. Caraglia, B. Caramés, E.H. Carchman, E. Cardenal-Muñoz, C. Cardenas, L. Cardenas, S.M. Cardoso, J.S. Carew, G.F. Carle, G. Carleton, S. Carloni, D. Carmona-Gutierrez, L.A. Carneiro, O. Carnevali, J.M. Carosi, S. Carra, A. Carrier, L. Carrier, B. Carroll, A.B. Carter, A.N. Carvalho, M. Casanova, C. Casas, J. Casas, C. Cassioli, E.F. Castillo, K. Castillo, S. Castillo-Lluva, F. Castoldi, M. Castori, A.F. Castro, M. Castro-Caldas, J. Castro-Hernandez, S. Castro-Obregon, S.D. Catz, C. Cavadas, F. Cavaliere, G. Cavallini, M. Cavinato, M.L. Cayuela, P. Cebollada Rica, V. Cecarini, F. Cecconi, M. Cechowska-Pasko, S. Cenci, V. Ceperuelo-Mallafré, J.J. Cerqueira, J.M. Cerutti, D. Cervia, V.B. Cetintas, S. Cetrullo, H.-J. Chae, A.S. Chagin, C.-Y. Chai, G. Chakrabarti, O. Chakrabarti, T. Chakraborty, T. Chakraborty, M. Chami, G. Chamilos, D.W. Chan, E.Y.W. Chan, E.D. Chan, H.Y.E. Chan, H.H. Chan, H. Chan, M.T. V Chan, Y.S. Chan, P.K. Chandra, C.-P. Chang, C. Chang, H.-C. Chang, K. Chang, J. Chao, T. Chapman, N. Charlet-Berguerand, S. Chatterjee, S.K. Chaube, A. Chaudhary, S. Chauhan, E. Chaum, F. Checler, M.E. Cheetham, C.-S. Chen, G.-C. Chen, J.-F. Chen, L.L. Chen, L. Chen, L. Chen, M. Chen, M.-K. Chen, N. Chen, Q. Chen, R.-H. Chen, S. Chen, W. Chen, W. Chen, X.-M. Chen, X.-W. Chen, X. Chen, Y. Chen, Y.-G. Chen, Y. Chen, Y. Chen, Y.-J. Chen, Y.-Q. Chen, Z.S. Chen, Z. Chen, Z.-H. Chen, Z.J. Chen, Z. Chen, H. Cheng, J. Cheng, S.-Y. Cheng, W. Cheng, X. Cheng, X.-T. Cheng, Y. Cheng, Z. Cheng, Z. Chen, H. Cheong, J.K. Cheong, B. V Chernyak, S. Cherry, C.F.R. Cheung, C.H.A. Cheung, K.-H. Cheung, E. Chevet, R.J. Chi, A.K.S. Chiang, F. Chiaradonna, R. Chiarelli, M. Chiariello, N. Chica, S. Chiocca, M. Chiong, S.-H. Chiou, A.I. Chiramel, V. Chiurchiù, D.-H. Cho, S.-K. Choe, A.M.K. Choi, M.E. Choi, K.R. Choudhury, N.S. Chow, C.T. Chu, J.P. Chua, J.J.E. Chua, H. Chung, K.P. Chung, S. Chung, S.-H. Chung, Y.-L. Chung, V. Cianfanelli, I.A. Ciechomska, M. Cifuentes, L. Cinque, S. Cirak, M. Cirone, M.J. Clague, R. Clarke, E. Clementi, E.M. Coccia, P. Codogno, E. Cohen, M.M. Cohen, T. Colasanti, F. Colasuonno, R.A. Colbert, A. Colell, M. Čolić, N.S. Coll, M.O. Collins, M.I. Colombo, D.A. Colón-Ramos, L. Combaret, S. Comincini, M.R. Cominetti, A. Consiglio, A. Conte, F. Conti, V.R. Contu, M.R. Cookson, K.M. Coombs, I. Coppens, M.T. Corasaniti, D.P. Corkery, N. Cordes, K. Cortese, M. do C. Costa, S. Costantino, P. Costelli, A. Coto-Montes, P.J. Crack, J.L. Crespo, A. Criollo, V. Crippa, R. Cristofani, T. Csizmadia, A. Cuadrado, B. Cui, J. Cui, Y. Cui, Y. Cui, E. Culetto, A.C. Cumino, A. V Cybulsky, M.J. Czaja, S.J. Czuczwar, S. D'Adamo, M. D'Amelio, D. D'Arcangelo, A.C. D'Lugos, G. D'Orazi, J.A. da Silva, H.S. Dafsari, R.K. Dagda, Y. Dagdas, M. Daglia, X. Dai, Y. Dai, Y. Dai, J. Dal Col, P. Dalhaimer, L. Dalla Valle, T. Dallenga, G. Dalmasso, M. Damme, I. Dando, N.P. Dantuma, A.L. Darling, H. Das, S. Dasarathy, S.K. Dasari, S. Dash, O. Daumke, A.N. Dauphinee, J.S. Davies, V.A. Dávila, R.J. Davis, T. Davis, S. Dayalan Naidu, F. De Amicis, K. De Bosscher, F. De Felice, L. De Franceschi, C. De Leonibus, M.G. de Mattos Barbosa, G.R.Y. De Meyer, A. De Milito, C. De Nunzio, C. De Palma, M. De Santi, C. De Virgilio, D. De Zio, J. Debnath, B.J. DeBosch, J.-P. Decuypere, M.A. Deehan, G. Deflorian, J. DeGregori, B. Dehay, G. Del Rio, J.R. Delaney, L.M.D. Delbridge, E. Delorme-Axford, M.V. Delpino, F. Demarchi, V. Dembitz, N.D. Demers, H. Deng, Z. Deng, J. Dengjel, P. Dent, D. Denton,

M.L. DePamphilis, C.J. Der, V. Deretic, A. Descoteaux, L. Devis, S. Devkota, O. Devuyst, G. Dewson, M. Dharmasivam, R. Dhiman, D. di Bernardo, M. Di Cristina, F. Di Domenico, P. Di Fazio, A. Di Fonzo, G. Di Guardo, G.M. Di Guglielmo, L. Di Leo, C. Di Malta, A. Di Nardo, M. Di Rienzo, F. Di Sano, G. Diallinas, J. Diao, G. Diaz-Araya, I. Díaz-Laviada, J.M. Dickinson, M. Diederich, M. Dieudé, I. Dikic, S. Ding, W.-X. Ding, L. Dini, J. Dinić, M. Dinic, A.T. Dinkova-Kostova, M.S. Dionne, J.H.W. Distler, A. Diwan, I.M.C. Dixon, M. Djavaheri-Mergny, I. Dobrinski, O. Dobrovinskaya, R. Dobrowolski, R.C.J. Dobson, J. Đokić, S. Dokmeci Emre, M. Donadelli, B. Dong, X. Dong, Z. Dong, G.W. Dorn II, V. Dotsch, H. Dou, J. Dou, M. Dowaidar, S. Dridi, L. Drucker, A. Du, C. Du, G. Du, H.-N. Du, L.-L. Du, A. du Toit, S.-B. Duan, X. Duan, S.P. Duarte, A. Dubrovska, E.A. Dunlop, N. Dupont, R. V Durán, B.S. Dwarakanath, S.A. Dyshlovoy, D. Ebrahimi-Fakhari, L. Eckhart, C.L. Edelstein, T. Efferth, E. Eftekharpour, L. Eichinger, N. Eid, T. Eisenberg, N.T. Eissa, S. Eissa, M. Ejarque, A. El Andaloussi, N. El-Hage, S. El-Naggar, A.M. Eleuteri, E.S. El-Shafey, M. Elgendy, A.G. Eliopoulos, M.M. Elizalde, P.M. Elks, H.-P. Elsasser, E.S. Elsherbiny, B.M. Emerling, N.C.T. Emre, C.H. Eng, N. Engedal, A.-M. Engelbrecht, A.S.T. Engelsen, J.M. Enserink, R. Escalante, A. Esclatine, M. Escobar-Henriques, E.-L. Eskelinen, L. Espert, M.-O. Eusebio, G. Fabrias, C. Fabrizi, A. Facchiano, F. Facchiano, B. Fadeel, C. Fader, A.C. Faesen, W.D. Fairlie, A. Falcó, B.H. Falkenburger, D. Fan, J. Fan, Y. Fan, E.F. Fang, Y. Fang, Y. Fang, M. Fanto, T. Farfel-Becker, M. Faure, G. Fazeli, A.O. Fedele, A.M. Feldman, D. Feng, J. Feng, L. Feng, Y. Feng, Y. Feng, W. Feng, T. Fenz Araujo, T.A. Ferguson, Á.F. Fernández, J.C. Fernandez-Checa, S. Fernández-Veledo, A.R. Fernie, A.W. Ferrante, A. Ferraresi, M.F. Ferrari, J.C.B. Ferreira, S. Ferro-Novick, A. Figueras, R. Filadi, N. Filigheddu, E. Filippi-Chiela, G. Filomeni, G.M. Fimia, V. Fineschi, F. Finetti, S. Finkbeiner, E.A. Fisher, P.B. Fisher, F. Flamigni, S.J. Fliesler, T.H. Flo, I. Florance, O. Florey, T. Florio, E. Fodor, C. Follo, E.A. Fon, A. Forlino, F. Fornai, P. Fortini, A. Fracassi, A. Fraldi, B. Franco, R. Franco, F. Franconi, L.B. Frankel, S.L. Friedman, L.F. Fröhlich, G. Frühbeck, J.M. Fuentes, Y. Fujiki, N. Fujita, Y. Fujiwara, M. Fukuda, S. Fulda, L. Furic, N. Furuya, C. Fusco, M.U. Gack, L. Gaffke, S. Galadari, A. Galasso, M.F. Galindo, S. Gallolu Kankanamalage, L. Galluzzi, V. Galy, N. Gammoh, B. Gan, I.G. Ganley, F. Gao, H. Gao, M. Gao, P. Gao, S.-J. Gao, W. Gao, X. Gao, A. Garcera, M.N. Garcia, V.E. Garcia, F. García-Del Portillo, V. Garcia-Escudero, A. Garcia-Garcia, M. Garcia-Macia, D. García-Moreno, C. Garcia-Ruiz, P. García-Sanz, A.D. Garg, R. Gargini, T. Garofalo, R.F. Garry, N.C. Gassen, D. Gatica, L. Ge, W. Ge, R. Geiss-Friedlander, C. Gelfi, P. Genschik, I.E. Gentle, V. Gerbino, C. Gerhardt, K. Germain, M. Germain, D.A. Gewirtz, E. Ghasemipour Afshar, S. Ghavami, A. Ghigo, M. Ghosh, G. Giamas, C. Giampietri, A. Giatromanolaki, G.E. Gibson, S.B. Gibson, V. Ginet, E. Giniger, C. Giorgi, H. Girao, S.E. Girardin, M. Giridharan, S. Giuliano, C. Giulivi, S. Giuriato, J. Giustiniani, A. Gluschko, V. Goder, A. Goginashvili, J. Golab, D.C. Goldstone, A. Golebiewska, L.R. Gomes, R. Gomez, R. Gómez-Sánchez, M.C. Gomez-Puerto, R. Gomez-Sintes, Q. Gong, F.M. Goni, J. González-Gallego, T. Gonzalez-Hernandez, R.A. Gonzalez-Polo, J.A. Gonzalez-Reyes, P. González-Rodríguez, I.S. Goping, M.S. Gorbatyuk, N. V Gorbunov, K. Görgülü, R.M. Gorojod, S.M. Gorski, S. Goruppi, C. Gotor, R.A. Gottlieb, I. Gozes, D. Gozuacik, M. Graef, M.H. Gräler, V. Granatiero, D. Grasso, J.P. Gray, D.R. Green, A. Greenhough, S.L. Gregory, E.F. Griffin, M.W. Grinstaff, F. Gros, C. Grose, A.S. Gross, F. Gruber, P. Grumati, T. Grune, X. Gu, J.-L. Guan, C.M. Guardia, K. Guda, F. Guerra, C. Guerri, P. Guha, C. Guillén, S. Gujar, A. Gukovskaya, I. Gukovsky, J. Gunst, A. Günther, A.R. Guntur, C. Guo, C. Guo, H. Guo, L.-

W. Guo, M. Guo, P. Gupta, S.K. Gupta, S. Gupta, V.B. Gupta, V. Gupta, A.B. Gustafsson, D.D. Gutterman, R. H.B., A. Haapasalo, J.E. Haber, A. Hać, S. Hadano, A.J. Hafrén, M. Haidar, B.S. Hall, G. Halldén, A. Hamacher-Brady, A. Hamann, M. Hamasaki, W. Han, M. Hansen, P.I. Hanson, Z. Hao, M. Harada, L. Harhaji-Trajkovic, N. Hariharan, N. Haroon, J. Harris, T. Hasegawa, N. Hasima Nagoor, J.A. Haspel, V. Haucke, W.D. Hawkins, B.A. Hay, C.M. Haynes, S.B. Hayrabedyan, T.S. Hays, C. He, Q. He, R.-R. He, Y.-W. He, Y.-Y. He, Y. Heakal, A.M. Heberle, J.F. Hejtmancik, G.V. Helgason, V. Henkel, M. Herb, A. Hergovich, A. Herman-Antosiewicz, A. Hernández, C. Hernandez, S. Hernandez-Diaz, V. Hernandez-Gea, A. Herpin, J. Herreros, J.H. Hervás, D. Hesselson, C. Hetz, V.T. Heussler, Y. Higuchi, S. Hilfiker, J.A. Hill, W.S. Hlavacek, E.A. Ho, I.H.T. Ho, P.W.-L. Ho, S.-L. Ho, W.Y. Ho, G.A. Hobbs, M. Hochstrasser, P.H.M. Hoet, D. Hofius, P. Hofman, A. Höhn, C.I. Holmberg, J.R. Hombrebueno, C.-W.H. Yi-Ren Hong, L. V Hooper, T. Hoppe, R. Horos, Y. Hoshida, I.-L. Hsin, H.-Y. Hsu, B. Hu, D. Hu, L.-F. Hu, M.C. Hu, R. Hu, W. Hu, Y.-C. Hu, Z.-W. Hu, F. Hua, J. Hua, Y. Hua, C. Huan, C. Huang, C. Huang, C. Huang, C. Huang, H. Huang, K. Huang, M.L.H. Huang, R. Huang, S. Huang, T. Huang, X. Huang, Y.J. Huang, T.B. Huber, V. Hubert, C.A. Hubner, S.M. Hughes, W.E. Hughes, M. Humbert, G. Hummer, J.H. Hurley, S. Hussain, S. Hussain, P.J. Hussey, M. Hutabarat, H.-Y. Hwang, S. Hwang, A. Ieni, F. Ikeda, Y. Imagawa, Y. Imai, C. Imbriano, M. Imoto, D.M. Inman, K. Inoki, J. Iovanna, R. V Iozzo, G. Ippolito, J.E. Irazoqui, P. Iribarren, M. Ishaq, M. Ishikawa, N. Ishimwe, C. Isidoro, N. Ismail, S. Issazadeh-Navikas, E. Itakura, D. Ito, D. Ivankovic, S. Ivanova, A.K. V Iyer, J.M. Izquierdo, M. Izumi, M. Jäättelä, M.S. Jabir, W.T. Jackson, N. Jacobo-Herrera, A.-C. Jacomin, E. Jacquin, P. Jadiya, H. Jaeschke, C. Jagannath, A.J. Jakobi, J. Jakobsson, B. Janji, P. Jansen-Dürr, P.J. Jansson, J. Jantsch, S. Januszewski, A. Jassey, S. Jean, H. Jeltsch-David, P. Jendelova, A. Jenny, T.E. Jensen, N. Jessen, J.L. Jewell, J. Ji, L. Jia, R. Jia, L. Jiang, Q. Jiang, R. Jiang, T. Jiang, X. Jiang, Y. Jiang, M. Jimenez-Sanchez, E.-J. Jin, F. Jin, H. Jin, L. Jin, L. Jin, M. Jin, S. Jin, E.-K. Jo, C. Joffre, T. Johansen, G.V.W. Johnson, S.A. Johnston, E. Jokitalo, M.K. Jolly, L.A.B. Joosten, J. Jordan, B. Joseph, D. Ju, J.-S. Ju, J. Ju, E. Juárez, D. Judith, G. Juhász, Y. Jun, C.H. Jung, S.-C. Jung, Y.K. Jung, H. Jungbluth, J. Jungverdorben, S. Just, K. Kaarniranta, A. Kaasik, T. Kabuta, D. Kaganovich, A. Kahana, R. Kain, S. Kajimura, M. Kalamvoki, M. Kalia, D.S. Kalinowski, N. Kaludercic, I. Kalvari, J. Kaminska, V.O. Kaminskyy, H. Kanamori, K. Kanasaki, C. Kang, R. Kang, S.S. Kang, S. Kaniyappan, T. Kanki, T.-D. Kanneganti, A.G. Kanthasamy, A. Kanthasamy, M. Kantorow, O. Kapuy, M. V Karamouzis, M.R. Karim, P. Karmakar, R.G. Katare, M. Kato, S.H.E. Kaufmann, A. Kauppinen, G.P. Kaushal, S. Kaushik, K. Kawasaki, K. Kazan, P.-Y. Ke, D.J. Keating, U. Keber, J.H. Kehrl, K.E. Keller, C.W. Keller, J.K. Kemper, C.M. Kenific, O. Kepp, S. Kermorgant, A. Kern, R. Ketteler, T.G. Keulers, B. Khalfin, H. Khalil, B. Khambu, S.Y. Khan, V.K.M. Khandelwal, R. Khandia, W. Kho, N. V Khobrekar, S. Khuansuwan, M. Khundadze, S.A. Killackey, D. Kim, D.R. Kim, D.-H. Kim, D.-E. Kim, E.Y. Kim, E.-K. Kim, H.-R. Kim, H.-S. Kim, H.-R. Kim, J.H. Kim, J.K. Kim, J.-H. Kim, J. Kim, J.H. Kim, K. Il Kim, P.K. Kim, S.-J. Kim, S.R. Kimball, A. Kimchi, A.C. Kimmelman, T. Kimura, M.A. King, K.J. Kinghorn, C.G. Kinsey, V. Kirkin, L.A. Kirshenbaum, S.L. Kiselev, S. Kishi, K. Kitamoto, Y. Kitaoka, K. Kitazato, R.N. Kitsis, J.T. Kittler, O. Kjaerulff, P.S. Klein, T. Klopstock, J. Klucken, H. Knævelsrud, R.L. Knorr, B.C.B. Ko, F. Ko, J.-L. Ko, H. Kobayashi, S. Kobayashi, I. Koch, J.C. Koch, U. Koenig, D. Kögel, Y.H. Koh, M. Koike, S.D. Kohlwein, N.M. Kocaturk, M. Komatsu, J. König, T. Kono, B.T. Kopp, T. Korcsmaros, G. Korkmaz, V.I. Korolchuk, M.S. Korsnes, A. Koskela, J. Kota, Y. Kotake, M.L. Kotler, Y. Kou, M.I.

Koukourakis, E. Koustas, A.L. Kovacs, T. Kovács, D. Koya, T. Kozako, C. Kraft, D. Krainc, H. Krämer, A.D. Krasnodembskaya, C. Kretz-Remy, G. Kroemer, N.T. Ktistakis, K. Kuchitsu, S. Kuenen, L. Kuerschner, T. Kukar, A. Kumar, A. Kumar, D. Kumar, D. Kumar, S. Kumar, S. Kume, C. Kumsta, C.N. Kundu, M. Kundu, A.B. Kunnumakkara, L. Kurgan, T.G. Kutateladze, O. Kutlu, S. Kwak, H.J. Kwon, T.K. Kwon, Y.T. Kwon, I. Kyrmizi, A. La Spada, P. Labonté, S. Ladoire, I. Laface, F. Lafont, D.C. Lagace, V. Lahiri, Z. Lai, A.S. Laird, A. Lakkaraju, T. Lamark, S.-H. Lan, A. Landajuela, D.J.R. Lane, J.D. Lane, C.H. Lang, C. Lange, Ü. Langel, R. Langer, P. Lapaquette, J. Laporte, N.F. LaRusso, I. Lastres-Becker, W.C.Y. Lau, G.W. Laurie, S. Lavandero, B.Y.K. Law, H.K. Law, R. Layfield, W. Le, H. Le Stunff, A.Y. Leary, J.-J. Lebrun, L.Y.W. Leck, J.-P. Leduc-Gaudet, C. Lee, C.-P. Lee, D.-H. Lee, E.B. Lee, E.F. Lee, G.M. Lee, H.-J. Lee, H.K. Lee, J.M. Lee, J.S. Lee, J.-A. Lee, J.-Y. Lee, J.H. Lee, M. Lee, M.G. Lee, M.J. Lee, M.-S. Lee, S.Y. Lee, S.-J. Lee, S.Y. Lee, S.B. Lee, W.H. Lee, Y.-R. Lee, Y. Lee, Y. Lee, C. Lefebvre, R. Legouis, Y.L. Lei, Y. Lei, S. Leikin, G. Leitinger, L. Lemus, S. Leng, O. Lenoir, G. Lenz, H.J. Lenz, P. Lenzi, Y. León, A.M. Leopoldino, C. Leschczyk, S. Leskelä, E. Letellier, C.-T. Leung, P.S. Leung, J.S. Leventhal, B. Levine, P.A. Lewis, K. Ley, B. Li, D.-Q. Li, J. Li, J. Li, J. Li, K. Li, L. Li, M. Li, M. Li, M. Li, M. Li, M. Li, P.-L. Li, M.-Q. Li, Q. Li, S. Li, T. Li, W. Li, W. Li, X. Li, Y.-P. Li, Y. Li, Z. Li, Z. Li, Z. Li, J. Lian, C. Liang, Q. Liang, W. Liang, Y. Liang, Y. Liang, G. Liao, L. Liao, M. Liao, Y.-F. Liao, M. Librizzi, P.P.Y. Lie, M.A. Lilly, H.J. Lim, T.R.R. Lima, F. Limana, C. Lin, C.-W. Lin, D.-S. Lin, F.-C. Lin, J.D. Lin, K.M. Lin, K.-H. Lin, L.-T. Lin, P.-H. Lin, Q. Lin, S. Lin, S.-J. Lin, W. Lin, X. Lin, Y.-X. Lin, Y.-S. Lin, R. Linden, P. Lindner, S.-C. Ling, P. Lingor, A.K. Linnemann, Y.-C. Liou, M.M. Lipinski, S. Lipovšek, V.A. Lira, N. Lisiak, P.B. Liton, C. Liu, C.-H. Liu, C.-F. Liu, C.H. Liu, F. Liu, H. Liu, H.-S. Liu, H. Liu, H. Liu, J. Liu, J. Liu, J. Liu, L. Liu, L. Liu, M. Liu, Q. Liu, W. Liu, W. Liu, X.-H. Liu, X. Liu, X. Liu, X. Liu, X. Liu, Y. Liu, Y. Liu, Y. Liu, Y. Liu, Y. Liu, J.A. Livingston, G. Lizard, J.M. Lizcano, S. Ljubojevic-Holzer, M.E. LLeonart, D. Llobet-Navàs, A. Llorente, C.H. Lo, D. Lobato-Márquez, Q. Long, Y.C. Long, B. Loos, J.A. Loos, M.G. López, G. López-Doménech, J.A. López-Guerrero, A.T. López-Jiménez, Ó. López-Pérez, I. López-Valero, M.J. Lorenowicz, M. Lorente, P. Lorincz, L. Lossi, S. Lotersztajn, P.E. Lovat, J.F. Lovell, A. Lovy, P. Lőw, G. Lu, H. Lu, J.-H. Lu, J.-J. Lu, M. Lu, S. Lu, A. Luciani, J.M. Lucocq, P. Ludovico, M.A. Luftig, M. Luhr, D. Luis-Ravelo, J.J. Lum, L. Luna-Dulcey, A.H. Lund, V.K. Lund, J.D. Lünemann, P. Lüningschrör, H. Luo, R. Luo, S. Luo, Z. Luo, C. Luparello, B. Lüscher, L. Luu, A. Lyakhovich, K.G. Lyamzaev, A.H. Lystad, L. Lytvynchuk, A.C. Ma, C. Ma, M. Ma, N.-F. Ma, Q.-H. Ma, X. Ma, Y. Ma, Z. Ma, O.A. MacDougald, F. Macian, G.C. MacIntosh, J.P. MacKeigan, K.F. Macleod, S. Maday, F. Madeo, M. Madesh, T. Madl, J. Madrigal-Matute, A. Maeda, Y. Maejima, M. Magarinos, P. Mahavadi, E. Maiani, K. Maiese, P. Maiti, M.C. Maiuri, B. Majello, M.B. Major, E. Makareeva, F. Malik, K. Mallilankaraman, W. Malorni, A. Maloyan, N. Mammadova, G.C.W. Man, F. Manai, J.D. Mancias, E.-M. Mandelkow, M.A. Mandell, A.A. Manfredi, M.H. Manjili, R. Manjithaya, P. Manque, B.B. Manshian, R. Manzano, C. Manzoni, K. Mao, C. Marchese, S. Marchetti, A.M. Marconi, F. Marcucci, S. Mardente, O.A. Mareninova, M. Margeta, M. Mari, S. Marinelli, O. Marinelli, G. Mariño, S. Mariotto, R.S. Marshall, M.R. Marten, S. Martens, A.P.J. Martin, K.R. Martin, S. Martin, S. Martin, A. Martín-Segura, M.A. Martín-Acebes, I. Martin-Burriel, M. Martin-Rincon, P. Martin-Sanz, J.A. Martina, W. Martinet, A. Martinez, A. Martinez, J. Martinez, M. Martinez Velazquez, N. Martinez-Lopez, M. Martinez-Vicente, D.O. Martins, J.O. Martins, W.K. Martins, T. Martins-Marques, E. Marzetti, S. Masaldan, C. Masclaux-Daubresse, D.G. Mashek, V.

Massa, L. Massieu, G.R. Masson, L. Masuelli, A.I. Masyuk, T. V Masyuk, P. Matarrese, A. Matheu, S. Matoba, S. Matsuzaki, P. Mattar, A. Matte, D. Mattoscio, J.L. Mauriz, M. Mauthe, C. Mauvezin, E. Maverakis, P. Maycotte, J. Mayer, G. Mazzoccoli, C. Mazzoni, J.R. Mazzulli, N. McCarty, C. McDonald, M.R. McGill, S.L. McKenna, B. McLaughlin, F. McLoughlin, M.A. McNiven, T.G. McWilliams, F. Mechta-Grigoriou, T.C. Medeiros, D.L. Medina, L.A. Megeney, K. Megyeri, M. Mehrpour, J.L. Mehta, A.J. Meijer, A.H. Meijer, J. Mejlvang, A. Meléndez, A. Melk, G. Memisoglu, A.F. Mendes, D. Meng, F. Meng, T. Meng, R. Menna-Barreto, M.B. Menon, C. Mercer, A.E. Mercier, J.-L. Mergny, A. Merighi, S.D. Merkley, G. Merla, V. Meske, A.C. Mestre, S.P. Metur, C. Meyer, H. Meyer, W. Mi, J. Mialet-Perez, J. Miao, L. Micale, Y. Miki, E. Milan, M. Milczarek, D.L. Miller, S.I. Miller, S. Miller, S.W. Millward, I. Milosevic, E.A. Minina, H. Mirzaei, H.R. Mirzaei, M. Mirzaei, A. Mishra, N. Mishra, P.K. Mishra, M. Misirkic Marjanovic, R. Misasi, A. Misra, G. Misso, C. Mitchell, G. Mitou, T. Miura, S. Miyamoto, M. Miyazaki, M. Miyazaki, T. Miyazaki, K. Miyazawa, N. Mizushima, T.H. Mogensen, B. Mograbi, R. Mohammadinejad, Y. Mohamud, A. Mohanty, S. Mohapatra, T. Möhlmann, A. Mohmmed, A. Moles, K.H. Moley, M. Molinari, V. Mollace, A.B. Møller, B. Mollereau, F. Mollinedo, C. Montagna, M.J. Monteiro, A. Montella, L.R. Montes, B. Montico, V.K. Mony, G. Monzio Compagnoni, M.N. Moore, M.A. Moosavi, A.L. Mora, M. Mora, D. Morales-Alamo, R. Moratalla, P.I. Moreira, E. Morelli, S. Moreno, D. Moreno-Blas, V. Moresi, B. Morga, A.H. Morgan, F. Morin, H. Morishita, O.L. Moritz, M. Moriyama, Y. Moriyasu, M. Morleo, E. Morselli, J.F. Moruno-Manchon, J. Moscat, S. Mostowy, E. Motori, A.F. Moura, N. Moustaid-Moussa, M. Mrakovcic, G. Muciño-Hernández, A. Mukherjee, S. Mukhopadhyay, J.M. Mulcahy Levy, V. Mulero, S. Muller, C. Münch, A. Munjal, P. Munoz-Canoves, T. Muñoz-Galdeano, C. Münz, T. Murakawa, C. Muratori, B.M. Murphy, J.P. Murphy, A. Murthy, T.T. Myöhänen, I.U. Mysorekar, J. Mytych, S.M. Nabavi, M. Nabissi, P. Nagy, J. Nah, A. Nahimana, I. Nakagawa, K. Nakamura, H. Nakatogawa, S.S. Nandi, M. Nanjundan, M. Nanni, G. Napolitano, R. Nardacci, M. Narita, M. Nassif, I. Nathan, M. Natsumeda, R.J. Naude, C. Naumann, O. Naveiras, F. Navid, S.T. Nawrocki, T.Y. Nazarko, F. Nazio, F. Negoita, T. Neill, A.L. Neisch, L.M. Neri, M.G. Netea, P. Neubert, T.P. Neufeld, D. Neumann, A. Neutzner, P.T. Newton, P.A. Ney, I.P. Nezis, C.C.W. Ng, T.B. Ng, H.T.T. Nguyen, L.T. Nguyen, H.-M. Ni, C. Ní Cheallaigh, Z. Ni, M.C. Nicolao, F. Nicoli, M. Nieto-Diaz, P. Nilsson, S. Ning, R. Niranjan, H. Nishimune, M. Niso-Santano, R.A. Nixon, A. Nobili, C. Nobrega, T. Noda, U. Nogueira-Recalde, T.M. Nolan, I. Nombela, I. Novak, B. Novoa, T. Nozawa, N. Nukina, C. Nussbaum-Krammer, J. Nylandsted, T.R. O'Donovan, S.M. O'Leary, E.J. O'Rourke, M.P. O'Sullivan, T.E. O'Sullivan, S. Oddo, I. Oehme, M. Ogawa, E. Ogier-Denis, M.H. Ogmundsdottir, B. Ogretmen, G.T. Oh, S.-H. Oh, Y.J. Oh, T. Ohama, Y. Ohashi, M. Ohmuraya, V. Oikonomou, R. Ojha, K. Okamoto, H. Okazawa, M. Oku, S. Oliván, J.M.A. Oliveira, M. Ollmann, J.A. Olzmann, S. Omari, M.B. Omary, G. Önal, M. Ondrej, S.-B. Ong, S.-G. Ong, A. Onnis, J.A. Orellana, S. Orellana-Muñoz, M.D.M. Ortega-Villaizan, X.R. Ortiz-Gonzalez, E. Ortona, H.D. Osiewacz, A.-H.K. Osman, R. Osta, M.S. Otegui, K. Otsu, C. Ott, L. Ottobrini, J.J. Ou, T.F. Outeiro, I. Oynebraten, M. Ozturk, G. Pagès, S. Pahari, M. Pajares, U.B. Pajvani, R. Pal, S. Paladino, N. Pallet, M. Palmieri, G. Palmisano, C. Palumbo, F. Pampaloni, L. Pan, Q. Pan, W. Pan, X. Pan, G. Panasyuk, R. Pandey, U.B. Pandey, V. Pandya, F. Paneni, S.Y. Pang, E. Panzarini, D.L. Papademetrio, E. Papaleo, D. Papinski, D. Papp, E.C. Park, H.T. Park, J.-M. Park, J.-I. Park, J.T. Park, J. Park, S.C. Park, S.-Y. Park, A.H. Parola, J.B. Parys, A. Pasquier, B. Pasquier, J.F. Passos,

N. Pastore, H.H. Patel, D. Patschan, S. Pattingre, G. Pedraza-Alva, J. Pedraza-Chaverri, Z. Pedrozo, G. Pei, J. Pei, H. Peled-Zehavi, J.M. Pellegrini, J. Pelletier, M.A. Peñalva, D. Peng, Y. Peng, F. Penna, M. Pennuto, F. Pentimalli, C.M.F. Pereira, G.J.S. Pereira, L.C. Pereira, L. Pereira de Almeida, N.D. Perera, Á. Pérez-Lara, A.B. Perez-Oliva, M.E. Pérez-Pérez, P. Periyasamy, A. Perl, C. Perrotta, I. Perrotta, R.G. Pestell, M. Petersen, I. Petrache, G. Petrovski, T. Pfirrmann, A.S. Pfister, J.A. Philips, H. Pi, A. Picca, A.M. Pickrell, S. Picot, G.M. Pierantoni, M. Pierdominici, P. Pierre, V. Pierrefite-Carle, K. Pierzynowska, F. Pietrocola, M. Pietruczuk, C. Pignata, F.X. Pimentel-Muiños, M. Pinar, R.O. Pinheiro, R. Pinkas-Kramarski, P. Pinton, K. Pircs, S. Piya, P. Pizzo, T.S. Plantinga, H.W. Platta, A. Plaza-Zabala, M. Plomann, E.Y. Plotnikov, H. Plun-Favreau, R. Pluta, R. Pocock, S. Pöggeler, C. Pohl, M. Poirot, A. Poletti, M. Ponpuak, H. Popelka, B. Popova, H. Porta, S. Porte Alcon, E. Portilla-Fernandez, M. Post, M.B. Potts, J. Poulton, T. Powers, V. Prahlad, T.K. Prajsnar, D. Praticò, R. Prencipe, M. Priault, T. Proikas-Cezanne, V.J. Promponas, C.G. Proud, R. Puertollano, L. Puglielli, T. Pulinilkunnil, D. Puri, R. Puri, J. Puyal, X. Qi, Y. Qi, W. Qian, L. Qiang, Y. Qiu, J. Quadrilatero, J. Quarleri, N. Raben, H. Rabinowich, D. Ragona, M.J. Ragusa, N. Rahimi, M. Rahmati, V. Raia, N. Raimundo, N.-S. Rajasekaran, S. Ramachandra Rao, A. Rami, I. Ramírez-Pardo, D.B. Ramsden, F. Randow, P.N. Rangarajan, D. Ranieri, H. Rao, L. Rao, R. Rao, S. Rathore, J.A. Ratnayaka, E.A. Ratovitski, P. Ravanan, G. Ravegnini, S.K. Ray, B. Razani, V. Rebecca, F. Reggiori, A. Régnier-Vigouroux, A.S. Reichert, D. Reigada, J.H. Reiling, T. Rein, S. Reipert, R.S. Rekha, H. Ren, J. Ren, W. Ren, T. Renault, G. Renga, K. Reue, K. Rewitz, B. Ribeiro de Andrade Ramos, S.A. Riazuddin, T.M. Ribeiro-Rodrigues, J.-E. Ricci, R. Ricci, V. Riccio, D.R. Richardson, Y. Rikihisa, M. V Risbud, R.M. Risueño, K. Ritis, S. Rizza, R. Rizzuto, H.C. Roberts, L.D. Roberts, K.J. Robinson, M.C. Roccheri, S. Rocchi, G.G. Rodney, T. Rodrigues, V.R. Rodrigues Silva, A. Rodriguez, R. Rodriguez-Barrueco, N. Rodriguez-Henche, H. Rodriguez-Rocha, J. Roelofs, R.S. Rogers, V. V Rogov, A.I. Rojo, K. Rolka, V. Romanello, L. Romani, A. Romano, P.S. Romano, D. Romeo-Guitart, L.C. Romero, M. Romero, J.C. Roney, C. Rongo, S. Roperto, M.T. Rosenfeldt, P. Rosenstiel, A.G. Rosenwald, K.A. Roth, L. Roth, S. Roth, K.M.A. Rouschop, B.D. Roussel, S. Roux, P. Rovere-Querini, A. Roy, A. Rozieres, D. Ruano, D.C. Rubinsztein, M.P. Rubtsova, K. Ruckdeschel, C. Ruckenstuhl, E. Rudolf, R. Rudolf, A. Ruggieri, A.A. Ruparelia, P. Rusmini, R.R. Russell, G.L. Russo, M. Russo, R. Russo, O.O. Ryabaya, K.M. Ryan, K.-Y. Ryu, M. Sabater-Arcis, U. Sachdev, M. Sacher, C. Sachse, A. Sadhu, J. Sadoshima, N. Safren, P. Saftig, A.P. Sagona, G. Sahay, A. Sahebkar, M. Sahin, O. Sahin, S. Sahni, N. Saito, S. Saito, T. Saito, R. Sakai, Y. Sakai, J.-I. Sakamaki, K. Saksela, G. Salazar, A. Salazar-Degracia, G.H. Salekdeh, A.K. Saluja, B. Sampaio-Marques, M.C. Sanchez, J.A. Sanchez-Alcazar, V. Sanchez-Vera, V. Sancho-Shimizu, J.T. Sanderson, M. Sandri, S. Santaguida, L. Santambrogio, M.M. Santana, G. Santoni, A. Sanz, P. Sanz, S. Saran, M. Sardiello, T.J. Sargeant, A. Sarin, C. Sarkar, S. Sarkar, M.-R. Sarrias, S. Sarkar, D.T. Sarmah, J. Sarparanta, A. Sathyanarayan, R. Sathyanarayanan, K.M. Scaglione, F. Scatozza, L. Schaefer, Z.T. Schafer, U.E. Schaible, A.H. V Schapira, M. Scharl, H.M. Schatzl, C.H. Schein, W. Scheper, D. Scheuring, M.V. Schiaffino, M. Schiappacassi, R. Schindl, U. Schlattner, O. Schmidt, R. Schmitt, S.D. Schmidt, I. Schmitz, E. Schmukler, A. Schneider, B.E. Schneider, R. Schober, A.C. Schoijet, M.B. Schott, M. Schramm, B. Schröder, K. Schuh, C. Schüller, R.J. Schulze, L. Schürmanns, J.C. Schwamborn, M. Schwarten, F. Scialo, S. Sciarretta, M.J. Scott, K.W. Scotto, A.I. Scovassi, A. Scrima, A. Scrivo, D. Sebastian, S. Sebti, S. Sedej, L. Segatori, N. Segev, P.O. Seglen, I. Seiliez, E.

Seki, S.B. Selleck, F.W. Sellke, J.T. Selsby, M. Sendtner, S. Senturk, E. Seranova, C. Sergi, R. Serra-Moreno, H. Sesaki, C. Settembre, S.R.G. Setty, G. Sgarbi, O. Sha, J.J. Shacka, J.A. Shah, D. Shang, C. Shao, F. Shao, S. Sharbati, L.M. Sharkey, D. Sharma, G. Sharma, K. Sharma, P. Sharma, S. Sharma, H.-M. Shen, H. Shen, J. Shen, M. Shen, W. Shen, Z. Shen, R. Sheng, Z. Sheng, Z.-H. Sheng, J. Shi, X. Shi, Y.-H. Shi, K. Shiba-Fukushima, J.-J. Shieh, Y. Shimada, S. Shimizu, M. Shimozawa, T. Shintani, C.J. Shoemaker, S. Shojaei, I. Shoji, B. V Shravage, V. Shridhar, C.-W. Shu, H.-B. Shu, K. Shui, A.K. Shukla, T.E. Shutt, V. Sica, A. Siddiqui, A. Sierra, V. Sierra-Torre, S. Signorelli, P. Sil, B.J. de A. Silva, J.D. Silva, E. Silva-Pavez, S. Silvente-Poirot, R.E. Simmonds, A.K. Simon, H.-U. Simon, M. Simons, A. Singh, L.P. Singh, R. Singh, S. V Singh, S.K. Singh, S.B. Singh, S. Singh, S.P. Singh, D. Sinha, R.A. Sinha, S. Sinha, A. Sirko, K. Sirohi, E.L. Sivridis, P. Skendros, A. Skirycz, I. Slaninová, S.S. Smaili, A. Smertenko, M.D. Smith, S.J. Soenen, E.J. Sohn, S.P.M. Sok, G. Solaini, T. Soldati, S.A. Soleimanpour, R.M. Soler, A. Solovchenko, J.A. Somarelli, A. Sonawane, F. Song, H.K. Song, J.-X. Song, K. Song, Z. Song, L.R. Soria, M. Sorice, A.A. Soukas, S.-F. Soukup, D. Sousa, N. Sousa, P.A. Spagnuolo, S.A. Spector, M.M. Srinivas Bharath, D. St. Clair, V. Stagni, L. Staiano, C.A. Stalnecker, M. V Stankov, P.B. Stathopulos, K. Stefan, S.M. Stefan, L. Stefanis, J.S. Steffan, A. Steinkasserer, H. Stenmark, J. Sterneckert, C. Stevens, V. Stoka, S. Storch, B. Stork, F. Strappazzon, A.M. Strohecker, D.G. Stupack, H. Su, L.-Y. Su, L. Su, A.M. Suarez-Fontes, C.S. Subauste, S. Subbian, P. V Subirada, G. Sudhandiran, C.M. Sue, X. Sui, C. Summers, G. Sun, J. Sun, K. Sun, M. Sun, Q. Sun, Y. Sun, Z. Sun, K.K.S. Sunahara, E. Sundberg, K. Susztak, P. Sutovsky, H. Suzuki, G. Sweeney, J.D. Symons, S.C.W. Sze, N.J. Szewczyk, A. Tabęcka-Łonczynska, C. Tabolacci, F. Tacke, H. Taegtmeyer, M. Tafani, M. Tagaya, H. Tai, S.W.G. Tait, Y. Takahashi, S. Takats, P. Talwar, C. Tam, S.Y. Tam, D. Tampellini, A. Tamura, C.T. Tan, E.-K. Tan, Y.-Q. Tan, M. Tanaka, M. Tanaka, D. Tang, J. Tang, T.-S. Tang, I. Tanida, Z. Tao, M. Taouis, L. Tatenhorst, N. Tavernarakis, A. Taylor, G.A. Taylor, J.M. Taylor, E. Tchetina, A.R. Tee, I. Tegeder, D. Teis, N. Teixeira, F. Teixeira-Clerc, K.A. Tekirdag, T. Tencomnao, S. Tenreiro, A. V Tepikin, P.S. Testillano, G. Tettamanti, P.-L. Tharaux, K. Thedieck, A.A. Thekkinghat, S. Thellung, J.W. Thinwa, V.P. Thirumalaikumar, S.M. Thomas, P.G. Thomes, A. Thorburn, L. Thukral, T. Thum, M. Thumm, L. Tian, A. Tichy, A. Till, V. Timmerman, V.I. Titorenko, S. V Todi, K. Todorova, J.M. Toivonen, L. Tomaipitinca, D. Tomar, C. Tomas-Zapico, S. Tomić, B.C.-K. Tong, C. Tong, X. Tong, S.A. Tooze, M.L. Torgersen, S. Torii, L. Torres-López, A. Torriglia, C.G. Towers, R. Towns, S. Toyokuni, V. Trajkovic, D. Tramontano, Q.-G. Tran, L.H. Travassos, C.B. Trelford, S. Tremel, I.P. Trougakos, B.P. Tsao, M.P. Tschan, H.-F. Tse, T.F. Tse, H. Tsugawa, A.S. Tsvetkov, D.A. Tumbarello, Y. Tumtas, M.J. Tuñón, S. Turcotte, B. Turk, V. Turk, B.J. Turner, R.I. Tuxworth, J.K. Tyler, E. V Tyutereva, Y. Uchiyama, A. Ugun-Klusek, H.H. Uhlig, M. Ułamek-Kozioł, I. V Ulasov, M. Umekawa, C. Ungermann, R. Unno, S. Urbe, E. Uribe-Carretero, S. Üstün, V.N. Uversky, T. Vaccari, M.I. Vaccaro, B.F. Vahsen, H. Vakifahmetoglu-Norberg, R. Valdor, M.J. Valente, A. Valko, R.B. Vallee, A.M. Valverde, G. Van den Berghe, S. van der Veen, L. Van Kaer, J. van Loosdregt, S.J.L. van Wijk, W. Vandenberghe, I. Vanhorebeek, M.A. Vannier-Santos, N. Vannini, M.C. Vanrell, C. Vantaggiato, G. Varano, I. Varela-Nieto, M. Varga, M.H. Vasconcelos, S. Vats, D.G. Vavvas, I. Vega-Naredo, S. Vega-Rubin-de-Celis, G. Velasco, A.P. Velázquez, T. Vellai, E. Vellenga, F. Velotti, M. Verdier, P. Verginis, I. Vergne, P. Verkade, M. Verma, P. Verstreken, T. Vervliet, J. Vervoorts, A.T. Vessoni, V.M. Victor, M. Vidal, C. Vidoni, O. V Vieira, R.D. Vierstra, S. Viganó, H. Vihinen, V.

Vijayan, M. Vila, M. Vilar, J.M. Villalba, A. Villalobo, B. Villarejo-Zori, F. Villarroya, J. Villarroya, O. Vincent, C. Vindis, C. Viret, M.T. Viscomi, D. Visnjic, I. Vitale, D.J. Vocadlo, O. V Voitsekhovskaja, C. Volonté, M. Volta, M. Vomero, C. Von Haefen, M.A. Vooijs, W. Voos, L. Vucicevic, R. Wade-Martins, S. Waguri, K.A. Waite, S. Wakatsuki, D.W. Walker, M.J. Walker, S.A. Walker, J. Walter, F.G. Wandosell, B. Wang, C.-Y. Wang, C. Wang, C. Wang, C. Wang, C.-Y. Wang, D. Wang, F. Wang, F. Wang, F. Wang, G. Wang, H. Wang, H. Wang, H. Wang, H.-G. Wang, J. Wang, J. Wang, J. Wang, J. Wang, K. Wang, L. Wang, L. Wang, M.H. Wang, M. Wang, N. Wang, P. Wang, P. Wang, P. Wang, P. Wang, Q.J. Wang, Q. Wang, Q.K. Wang, Q.A. Wang, W.-T. Wang, W. Wang, X. Wang, X. Wang, Y. Wang, Y. Wang, Y. Wang, Y.-Y. Wang, Y. Wang, Y. Wang, Y. Wang, Y. Wang, Z. Wang, Z. Wang, Z. Wang, G. Warnes, V. Warnsmann, H. Watada, E. Watanabe, M. Watchon, A. Wawrzyńska, T.E. Weaver, G. Wegrzyn, A.M. Wehman, H. Wei, L. Wei, T. Wei, Y. Wei, O.H. Weiergräber, C.C. Weihl, G. Weindl, R. Weiskirchen, A. Wells, R.H. Wen, X. Wen, A. Werner, B. Weykopf, S.P. Wheatley, J.L. Whitton, A.J. Whitworth, K. Wiktorska, M.E. Wildenberg, T. Wileman, S. Wilkinson, D. Willbold, B. Williams, R.S.B. Williams, R.L. Williams, P.R. Williamson, R.A. Wilson, B. Winner, N.J. Winsor, S.S. Witkin, H. Wodrich, U. Woehlbier, T. Wollert, E. Wong, J.H. Wong, R.W. Wong, V.K.W. Wong, W.W.-L. Wong, A.-G. Wu, C. Wu, J. Wu, J. Wu, K.K. Wu, M. Wu, S.-Y. Wu, S. Wu, S.-Y. Wu, S. Wu, W.K.K. Wu, X. Wu, X. Wu, Y.-W. Wu, Y. Wu, R.J. Xavier, H. Xia, L. Xia, Z. Xia, G. Xiang, J. Xiang, M. Xiang, W. Xiang, B. Xiao, G. Xiao, H. Xiao, H. Xiao, J. Xiao, L. Xiao, S. Xiao, Y. Xiao, B. Xie, C.-M. Xie, M. Xie, Y. Xie, Z. Xie, Z. Xie, M. Xilouri, C. Xu, E. Xu, H. Xu, J. Xu, J. Xu, L. Xu, W.W. Xu, X. Xu, Y. Xue, S.M.S. Yakhine-Diop, M. Yamaguchi, O. Yamaguchi, A. Yamamoto, S. Yamashina, S. Yan, S.-J. Yan, Z. Yan, Y. Yanagi, C. Yang, D.-S. Yang, H. Yang, H.-T. Yang, H. Yang, J.-M. Yang, J. Yang, J. Yang, L. Yang, L. Yang, M. Yang, P.-M. Yang, Q. Yang, S. Yang, S. Yang, S.-F. Yang, W. Yang, W.Y. Yang, X. Yang, X. Yang, Y. Yang, Y. Yang, H. Yao, S. Yao, X. Yao, Y.-G. Yao, Y.-M. Yao, T. Yasui, M. Yazdankhah, P.M. Yen, C. Yi, X.-M. Yin, Y. Yin, Z. Yin, Z. Yin, M. Ying, Z. Ying, C.K. Yip, S.P.T. Yiu, Y.H. Yoo, K. Yoshida, S.R. Yoshii, T. Yoshimori, B. Yousefi, B. Yu, H. Yu, J. Yu, J. Yu, L. Yu, M.-L. Yu, S.-W. Yu, V.C. Yu, W.H. Yu, Z. Yu, Z. Yu, J. Yuan, L.-Q. Yuan, S. Yuan, S.-S.F. Yuan, Y. Yuan, Z. Yuan, J. Yue, Z. Yue, J. Yun, R.L. Yung, D.N. Zacks, G. Zaffagnini, V.O. Zambelli, I. Zanella, Q.S. Zang, S. Zanivan, S. Zappavigna, P. Zaragoza, K.S. Zarbalis, A. Zarebkohan, A. Zarrouk, S.O. Zeitlin, J. Zeng, J. Zeng, E. Žerovnik, L. Zhan, B. Zhang, D.D. Zhang, H. Zhang, H. Zhang, H. Zhang, H. Zhang, H. Zhang, H. Zhang, H. Zhang, H.-L. Zhang, J. Zhang, J. Zhang, J.-P. Zhang, K.Y.B. Zhang, L.W. Zhang, L. Zhang, L. Zhang, L. Zhang, L. Zhang, M. Zhang, P. Zhang, S. Zhang, W. Zhang, X. Zhang, X.-W. Zhang, X. Zhang, X. Zhang, X. Zhang, X. Zhang, X.D. Zhang, Y. Zhang, Y. Zhang, Y. Zhang, Y.-D. Zhang, Y. Zhang, Y.-Y. Zhang, Y. Zhang, Z. Zhang, Z. Zhang, Z. Zhang, Z. Zhang, Z. Zhang, Z. Zhang, H. Zhao, L. Zhao, S. Zhao, T. Zhao, X.-F. Zhao, Y. Zhao, Y. Zhao, Y. Zhao, Y. Zhao, G. Zheng, K. Zheng, L. Zheng, S. Zheng, X.-L. Zheng, Y. Zheng, Z.-G. Zheng, B. Zhivotovsky, Q. Zhong, A. Zhou, B. Zhou, C. Zhou, G. Zhou, H. Zhou, H. Zhou, H. Zhou, J. Zhou, J. Zhou, J. Zhou, J. Zhou, K. Zhou, R. Zhou, X.-J. Zhou, Y. Zhou, Y. Zhou, Y. Zhou, Z.-Y. Zhou, Z. Zhou, B. Zhu, C. Zhu, G.-Q. Zhu, H. Zhu, H. Zhu, H. Zhu, W.-G. Zhu, Y. Zhu, Y. Zhu, H. Zhuang, X. Zhuang, K. Zientara-Rytter, C.M. Zimmermann, E. Ziviani, T. Zoladek, W.-X. Zong, D.B. Zorov, A. Zorzano, W. Zou, Z. Zou, Z. Zou, S. Zuryn, W. Zwerschke, B. Brand-Saberi, X.C. Dong, C.S. Kenchappa, Z. Li, Y. Lin, S. Oshima, Y. Rong, J.C. Sluimer, C.L. Stallings, C.-K. Tong, Guidelines for the use and interpretation of assays for monitoring autophagy,

Autophagy. (2021) 1–382. https://doi.org/10.1080/15548627.2020.1797280.

[244] D.J. Klionsky, Z. Elazar, P.O. Seglen, D.C. Rubinsztein, Does bafilomycin A1 block the fusion of autophagosomes with lysosomes?, Autophagy. 4 (2008) 849–850. https://doi.org/10.4161/auto.6845.

[245] A. Yamamoto, Y. Tagawa, T. Yoshimori, Y. Moriyama, R. Masaki, Y. Tashiro, Bafilomycin A1 prevents maturation of autophagic vacuoles by inhibiting fusion between autophagosomes and lysosomes in rat hepatoma cell line, H-4-II-E cells, Cell Struct. Funct. 23 (1998) 33–42. https://doi.org/10.1247/csf.23.33.

[246] M. Mauthe, I. Orhon, C. Rocchi, X. Zhou, M. Luhr, K.J. Hijlkema, R.P. Coppes, N. Engedal, M. Mari, F. Reggiori, Chloroquine inhibits autophagic flux by decreasing autophagosome-lysosome fusion, Autophagy. 14 (2018) 1435–1455. https://doi.org/10.1080/15548627.2018.1474314.

[247] E.F.C. Blommaart, U. Krause, J.P.M. Schellens, H. Vreeling-Sindelárová, A.J. Meijer, The phosphatidylinositol 3-kinase inhibitors wortmannin and LY294002 inhibit in isolated rat hepatocytes, Eur. J. Biochem. 243 (1997) 240–246. https://doi.org/10.1111/j.1432-1033.1997.0240a.x.

[248] P.O. Seglen, P.B. Gordon, 3-Methyladenine: Specific inhibitor of autophagic/lysosomal protein degradation in isolated rat hepatocytes, Proc. Natl. Acad. Sci. U. S. A. 79 (1982) 1889–1892. https://doi.org/10.1073/pnas.79.6.1889.

[249] Y.T. Wu, H.L. Tan, G. Shui, C. Bauvy, Q. Huang, M.R. Wenk, C.N. Ong, P. Codogno, H.M. Shen, Dual role of 3-methyladenine in modulation of autophagy via different temporal patterns of inhibition on class I and III phosphoinositide 3-kinase, J. Biol. Chem. 285 (2010) 10850–10861. https://doi.org/10.1074/jbc.M109.080796.

[250] M. Ihara, K. Shichijo, S. Takeshita, T. Kudo, Wortmannin, a specific inhibitor of phosphatidylinositol-3-kinase, induces accumulation of DNA double-strand breaks, J. Radiat. Res. 61 (2020) 171–176. https://doi.org/10.1093/jrr/rrz102.

[251] J.N. Sarkaria, R.S. Tibbetts, E.C. Busby, A.P. Kennedy, D.E. Hill, R.T. Abraham, Inhibition of phosphoinositide 3-kinase related kinases by the radiosensitizing agent wortmannin, Cancer Res. 58 (1998) 4375–4382.

[252] W.H. Baricos, S.E. O'Connor, S.L. Cortez, L.T. Wu, S. V. Shah, The cysteine proteinase inhibitor, E-64, reduces proteinuria in an experimental model of glomerulonephritis, Biochem. Biophys. Res. Commun. 155 (1988) 1318–1323. https://doi.org/10.1016/S0006-291X(88)81285-3.

[253] D.H. Rich, P.G. Schmidt, M.S. Bernatowicz, N.S. Agarwal, M. Kawai, F.G. Salituro, Inhibition of Aspartic Proteases by Pepstatin and 3-Methylstatine Perivatives of Pepstatin. Evidence for Collected-Substrate Enzyme Inhibition, Biochemistry. 24 (1985) 3165–3173. https://doi.org/10.1021/bi00334a014.

[254] N. Hosokawa, Y. Hara, N. Mizushima, Generation of cell lines with tetracycline-regulated autophagy and a role for autophagy in controlling cell size, FEBS Lett. 580 (2006) 2623–2629. https://doi.org/10.1016/j.febslet.2006.04.008.

[255] G. Bjørkøy, T. Lamark, S. Pankiv, A. Øvervatn, A. Brech, T. Johansen, Chapter 12 Monitoring Autophagic Degradation of p62/SQSTM1, Methods Enzymol. 451 (2009) 181–197. https://doi.org/10.1016/S0076-6879(08)03612-4.

[256] G. Bjørkøy, T. Lamark, A. Brech, H. Outzen, M. Perander, A. Øvervatn, H. Stenmark, T. Johansen, p62/SQSTM1 forms protein aggregates degraded by autophagy and has a protective effect on huntingtin-induced cell death, J. Cell Biol. 171 (2005) 603–614. https://doi.org/10.1083/jcb.200507002.

[257] A.S. Tsvetkov, J. Miller, M. Arrasate, J.S. Wong, M.A. Pleiss, S. Finkbeiner, A small-molecule scaffold induces autophagy in primary neurons and protects against toxicity in a Huntington disease model, Proc. Natl. Acad. Sci. U. S. A. 107 (2010) 16982–16987. https://doi.org/10.1073/pnas.1004498107.

[258] E.L. Eskelinen, Maturation of autophagic vacuoles in Mammalian cells., Autophagy. 1 (2005) 1–10. https://doi.org/10.4161/auto.1.1.1270.

[259] T.M. Mayhew, Quantitative Immunoelectron Microscopy, in: Methods Mol. Biol., Methods Mol Biol, 2007: pp. 309–329. https://doi.org/10.1007/978-1-59745-294-6_15.

[260] T.M. Mayhew, J.M. Lucocq, G. Griffiths, Relative labelling index: a novel stereological approach to test for non-random immunogold labelling of organelles and membranes on transmission electron microscopy thin sections, J. Microsc. 205 (2002) 153–164. https://doi.org/10.1046/j.0022-2720.2001.00977.x.

[261] C. Behrends, M.E. Sowa, S.P. Gygi, J.W. Harper, Network organization of the human autophagy system, Nature. 466 (2010) 68–76. https://doi.org/10.1038/nature09204.

[262] J. Dengjel, M. Høyer-Hansen, M.O. Nielsen, T. Eisenberg, L.M. Harder, S. Schandorff, T. Farkas, T. Kirkegaard, A.C. Becker, S. Schroeder, K. Vanselow, E. Lundberg, M.M. Nielsen, A.R. Kristensen, V. Akimov, J. Bunkenborg, F. Madeo, M. Jäättelä, J.S. Andersen, Identification of autophagosome-associated proteins and regulators by quantitative proteomic analysis and genetic screens., Mol. Cell. Proteomics. 11 (2012) M111.014035. https://doi.org/10.1074/mcp.M111.014035.

[263] J.D. Mancias, X. Wang, S.P. Gygi, J.W. Harper, A.C. Kimmelman, Quantitative proteomics identifies NCOA4 as the cargo receptor mediating ferritinophagy, Nature. 509 (2014) 105–109. https://doi.org/10.1038/nature13148.

[264] S. Zellner, M. Schifferer, C. Behrends, Systematically defining selective autophagy receptor-specific cargo using autophagosome content profiling, Mol. Cell. (2021). https://doi.org/10.1016/j.molcel.2021.01.009.

[265] R. Aebersold, M. Mann, Mass spectrometry-based proteomics., Nature. 422 (2003) 198–207. https://doi.org/10.1038/nature01511.

[266] J.W. Gouw, J. Krijgsveld, A.J.R. Heck, Quantitative proteomics by metabolic labeling of model organisms, Mol. Cell. Proteomics. 9 (2010) 11–24. https://doi.org/10.1074/mcp.R900001-MCP200.

[267] J. Cox, M. Mann, Quantitative, High-Resolution Proteomics for Data-Driven Systems Biology, Annu. Rev. Biochem. 80 (2011) 273–299. https://doi.org/10.1146/annurev-biochem-061308-093216.

[268] J.B. Fenn, M. Mann, C.K. Meng, S.F. Wong, C.M. Whitehouse, Electrospray ionization for mass spectrometry of large biomolecules, Science (80-.). 246 (1989) 64–71. https://doi.org/10.1126/science.2675315.

[269] M. Karas, F. Hillenkamp, Laser Desorption Ionization of Proteins with Molecular Masses Exceeding 10 000 Daltons, Anal. Chem. 60 (1988) 2299–2301. https://doi.org/10.1021/ac00171a028.

[270] Y. Ishihama, J. Rappsilber, J.S. Andersen, M. Mann, Microcolumns with self-assembled particle frits for proteomics, J. Chromatogr. A. 979 (2002) 233–239. https://doi.org/10.1016/S0021-9673(02)01402-4.

[271] H. Steen, M. Mann, The abc's (and xyz's) of peptide sequencing, Nat. Rev. Mol. Cell Biol. 5 (2004) 699–711. https://doi.org/10.1038/nrm1468.

[272] J. V Olsen, L.M.F. de Godoy, G. Li, B. Macek, P. Mortensen, R. Pesch, A. Makarov, O. Lange, S. Horning, M. Mann, Parts per million mass accuracy on an Orbitrap mass spectrometer via lock mass injection into a C-trap., Mol. Cell. Proteomics. 4 (2005) 2010–21. https://doi.org/10.1074/mcp.T500030-MCP200.

[273] M.J. Wither, K.C. Hansen, J.A. Reisz, Mass Spectrometry-Based Bottom-Up Proteomics: Sample Preparation, LC-MS/MS Analysis, and Database Query Strategies, Curr. Protoc. Protein Sci. 86 (2016) 16.4.1-16.4.20. https://doi.org/10.1002/cpps.18.

[274] J. Cox, M. Mann, MaxQuant enables high peptide identification rates, individualized p.p.b.-range mass accuracies and proteome-wide protein quantification, Nat. Biotechnol. 26 (2008) 1367–1372. https://doi.org/10.1038/nbt.1511.

[275] J. Cox, N. Neuhauser, A. Michalski, R.A. Scheltema, J. V. Olsen, M. Mann, Andromeda: A Peptide Search Engine Integrated into the MaxQuant Environment, J. Proteome Res. 10 (2011) 1794–1805. https://doi.org/10.1021/pr101065j.

[276] M. Bantscheff, M. Schirle, G. Sweetman, J. Rick, B. Kuster, Quantitative mass spectrometry in proteomics: A critical review, Anal. Bioanal. Chem. 389 (2007) 1017–1031. https://doi.org/10.1007/s00216-007-1486-6.

[277] J. Cox, M.Y. Hein, C.A. Luber, I. Paron, N. Nagaraj, M. Mann, Accurate proteome-wide label-free quantification by delayed normalization and maximal peptide ratio extraction, termed MaxLFQ, Mol. Cell. Proteomics. 13 (2014) 2513–2526. https://doi.org/10.1074/mcp.M113.031591.

[278] A. Thompson, J. Schäfer, K. Kuhn, S. Kienle, J. Schwarz, G. Schmidt, T. Neumann, R. Johnstone, a K. a Mohammed, C. Hamon, Tandem mass tags: a novel quantification strategy for comparative analysis of complex protein mixtures by MS/MS., Anal. Chem. 75 (2003) 1895–904. https://doi.org/10.1021/ac0262560.

[279] J. Li, J.G. Van Vranken, L. Pontano Vaites, D.K. Schweppe, E.L. Huttlin, C. Etienne, P.

Nandhikonda, R. Viner, A.M. Robitaille, A.H. Thompson, K. Kuhn, I. Pike, R.D. Bomgarden, J.C. Rogers, S.P. Gygi, J.A. Paulo, TMTpro reagents: a set of isobaric labeling mass tags enables simultaneous proteome-wide measurements across 16 samples, Nat. Methods. 17 (2020) 399–404. https://doi.org/10.1038/s41592-020-0781-4.

[280] J. Zecha, S. Satpathy, T. Kanashova, S.C. Avanessian, M.H. Kane, K.R. Clauser, P. Mertins, S.A. Carr, B. Kuster, TMT labeling for the masses: A robust and cost-efficient, in-solution labeling approach, Mol. Cell. Proteomics. 18 (2019) 1468–1478. https://doi.org/10.1074/mcp.TIR119.001385.

[281] L. Ting, R. Rad, S.P. Gygi, W. Haas, MS3 eliminates ratio distortion in isobaric multiplexed quantitative proteomics, Nat. Methods. 8 (2011) 937–940. https://doi.org/10.1038/nmeth.1714.

[282] S.-E. Ong, B. Blagoev, I. Kratchmarova, D.B. Kristensen, H. Steen, A. Pandey, M. Mann, Stable isotope labeling by amino acids in cell culture, SILAC, as a simple and accurate approach to expression proteomics., Mol. Cell. Proteomics. 1 (2002) 376–86. https://doi.org/10.1074/MCP.M200025-MCP200.

[283] S.-E. Ong, M. Mann, A practical recipe for stable isotope labeling by amino acids in cell culture (SILAC), Nat. Protoc. 1 (2007) 2650–2660. https://doi.org/10.1038/nprot.2006.427.

[284] P. Jiang, N. Mizushima, LC3- and p62-based biochemical methods for the analysis of autophagy progression in mammalian cells, Methods. 75 (2015) 13–18. https://doi.org/10.1016/J.YMETH.2014.11.021.

[285] D. Fracchiolla, S. Martens, Sorting out “non-canonical” autophagy., EMBO J. 37 (2018) e98895. https://doi.org/10.15252/embj.201798895.

[286] M.B.E. Schaaf, T.G. Keulers, M.A. Vooijs, K.M.A. Rouschop, LC3/GABARAP family proteins: autophagy-(un)related functions., FASEB J. 30 (2016) 3961–3978. https://doi.org/10.1096/fj.201600698R.

[287] L. Galluzzi, D.R. Green, Autophagy-Independent Functions of the Autophagy Machinery, Cell. 177 (2019) 1682–1699. https://doi.org/10.1016/j.cell.2019.05.026.

[288] K.J. Simpson-Lavy, A. Bronstein, M. Kupiec, M. Johnston, Cross-Talk between Carbon Metabolism and the DNA Damage Response in S. cerevisiae, Cell Rep. 12 (2015) 1865–1875. https://doi.org/10.1016/J.CELREP.2015.08.025.

[289] D.N. Tripathi, R. Chowdhury, L.J. Trudel, A.R. Tee, R.S. Slack, C.L. Walker, G.N. Wogan, Reactive nitrogen species regulate autophagy through ATM-AMPK-TSC2-mediated suppression of mTORC1., Proc. Natl. Acad. Sci. U. S. A. 110 (2013) E2950-7. https://doi.org/10.1073/pnas.1307736110.

[290] C. Yi, J. Tong, P. Lu, Y. Wang, J. Zhang, C. Sun, K. Yuan, R. Xue, B. Zou, N. Li, S. Xiao, C. Dai, Y. Huang, L. Xu, L. Li, S. Chen, D. Miao, H. Deng, H. Li, L. Yu, Formation of a Snf1-Mec1-Atg1 Module on Mitochondria Governs Energy Deprivation-Induced Autophagy by Regulating Mitochondrial Respiration, Dev. Cell. 41 (2017) 59–71.e4.

https://doi.org/10.1016/J.DEVCEL.2017.03.007.

[291] M.E. Borisova, A. Voigt, M.A.X. Tollenaere, S.K. Sahu, T. Juretschke, N. Kreim, N. Mailand, C. Choudhary, S. Bekker-Jensen, M. Akutsu, S.A. Wagner, P. Beli, p38-MK2 signaling axis regulates RNA metabolism after UV-light-induced DNA damage, Nat. Commun. 9 (2018) 1017. https://doi.org/10.1038/s41467-018-03417-3.

[292] E. Keil, R. Höcker, M. Schuster, F. Essmann, N. Ueffing, B. Hoffman, D.A. Liebermann, K. Pfeffer, K. Schulze-Osthoff, I. Schmitz, Phosphorylation of Atg5 by the Gadd45β-MEKK4-p38 pathway inhibits autophagy, Cell Death Differ. 20 (2013) 321–332. https://doi.org/10.1038/cdd.2012.129.

[293] B. Dérijard, M. Hibi, I.H. Wu, T. Barrett, B. Su, T. Deng, M. Karin, R.J. Davis, JNK1: A protein kinase stimulated by UV light and Ha-Ras that binds and phosphorylates the c-Jun activation domain, Cell. 76 (1994) 1025–1037. https://doi.org/10.1016/0092-8674(94)90380-8.

[294] Y. Wei, S. Pattingre, S. Sinha, M. Bassik, B. Levine, JNK1-mediated phosphorylation of Bcl-2 regulates starvation-induced autophagy, Mol. Cell. 30 (2008) 678–688. https://doi.org/10.1016/j.molcel.2008.06.001.

[295] T. Kaizuka, H. Morishita, Y. Hama, S. Tsukamoto, T. Matsui, Y. Toyota, A. Kodama, T. Ishihara, T. Mizushima, N. Mizushima, An Autophagic Flux Probe that Releases an Internal Control, Mol. Cell. 64 (2016) 835–849. https://doi.org/10.1016/j.molcel.2016.09.037.

[296] Y. Peng, R.G. Woods, H. Beamish, R. Ye, S.P. Lees-Miller, M.F. Lavin, J.S. Bedford, Deficiency in the catalytic subunit of DNA-dependent protein kinase causes down-regulation of ATM, Cancer Res. 65 (2005) 1670–1677. https://doi.org/10.1158/0008-5472.CAN-04-3451.

[297] E.Y. Chen, C.M. Tan, Y. Kou, Q. Duan, Z. Wang, G. V. Meirelles, N.R. Clark, A. Ma'ayan, Enrichr: Interactive and collaborative HTML5 gene list enrichment analysis tool, BMC Bioinformatics. 14 (2013) 128. https://doi.org/10.1186/1471-2105-14-128.

[298] D.C. Rubinsztein, A.M. Cuervo, B. Ravikumar, S. Sarkar, V. Korolchuk, S. Kaushik, D.J. Klionsky, In search of an "autophagomometer," Autophagy. 5 (2009) 585–589. https://doi.org/10.4161/auto.5.5.8823.

[299] E.I. Azzam, J.P. Jay-Gerin, D. Pain, Ionizing radiation-induced metabolic oxidative stress and prolonged cell injury, Cancer Lett. 327 (2012) 48–60. https://doi.org/10.1016/j.canlet.2011.12.012.

[300] J. Kim, M. Kundu, B. Viollet, K.L. Guan, AMPK and mTOR regulate autophagy through direct phosphorylation of Ulk1, Nat. Cell Biol. 13 (2011) 132–141. https://doi.org/10.1038/ncb2152.

[301] A.K. Ajay, A.S. Meena, M.K. Bhat, Human papillomavirus 18 E6 inhibits phosphorylation of p53 expressed in HeLa cells, Cell Biosci. 2 (2012) 2. https://doi.org/10.1186/2045-3701-2-2.

[302] J.W. Yi, M. Jang, S.J. Kim, S.S. Kim, J.E. Rhee, Degradation of p53 by natural variants of the E6 protein of human papillomavirus type 16, Oncol. Rep. 29 (2013) 1617–1622. https://doi.org/10.3892/or.2013.2281.

[303] T. Farkas, M. Daugaard, M. Jäättelä, Identification of small molecule inhibitors of phosphatidylinositol 3-kinase and autophagy, J. Biol. Chem. 286 (2011) 38904–38912. https://doi.org/10.1074/jbc.M111.269134.

[304] J. Shortt, B.P. Martin, A. Newbold, K.M. Hannan, J.R. Devlin, A.J. Baker, R. Ralli, C. Cullinane, C.A. Schmitt, M. Reimann, M.N. Hall, M. Wall, R.D. Hannan, R.B. Pearson, G.A. McArthur, R.W. Johnstone, Combined inhibition of PI3K-related DNA damage response kinases and mTORC1 induces apoptosis in MYC-driven B-cell lymphomas, Blood. 121 (2013) 2964–2974. https://doi.org/10.1182/blood-2012-08-446096.

[305] T. Zhang, S. Shen, J. Qu, S. Ghaemmaghami, Global Analysis of Cellular Protein Flux Quantifies the Selectivity of Basal Autophagy, Cell Rep. 14 (2016) 2426–2439. https://doi.org/10.1016/j.celrep.2016.02.040.

[306] J.T. Parsons, A.R. Horwitz, M.A. Schwartz, Cell adhesion: Integrating cytoskeletal dynamics and cellular tension, Nat. Rev. Mol. Cell Biol. 11 (2010) 633–643. https://doi.org/10.1038/nrm2957.

[307] C.M. Kenific, T. Wittmann, J. Debnath, Autophagy in adhesion and migration, J. Cell Sci. 129 (2016) 3685–3693. https://doi.org/10.1242/jcs.188490.

[308] C.M. Kenific, S.J. Stehbens, J. Goldsmith, A.M. Leidal, N. Faure, J. Ye, T. Wittmann, J. Debnath, NBR 1 enables autophagy-dependent focal adhesion turnover, J. Cell Biol. 212 (2016) 577–590. https://doi.org/10.1083/jcb.201503075.

[309] M.N. Sharifi, E.E. Mowers, L.E. Drake, C. Collier, H. Chen, M. Zamora, S. Mui, K.F. Macleod, Autophagy Promotes Focal Adhesion Disassembly and Cell Motility of Metastatic Tumor Cells through the Direct Interaction of Paxillin with LC3, Cell Rep. 15 (2016) 1660–1672. https://doi.org/10.1016/J.CELREP.2016.04.065.

[310] H. An, J.W. Harper, Systematic analysis of ribophagy in human cells reveals bystander flux during selective autophagy, Nat. Cell Biol. 20 (2017) 135. https://doi.org/10.1038/s41556-017-0007-x.

[311] H. An, A. Ordureau, M. Körner, J.A. Paulo, J.W. Harper, Systematic quantitative analysis of ribosome inventory during nutrient stress, Nature. 583 (2020) 303–309. https://doi.org/10.1038/s41586-020-2446-y.

[312] G.A. Wyant, M. Abu-Remaileh, E.M. Frenkel, N.N. Laqtom, V. Dharamdasani, C.A. Lewis, S.H. Chan, I. Heinze, A. Ori, D.M. Sabatini, NUFIP1 is a ribosome receptor for starvation-induced ribophagy., Science. (2018) eaar2663. https://doi.org/10.1126/science.aar2663.

[313] L. Jiao, H.L. Zhang, D.D. Li, K.L. Yang, J. Tang, X. Li, J. Ji, Y. Yu, R.Y. Wu, S. Ravichandran, J.J. Liu, G.K. Feng, M.S. Chen, Y.X. Zeng, R. Deng, X.F. Zhu, Regulation of glycolytic metabolism by autophagy in liver cancer involves selective autophagic degradation of HK2 (hexokinase 2), Autophagy. 14 (2018) 671–684.

https://doi.org/10.1080/15548627.2017.1381804.

[314] D. Zhao, S.W. Zou, Y. Liu, X. Zhou, Y. Mo, P. Wang, Y.H. Xu, B. Dong, Y. Xiong, Q.Y. Lei, K.L. Guan, Lysine-5 acetylation negatively regulates lactate dehydrogenase a and is decreased in pancreatic cancer, Cancer Cell. 23 (2013) 464–476. https://doi.org/10.1016/j.ccr.2013.02.005.

[315] L. Lv, D. Li, D. Zhao, R. Lin, Y. Chu, H. Zhang, Z. Zha, Y. Liu, Z. Li, Y. Xu, G. Wang, Y. Huang, Y. Xiong, K.L. Guan, Q.Y. Lei, Acetylation Targets the M2 Isoform of Pyruvate Kinase for Degradation through Chaperone-Mediated Autophagy and Promotes Tumor Growth, Mol. Cell. 42 (2011) 719–730. https://doi.org/10.1016/j.molcel.2011.04.025.

[316] A. Forrester, C. De Leonibus, P. Grumati, E. Fasana, M. Piemontese, L. Staiano, I. Fregno, A. Raimondi, A. Marazza, G. Bruno, M. Iavazzo, D. Intartaglia, M. Seczynska, E. van Anken, I. Conte, M.A. De Matteis, I. Dikic, M. Molinari, C. Settembre, A selective ER-phagy exerts procollagen quality control via a Calnexin-FAM134B complex, EMBO J. 38 (2019) e99847. https://doi.org/10.15252/embj.201899847.

[317] Y. Wei, W.-C. Chiang, R. Sumpter, P. Mishra, B. Levine, Prohibitin 2 Is an Inner Mitochondrial Membrane Mitophagy Receptor., Cell. 168 (2017) 224–238.e10. https://doi.org/10.1016/j.cell.2016.11.042.

[318] A.J.L. Cook, Z.A. Gurard-Levin, I. Vassias, G. Almouzni, A Specific Function for the Histone Chaperone NASP to Fine-Tune a Reservoir of Soluble H3-H4 in the Histone Supply Chain, Mol. Cell. 44 (2011) 918–927. https://doi.org/10.1016/j.molcel.2011.11.021.

[319] C. Lenain, O. Gusyatiner, S. Douma, B. van den Broek, D.S. Peeper, Autophagy-mediated degradation of nuclear envelope proteins during oncogene-induced senescence, Carcinogenesis. 36 (2015) 1263–1274. https://doi.org/10.1093/carcin/bgv124.

[320] Y. Li, X. Jiang, Y. Zhang, Z. Gao, Y. Liu, J. Hu, X. Hu, L. Li, J. Shi, N. Gao, Nuclear accumulation of UBC9 contributes to SUMOylation of lamin A/C and nucleophagy in response to DNA damage, J. Exp. Clin. Cancer Res. 38 (2019) 67. https://doi.org/10.1186/s13046-019-1048-8.

[321] A.P. Borroni, A. Emanuelli, P.A. Shah, N. Ilić, L. Apel-Sarid, B. Paolini, D. Manikoth Ayyathan, P. Koganti, G. Levy-Cohen, M. Blank, Smurf2 regulates stability and the autophagic–lysosomal turnover of lamin A and its disease-associated form progerin, Aging Cell. 17 (2018). https://doi.org/10.1111/acel.12732.

[322] H. Takai, K. Masuda, T. Sato, Y. Sakaguchi, T. Suzuki, T. Suzuki, R. Koyama-Nasu, Y. Nasu-Nishimura, Y. Katou, H. Ogawa, Y. Morishita, H. Kozuka-Hata, M. Oyama, T. Todo, Y. Ino, A. Mukasa, N. Saito, C. Toyoshima, K. Shirahige, T. Akiyama, 5-Hydroxymethylcytosine plays a critical role in glioblastomagenesis by recruiting the CHTOP-Methylosome complex, Cell Rep. 9 (2014) 48–60. https://doi.org/10.1016/j.celrep.2014.08.071.

[323] S.J. Kim, B.C. Yoo, C.S. Uhm, S.W. Lee, Posttranslational arginine methylation of lamin

A/C during myoblast fusion, Biochim. Biophys. Acta - Proteins Proteomics. 1814 (2011) 308–317. https://doi.org/10.1016/j.bbapap.2010.11.006.

[324] S. Li, P. Yang, E. Tian, H. Zhang, Arginine Methylation Modulates Autophagic Degradation of PGL Granules in C.elegans, Mol. Cell. 52 (2013) 421–433. https://doi.org/10.1016/j.molcel.2013.09.014.

[325] Y. Chen, V. Scarcelli, R. Legouis, Approaches for Studying Autophagy in Caenorhabditis elegans, Cells. 6 (2017) 27. https://doi.org/10.3390/cells6030027.

[326] L.S. Fiore, S.S. Ganguly, J. Sledziona, M.L. Cibull, C. Wang, D.L. Richards, J.M. Neltner, C. Beach, J.R. McCorkle, D.M. Kaetzel, R. Plattner, C-Abl and Arg induce cathepsin-mediated lysosomal degradation of the NM23-H1 metastasis suppressor in invasive cancer, Oncogene. 33 (2014) 4508–4520. https://doi.org/10.1038/onc.2013.399.

[327] G.S. Puts, M.K. Leonard, N. V. Pamidimukkala, D.E. Snyder, D.M. Kaetzel, Nuclear functions of NME proteins, Lab. Investig. 98 (2018) 211–218. https://doi.org/10.1038/labinvest.2017.109.

[328] Q. Zhang, J.R. McCorkle, M. Novak, M. Yang, D.M. Kaetzel, Metastasis suppressor function of NM23-H1 requires its 3'-5' exonuclease activity, Int. J. Cancer. 128 (2011) 40–50. https://doi.org/10.1002/ijc.25307.

[329] N. Pamidimukkala, G.S. Puts, M. Kathryn Leonard, D. Snyder, S. Dabernat, E.C. De Fabo, F.P. Noonan, A. Slominski, G. Merlino, D.M. Kaetzel, Nme1 and Nme2 genes exert metastasis-suppressor activities in a genetically engineered mouse model of UV-induced melanoma, Br. J. Cancer. 124 (2021) 161–165. https://doi.org/10.1038/s41416-020-01096-w.

[330] Z. Fan, P.J. Beresford, D.Y. Oh, D. Zhang, J. Lieberman, Tumor suppressor NM23-H1 is a granzyme A-activated DNase during CTL-mediated apoptosis, and the nucleosome assembly protein set is its inhibitor, Cell. 112 (2003) 659–672. https://doi.org/10.1016/S0092-8674(03)00150-8.

[331] D. Chowdhury, P.J. Beresford, P. Zhu, D. Zhang, J.S. Sung, B. Demple, F.W. Perrino, J. Lieberman, The Exonuclease TREX1 Is in the SET Complex and Acts in Concert with NM23-H1 to Degrade DNA during Granzyme A-Mediated Cell Death, Mol. Cell. 23 (2006) 133–142. https://doi.org/10.1016/j.molcel.2006.06.005.

[332] L. Mohr, E. Toufektchan, P. von Morgen, K. Chu, A. Kapoor, J. Maciejowski, ER-directed TREX1 limits cGAS activation at micronuclei, Mol. Cell. 0 (2021). https://doi.org/10.1016/j.molcel.2020.12.037.

[333] M.H. Hauer, S.M. Gasser, Chromatin and nucleosome dynamics in DNA damage and repair, Genes Dev. 31 (2017) 2204–2221. https://doi.org/10.1101/gad.307702.117.

[334] M. Okuwaki, K. Kato, K. Nagata, Functional characterization of human nucleosome assembly protein 1-like proteins as histone chaperones, Genes to Cells. 15 (2010) 13–27. https://doi.org/10.1111/j.1365-2443.2009.01361.x.

[335] H. Ohtomo, S. Akashi, Y. Moriwaki, M. Okuwaki, A. Osakabe, K. Nagata, H. Kurumizaka,

Y. Nishimura, C-terminal acidic domain of histone chaperone human NAP1 is an efficient binding assistant for histone H2A-H2B, but not H3-H4, Genes to Cells. 21 (2016) 252–263. https://doi.org/10.1111/gtc.12339.

[336] N.E. Bernardes, Y.M. Chook, Nuclear import of histones, Biochem. Soc. Trans. 48 (2020) 2753–2767. https://doi.org/10.1042/BST20200572.

[337] N. Mosammaparast, K.R. Jackson, Y. Guo, C.J. Brame, J. Shabanowitz, D.F. Hunt, L.F. Pemberton, Nuclear import of histone H2A and H2B is mediated by a network of karyopherins, J. Cell Biol. 153 (2001) 251–262. https://doi.org/10.1083/jcb.153.2.251.

[338] M. Kimura, Y. Morinaka, K. Imai, S. Kose, P. Horton, N. Imamoto, Extensive cargo identification reveals distinct biological roles of the 12 importin pathways, Elife. 6 (2017). https://doi.org/10.7554/eLife.21184.

[339] Y. Yamamoto, H. Chino, S. Tsukamoto, K.L. Ode, H.R. Ueda, N. Mizushima, NEK9 regulates primary cilia formation by acting as a selective autophagy adaptor for MYH9/myosin IIA, Nat. Commun. 12 (2021). https://doi.org/10.1038/s41467-021-23599-7.

[340] I. Kalvari, S. Tsompanis, N.C. Mulakkal, R. Osgood, T. Johansen, I.P. Nezis, V.J. Promponas, iLIR: A web resource for prediction of Atg8-family interacting proteins, Autophagy. 10 (2014) 913–925. https://doi.org/10.4161/auto.28260.

[341] B.K. Shrestha, M. Skytte Rasmussen, Y.P. Abudu, J.-A. Bruun, K.B. Larsen, E.A. Alemu, E. Sjøttem, T. Lamark, T. Johansen, NIMA-related kinase 9–mediated phosphorylation of the microtubule-associated LC3B protein at Thr-50 suppresses selective autophagy of p62/sequestosome 1, J. Biol. Chem. 295 (2020) 1240–1260. https://doi.org/10.1016/s0021-9258(17)49883-8.

[342] G. Puts, S. Jarrett, M. Leonard, N. Matsangos, D. Snyder, Y. Wang, R. Vincent, B. Portney, R. Abbotts, L. McLaughlin, M. Zalzman, F. Rassool, D. Kaetzel, Metastasis Suppressor NME1 Modulates Choice of Double-Strand Break Repair Pathways in Melanoma Cells by Enhancing Alternative NHEJ while Inhibiting NHEJ and HR, Int. J. Mol. Sci. 21 (2020) 5896. https://doi.org/10.3390/ijms21165896.

[343] C.M. Dower, C.A. Wills, S.M. Frisch, H.G. Wang, Mechanisms and context underlying the role of autophagy in cancer metastasis, Autophagy. 14 (2018) 1110–1128. https://doi.org/10.1080/15548627.2018.1450020.

[344] E.E. Mowers, M.N. Sharifi, K.F. Macleod, Autophagy in cancer metastasis, Oncogene. 36 (2017) 1619–1630. https://doi.org/10.1038/onc.2016.333.

[345] A. Cheblal, K. Challa, A. Seeber, K. Shimada, H. Yoshida, H.C. Ferreira, A. Amitai, S.M. Gasser, DNA Damage-Induced Nucleosome Depletion Enhances Homology Search Independently of Local Break Movement, Mol. Cell. 80 (2020) 311–326.e4. https://doi.org/10.1016/j.molcel.2020.09.002.

[346] K. Challa, C.D. Schmid, S. Kitagawa, A. Cheblal, V. Iesmantavicius, A. Seeber, A. Amitai, J. Seebacher, M.H. Hauer, K. Shimada, S.M. Gasser, Damage-induced chromatome dynamics link Ubiquitin ligase and proteasome recruitment to histone loss and

efficient DNA repair, Mol. Cell. 81 (2021) 811–829.e6. https://doi.org/10.1016/j.molcel.2020.12.021.

[347] Q. Luo, B. Wang, Z. Wu, W. Jiang, Y. Wang, K. Du, N. Zhou, L. Zheng, J. Gan, W.H. Shen, J. Ma, A. Dong, NAP1-Related Protein 1 (NRP1) has multiple interaction modes for chaperoning histones H2A-H2B, Proc. Natl. Acad. Sci. U. S. A. 117 (2020) 30391–30399. https://doi.org/10.1073/pnas.2011089117.

[348] A. Dong, Y. Zhu, Y. Yu, K. Cao, C. Sun, W.H. Shen, Regulation of biosynthesis and intracellular localization of rice and tobacco homologues of nucleosome assembly protein 1, Planta. 216 (2003) 561–570. https://doi.org/10.1007/s00425-002-0910-6.

[349] C.J. Bonangelino, E.M. Chavez, J.S. Bonifacino, Genomic screen for vacuolar protein sorting genes in Saccharomyces cerevisiae, Mol. Biol. Cell. 13 (2002) 2486–2501. https://doi.org/10.1091/mbc.02-01-0005.

[350] L. Selth, J.Q. Svejstrup, Vps75, a new yeast member of the NAP histone chaperone, J. Biol. Chem. 282 (2007) 12358–12362. https://doi.org/10.1074/jbc.C700012200.

[351] G. Chen, Z. Han, D. Feng, Y. Chen, L. Chen, H. Wu, L. Huang, C. Zhou, X. Cai, C. Fu, L. Duan, X. Wang, L. Liu, X. Liu, Y. Shen, Y. Zhu, Q. Chen, A regulatory signaling loop comprising the PGAM5 phosphatase and CK2 controls receptor-mediated mitophagy., Mol. Cell. 54 (2014) 362–77. https://doi.org/10.1016/j.molcel.2014.02.034.

[352] J. Rappsilber, M. Mann, Y. Ishihama, Protocol for micro-purification, enrichment, pre-fractionation and storage of peptides for proteomics using StageTips, Nat. Protoc. 2 (2007) 1896–1906. https://doi.org/10.1038/nprot.2007.261.

[353] J. V Olsen, B. Macek, O. Lange, A. Makarov, S. Horning, M. Mann, Higher-energy C-trap dissociation for peptide modification analysis, Nat. Methods. 4 (2007) 709–712. https://doi.org/10.1038/nmeth1060.

[354] J.E. Elias, S.P. Gygi, Target-decoy search strategy for increased confidence in large-scale protein identifications by mass spectrometry, Nat. Methods. 4 (2007) 207–214. https://doi.org/10.1038/nmeth1019.

[355] A. Franceschini, D. Szklarczyk, S. Frankild, M. Kuhn, M. Simonovic, A. Roth, J. Lin, P. Minguez, P. Bork, C. Von Mering, L.J. Jensen, STRING v9.1: Protein-protein interaction networks, with increased coverage and integration, Nucleic Acids Res. 41 (2013) D808–D815. https://doi.org/10.1093/nar/gks1094.

[356] R. Saito, M.E. Smoot, K. Ono, J. Ruscheinski, P.L. Wang, S. Lotia, A.R. Pico, G.D. Bader, T. Ideker, A travel guide to Cytoscape plugins, Nat. Methods. 9 (2012) 1069–1076. https://doi.org/10.1038/nmeth.2212.

[357] H. Mi, A. Muruganujan, J.T. Casagrande, P.D. Thomas, Large-scale gene function analysis with the panther classification system, Nat. Protoc. 8 (2013) 1551–1566. https://doi.org/10.1038/nprot.2013.092.

11 APPENDIX II

11.1 ACKNOWLEDGEMENT

11.2 CURRICULUM VITAE

Appendix II: 11.2 Curriculum vitae